A unique way of energy conservation in glutamate fermenting clostridia

Dissertation

zur

Erlangung des Doktorgrades

der Naturwissenschaften

(Dr. rer. nat.)

dem

Fachbereich Biologie

der Philipps-Universität Marburg

vorgelegt von

Elamparithi Jayamani

aus Chennai, Indien

Marburg/Lahn 2008

Die Untersuchungen zur vorliegenden Arbeit wurden von April 2004 bis Dezember 2008 am Fachbereich Biologie der Philipps-Universität Marburg unter der Leitung von Herrn Prof. Dr. W. Buckel durchgeführt.

Vom Fachbereich Biologie

der Philipps-Universität Marburg als Dissertation am _____ angenommen.

Erstgutachter: Prof. Dr. Wolfgang Buckel

Zweitgutachter: Prof. Dr. Rudolf K. Thauer

Tag der mündlichen Prüfung: _____

Die im zeitlichen Rahmen dieser Dissertation erzielten Ergebnisse sind in folgenden Publikationen veröffentlicht:

Boiangiu, C. D., Jayamani, E., Brügel, D., Herrmann, G., Kim, J., Forzi, L., Hedderich, R., Vgenopoulou, I., Pierik, A. J., Steuber, J. & Buckel, W. (2005) Sodium ion pumps and hydrogen production in glutamate fermenting anaerobic bacteria. *J. Mol. Microbiol. Biotechnol. 10*, 105-119.

Herrmann, G., Jayamani, E., Mai, G. & Buckel, W. (2008) Energy conservation via electron transferring flavoprotein (ETF) in anaerobic bacteria. *J. Bacteriol. 190*, 784-791.

Frank, I., Biegel, E., Jayamani, E., Buckel, W., Müller, V. (2007) Dissection of the caffeate respiratory chain in the acetogen *Acetobacterium woodii*: identification of an Rnf-type NADH dehydrogenase as a potential coupling site. *J. Bacteriol. 189*, 8145-8153.

Jayamani, E*., Boiangiu, C. D*., Dietmar, L., and Buckel, W. Rnf-related ferredoxin-NAD$^+$ reductases from *Clostridium tetanomorphum.* (Manuscript in preparation).
*equally contributed to this work.

CONTENTS

Abbreviations:

Kpp	Potassium phosphate buffer
DTT	Dithiothreitol
FPLC	Fast Protein Liquid Chromatography
HPLC	High Performance Liquid Chromatography
FMN	Flavin Riboflavin-5'-phosphate
FAD	Flavin Adenine Dinucleotide
OD	Optical Density
SDS	Sodium dodecylsulfate
TEMED	N,N,N',N'-Tetraethylethylenediamine
TCA	Trichloroacetic acid
UV-vis	Ultraviolet visible
CCCP	Carbonylcyanide-*m*-chlorophenylhydrazone
Bcd	Butyryl-CoA dehydrogenase
Etf	Electron transferring flavoprotein

Zusammenfassung

Genetische Analysen ergaben, dass *Rhodobacter capsulatus* sechs *rnfABCDEG*-Gene enthält, die für den Elektronentransport bei der Stickstofffixierung verantwortlich sind (*rnf* = *R*hodobacter *n*itrogen *f*ixation). Homologe Gene wurden im Genom von *Clostridium tetani* entdeckt. In dieser Arbeit wurde aus dem nahe verwandten *Clostridium tetanomorphum* ein Membrankomplex gereinigt, der die Reduktion von NAD^+ ($E^{\circ'}$ = −320 mV) mit Ferredoxin ($E^{\circ'}$ ≤ −420 mV) katalysiert. Die Potentialdifferenz von ≥ 100 mV könnte zur Energiekonservierung in der Fermentation von Glutamat zu Ammonium, CO_2, Acetat, Butyrat und H_2 beitragen. Der Komplex besteht aus sechs Untereinheiten (RnfABCDEG), von denen vier (RnfCDEG) N-terminal ansequenziert werden konnten. Ihre Sequenzen sind zu 60-80% mit den abgeleiteten Sequenzen der Rnf-Untereinheiten aus *C. tetani* identisch. Auch die Reihenfolge. Der Komplex enthält kovalent und nicht-kovalent gebundenes Flavin. Letzteres wurde als FMN und Riboflavin identifiziert, je 0.3 mol/mol Komplex (180 kDa). Die Untereinheiten RnfG und RnfD enthalten das kovalent gebundene Flavin, das mit Phosphodiesterase abgelöst werden kann. Der Eisengehalt wurde zu 25 ± 1 mol Fe/mol bestimmt. Routinemäßig wird die Rnf-Aktivität mit NADH und Ferricyanid bei 420 nm gemessen. Für Aktivitätsmessungen über die NAD^+-Reduktion bei 340 nm wurde Ferredoxin aus *C. tetanomorphum* isoliert und mit Ti(III)Citrat bei pH 7.0 in der Küvette reduziert. Mit diesem Verfahren konnte weder mit invertierten Vesikeln noch mit dem in Liposomen rekonstituierten Enzym die postulierte Bildung eines elektrochemischen Na^+ oder H^+-Gradienten nachgewiesen werden. Hohe Rnf-Aktivität wurde auch in Membranpräparationen von *Clostridium aminobutyricum*, *Clostridium pascui* und *Clostridium propionicum* gefunden, nicht dagegen in denen des Nikotinat-Fermentierers *Eubacterium barkeri*.

Der Butyryl-CoA-Dehydrogenase/Elektron-Transfer-Protein (Bcd/Etf) Komplex wurde aus *C. pascui* und *C. tetanomorphum* isoliert. Die N-terminalen Sequenzen der drei verschiedenen Untereinheiten ($\alpha_2\beta\gamma$) aus beiden Organismen zeigten hohe Ähnlichkeiten zu denen der abgeleiteten Sequenzen aus dem Genom von *C. tetani*. Der Komplex aus *C. tetanomorphum* katalysiert die exergone Reduktion von Crotonyl-CoA zu Butyryl-CoA, an die die endergone Reduktion von Ferredoxin mit einem zweiten

NADH gekoppelt ist. Das reduzierte Ferredoxin kann entweder mit einer Hydrogenase H_2 bilden oder vermutlich über Rnf zur Energiekonservierung beitragen (ca. 0.3 mol ATP/mol Glutamat). Zukünftige Versuche mit gereinigtem Rnf und Bcd/Etf in Gegenwart von NADH und katalytischen Mengen an Ferredoxin könnten vielleicht den gesuchten Ionengradienten herstellen.

Versuche mit deuteriertem Glutamat und dem Nachweis von Citramalat-Lyase-Aktivität zeigten, dass *C. pascui* wie *C. tetanomorphum* den Methylaspartat-Weg zur Glutamatfermentation benutzt.

Summary

Genetic analysis revealed that *Rhodobacter capsulatus* contains six *rnfABCDEG*-genes that are responsible for the electron flow in nitrogen fixation (*rnf* = <u>*R*</u>*hodobacter* <u>n</u>itrogen <u>f</u>ixation). Homolgous genes have been detected in *Clostridium tetani*. In this work, a membrane complex has been purified from the related *Clostridium tetanomorphum* that catalyses the reduction of NAD^+ ($E^{\circ\prime} = -320$ mV) with ferredoxin ($E^{\circ\prime} \leq -420$ mV). The difference in the redox potential of ≥ 100 mV could be useful for additional energy conservation in the fermentation of glutamate to ammonia, CO_2, acetate, butyrate, and H_2. The complex consists of six subunits (RnfABCDEG), of which four N-termini (RnfCDEG) could be sequenced. The sequences are 60-80% identical to the deduced sequences of the Rnf-subunits from *C. tetani*. The *rnf* operon has been completely sequenced and aligned with the sequences of *C. tetani*.

The complex contains both non-covalently bound flavin as well as covalently bound flavin. The non-covalently bound flavin was identified as FMN and riboflavin in 1:1 stochiometric ratio, each 0.3 mol/mol Rnf complex (180 kDa). The subunits RnfG and RnfD contain covalently bound flavin linked via phosphodiester bond. The iron was determined as 25 ± 1 mol per Rnf complex. Usually, Rnf activity was measured with NADH and ferricyanide at 420 nm. In order to measure NAD^+ reduction with reduced ferredoxin catalysed by Rnf complex, the ferredoxin was purified from *C. tetanomorphum* and reduced by Ti(III)citrate at pH 7.0. High Rnf activities were observed in the membrane preparations of *Clostridium aminobutyricum*, *Clostridium pascui* and *Clostridium propionicum*. Thus, additional energy conservation can be explained in these bacteria. However Rnf activity was absent in *Eubacterium barkeri*, a nicotinate fermenting bacteria.

The soluble butyryl-CoA-dehydrogenase/electron transferring flavoprotein (Bcd/Etf) complex was purified from *C. pascui* as well as from *C. tetanomorphum*. The N-terminal sequences of the three subunits (αβγ) showed high identities with the deduced sequences of *C. tetani*. The Bcd/Etf complex purified from *C. tetanomorphum* was shown to catalyze the endergonic reduction of ferredoxin with NADH coupled to the exergonic reduction of crotonyl-CoA to butyryl-CoA ($E^{\circ\prime} = -10$ mV) with NADH. The

reduced ferredoxin could be used for H_2 production catalysed by a hydrogenase or probably used for additional energy conservation via Rnf (about 0.3 mol ATP/ mol glutamate).

Experiments with [2,4,4-^{2}H]glutamate and detection of citramalate-lyase activity showed that *C. pascui* and *C. tetanomorphum* ferment glutamate via the methylaspartate pathway.

1. Introduction

1.1 A brief overview on anaerobic metabolism

Organisms obtain their energy from the sun termed as prototroph or by using chemical energy termed as chemotroph. It has been suggested that the photosynthetic apparatus is a relatively late acquisition of anaerobes; therefore anaerobic chemotrophic metabolism might have been the source of energy at the start of life on earth. Nowadays life without oxygen is found in the mud at the bottom of marshes, buried organic material, sewage sludge, human intestine and also where putrefactive processes or excessive oxygen consumption by aerobic cells gives rise to niches of oxygen deficiency. Wachtershäuser's theory says pyrite-pulled chemoautotrophic anaerobic metabolism should be the origin of life [1,2].

Biological redox reactions are very important for the synthesis of energy rich compounds, one of which is the universal energy carrier adenosine triphosphate (ATP). In general the biological energy transformations are carried out in two ways, one as substrate level phosphorylation (SLP) that oxidises a substrate to an energy rich phosphate, which is transferred to ADP to generate ATP. Electron transport phospohorylation (ETP) converts the electrochemical potential between two redox partners into an electrochemical ion gradient, which drives ATP-synthesis [2,3].

In the biological redox processes, electron donor and acceptor processes differ in the mechanism of energy conservation. Substrate level phosphorylations are carried out almost exclusively by donor processes and it is the same scenario in both aerobic and anaerobic organisms. But in the electron acceptor processes, it differs substantially by using oxygen as terminal oxidant in the case of aerobic bacteria and anaerobic bacteria use organic and inorganic acceptors.

In aerobic bacteria, ATP synthesis is quite efficient by the reduction of oxygen in the respiratory chain. In respiring anaerobes oxygen is replaced by electron acceptors like nitrate, nitrite, fumarate, sulphate, sulphur and CO_2. Fermentative anaerobes use part of the substrates as electron acceptors and/or protons to yield molecular hydrogen. This increases the number of anaerobically possible electron donor processes, since electrons can be removed as hydrogen. However this process is expensive in terms of energy

production. It is known that anaerobes are able to ferment besides carbohydrates also amino acids which act as donor and acceptor; these processes are named Stickland reaction.

In the anaerobic food chain, conversion of organic matter like carbohydrates and proteins is only possible by the collective action of at least five different groups of bacteria, including primary fermenting bacteria, acetogenic bacteria, secondary fermenting bacteria, and two types of methanogens [4]. Polymers are first converted to oligomers and monomers, typically through the action of extracellular hydrolytic enzymes produced by primary fermenting bacteria like clostridia, which also ferment the resulting monomers further to fatty acids, succinate, lactate and alcohol. Some of these fermentation products, especially H_2 and CO_2 can be converted into acetate by acetogens. Acetate and other one-carbon compounds can be converted directly by methanogenic bacteria into methane and carbon dioxide. Fatty acids longer than two carbon atoms, alcohols longer than one carbon atom, longer branched-chain and aromatic fatty acids are fermented by secondary fermenters or obligate proton reducers. Acetate, CO_2, hydrogen, and perhaps formate are formed which are subsequently used by the methanogens. This interaction of two different organisms is called syntrophy [5].

The energy process of anaerobic organisms revolves around the oxidation and reduction of organic substrates. The oxidation shares high similarity with corresponding reactions carried out by aerobic organisms except for certain limitations imposed by the anaerobic conditions. The oxidative deamination of amino acids and oxidative decarboxylation of keto acids is identical in both aerobic as well as anaerobic energy metabolism. The exceptions are degradation of hydrocarbons, because for those therefore oxygen is required not only as electron acceptor but also as substrate for hydroxylation and ring opening. Therefore in the anaerobic degradation of hydrocarbon and aromatic compounds, special radical enzymes are required which have only been discovered and studied in the past decade. The reduction reactions, however, are quite unique in fermentative organisms. In Clostridia the problem of providing organic oxidants has been solved in a variety of ways. Some species use a substrate directly as the oxidant and the same as reductant, this process called as disproportionation. For example, *Clostridium propionicum* converts serine to pyruvate which is oxidised to acetyl-CoA

and reduced to propionyl-CoA and *Clostridium tetanomorphum* oxidises glutamate via pyruvate to acetyl-CoA, which is then reduced to butyrate.

1.2 Glutamate fermentation by clostridia

Clostridia ferment glutamate by 5 different pathways. Three of these pathways lead to the formation of butyrate. The major two pathways that occur in glutamate fermentation are the methylaspartate and the hydroxyglutarate pathway named after their intermediates. The methylaspartate pathway and hydroxyglutarate pathway lead to ammonia, carbon dioxide, acetate, butyrate and hydrogen as shown in the equation 1[6,7].

5 Glutamate$^-$ + 6 H_2O + 2 H^+ = 5 NH_4^+ + 5 CO_2 + 6 Acetate$^-$ + 2 Butyrate$^-$ + H_2 (Equation 1)
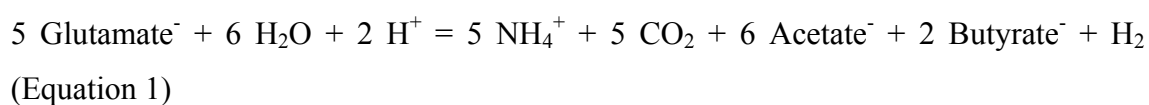
$\Delta G°' = -63.4$ kJ/mol Glutamate
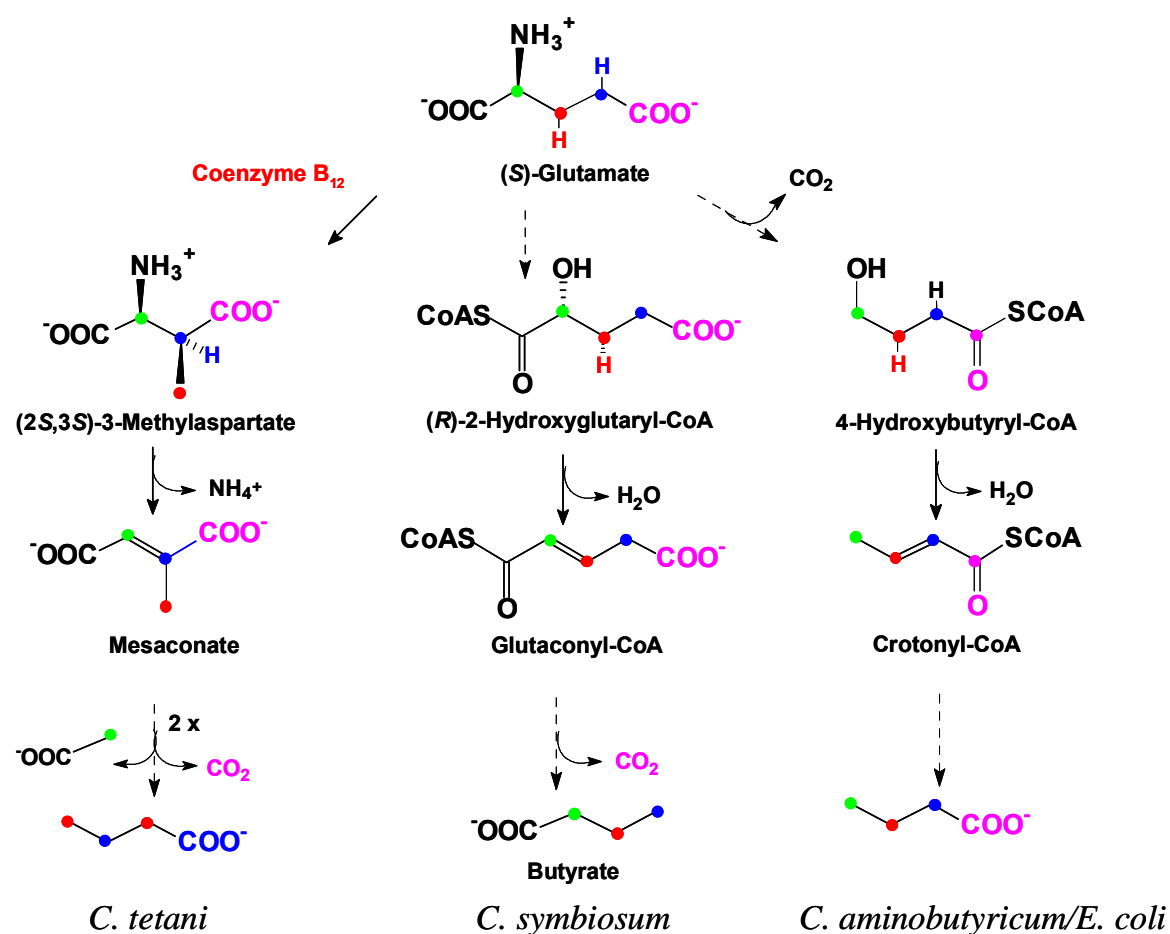
The third pathway of glutamate fermentation has 4-aminobutyrate as intermediate. The pathway is completed by two organisms, one to decarboxylate glutamate to 4-aminobutyrate and a second to ferment this product to acetate and butyrate.

$$Glutamate^- + H^+ \rightarrow CO_2 + 4\text{-aminobutyrate};$$

$\Delta G°'$ ca. -30 kJ/mol glutamate

$$2 \times 4\text{-Aminobutyrate} + 2\ H_2O \rightarrow 2\ NH_4^+ + 2\ acetate^- + butyrate^- + H^+;$$
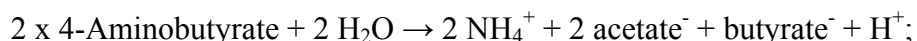
$\Delta G°'$ ca. -37 kJ/mol 4-aminobutyrate

Interestingly *C. aminobutyricum* is the only known organism which ferments 4-aminobutyrate to ammonia, acetate and butyrate but no hydrogen is formed in this oraganism.

The fourth pathway shares similar intermediates with methylaspartate pathway but propionate is the end product instead of butyrate. The fifth pathway proceeds via proline and 5-aminovalerate to acetate, propionate and *n*-valerate.

1.2.1 The methylaspartate pathway

The methylaspartate pathway was discovered in *C. tetanomorphum* [8] but it also widespread in closely related clostridia as are *Clostridium tetani*, *Clostridium cochlearium* and *Clostridium limosum* [6]. The completed genome sequence of *C. tetani* has been revealed and all genes encoding for the enzymes which are involved in the methylaspartate pathway have been annotated [9]. The first step in this pathway is the carbon skeleton rearrangement of (*S*)-glutamate into (2*S*,3*S*)-3-methylaspartate which is carried out by coenzyme B_{12}-dependent glutamate mutase (GlmSE). The enzyme has been characterised and the crystal structure was solved [10].

 The unusual carbon skeleton rearrangement of glutamate to 3-methylaspartate has two interesting purposes, one is the facile elimination of ammonia from the α,β-aminoacid 3-methylaspartate to mesaconate catalysed by methylaspartate ammonia lyase and the subsequent two-step conversion to pyruvate which is an central metabolite. It is also reported that the heterodimeric iron-sulfur protein mesaconase (MesAB, citramalate

hydrolyase) is responsible for the hydration of mesaconate to give (*S*)-citramalate, which is further cleaved to acetate and pyruvate. Citramalate lyase is an enzyme complex with an acetyl-CoA-like prosthetic group on a small carrier protein (ClmA) for whose synthesis requires six genes are required. Firstly, citramalyl-CoA is formed and acetate is released (ClmC) and secondly, citramalyl-CoA is cleaved to pyruvate, whereby acetyl-CoA is regenerated (ClmB). The biosynthesis of acetyl-bound ClmA in the active citramalate lyase complex probably proceeds exactly as that of citrate lyase in *Escherichia coli* [11]. It requires three enzymes; the first CmlF related to CitG catalyzes the triphosphoribosylation of 3-dephospho-CoA by ATP to yield adenosine and 2-(5-triphosphoribosyl)-3-dephospho- CoASH, which is incorporated into the *apo*-citramalate lyase complex at serine 14 of ClmA concomitant with the release of diphosphate mediated by CmlE, related to CitX. Finally the prosthetic group is acetylated at the SH group by the acetyl-CoA synthetase-like GmlD [12].
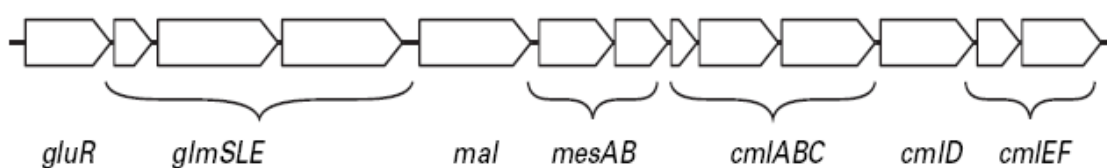
Fig. 1: Genes from *C. tetani* encoding the specific part of the methylaspartate pathway from glutamate to pyruvate (The first gene of the cluster shown in above figure encodes the protein GluR with helix-turn-helix motif, which probably controls the glutamate fermentation).

The formation of pyruvate finishes the special part of the methylaspartate pathway [13]. Pyruvate is then oxidatively decarboxylated by pyruvate ferredoxin oxidoreductase to yield acetyl-CoA, CO_2 and reduced ferredoxin. Ferredoxin is reoxidised in two ways. Approximately 80% of the reduced ferredoxin is used for butyrate synthesis together with two acetyl-CoA and the remaining 20% is used to reduce protons to molecular hydrogen by a [Fe-Fe] hydrogenase. Butyrate synthesis is carried out by two NADH dependent reductions, acetoacetyl-CoA to (*S*)-3-hydroxybutyryl-CoA and crotonyl-CoA (2 butenoyl-CoA) to butyryl-CoA [14]. The crotonyl-CoA reductase from *C. tetanomorphum* is purified as a complex. It consists of 3 subunits with a stochiometry of

$\alpha_2\beta\gamma$ by sequence comparisions revealed that $\alpha2$ is butyryl-CoA dehydrogenase (Bcd) and the $\beta\gamma$ subunits are heterodimeric electron-transferring flavoprotein (Etf). The artificial electron acceptor like ferrecenium hexaflurophosphate is used to monitor the conversion of butyryl CoA to crotonyl-CoA by butyryl-CoA dehydrogenase [15,16]. The reduction of crotonyl-CoA with NADH requires substrates amount of additional FAD [17]. A related propionyl-CoA dehydrogenase-Etf complex was isolated from *C. propionicum* which ferments besides serine also alanine [18]. This complex is composed of propinyl- CoA dehydrogenase and electron-transferring flavoprotein. It readily catalysed the reduction of acryloyl-CoA or crotonyl-CoA also in the absence of FAD. Whereas Bcd and Etf from *Acidominococcus fermentans,* which ferments glutamate via hydroxyglutarate pathway, and *Megasphaera elsdenii* do not form tight complexes. ATP is synthesized by substrate level phosphorylation from butyryl-CoA via butyryl phosphate.

The total energy conserved from 5 glutamates would amount to 3 ATP via SLP. In the traditional scheme of glutamate fermentation via methylaspartate pathway, five pyruvates derived from 5 glutamtes are oxidised by 5 ferredoxins to 5 CO_2 and 5 acetyl-CoA, 5 reduced ferredoxin (Fd^{2-}) are reoxidised by 6 H^+ and 4 NAD^+, yielding 1 H_2 and 4 NADH, respectively. Four of the 5 acetyl-CoA are reduced by 4 NADH to 2 butyryl-CoA. In total 3 ATP are generated from 2 butyryl-CoA and the remaining one acetyl-CoA.

One open question in this pathway is the reduction of NAD^+ by reduced ferredoxin generated by pyruvate oxidation, in order to obtain NADH necessary for butyrate synthesis which will be shown to be catalysed by the Rnf complex. The other question was the mode of coupling of butyryl-CoA dehydrogenase-ETF complex, which catalyses a highly exergonic reaction, to energy conservation that has been an enigma for about 70 years.

1.2.2 Rnf complex

The purple non sulfur bacterium *Rhodobacter capsulatus* is able to fix nitrogen. The reducing power for the nitrogen fixation in these bacteria is a limiting factor. The

missing link in the electron transport pathway to ferredoxin and flavodoxin could be answered by *rnf* genes which play a vital role in nitrogen fixation. Hence *rnf* mutant strains failed to grow diazotrophically. In vivo analysis demonstrated that *rnf* mutants of *R. capsulatus* exhibited no acetylene reduction activity. Insertion and deletion of *rnf* genes showed that the Rnf complex plays a vital role in electron transfer reaction to nitrogenase. In cell free extracts, however, nitrogenase activities could be determined using dithionite as an artificial electron donor in this *rnf* mutunat strain. These studies confirmed the fact that the Rnf system is involved in nitrogen fixation by acting as electron donor for nitrogenise, most likely by the endergonic reduction of ferredoxin by NADH driven by the proton motive force (PMF).

In 1993, Manfred Schmehl et al [19]. showed that *rnf* cluster comprises 7 genes which are all required for nitrogen fixation. They proposed to call these genes *rnfA*, *rnfB*, *rnfC*, *rnfD*, *rnfE* and *rnfF* (*rnf-R*hodobactor *n*itrogen *f*ixation). The structure predictions based on deduced amino acid sequences showed that RnfA, RnfD, RnfE and RnfG are membrane proteins. RnfA contains six transmembrane segments, both RnfD and RnfE include seven of these elements and RnfF contains only three transmembrane segments. The gene products of RnfB and RnfC are characterised by cysteine motifs typical for a clostridial ferredoxin-like [4Fe-4S] cluster. Both proteins contain two $C-X_2-C-X_2-C-X_3-C-P$ motifs, which are separated by 18 amino acid residues in RnfB and 27 residues in RnfC. In addition to these motifs, RnfB contains a further cysteine cluster $C-X_2-C-X_4-C-X_{16}-C$ in the N-terminal region. RnfB also contains a putative transmembrane helix, whereas RnfC is predicted to be a soluble protein.

1.2.3 Putative role of the Rnf system in *Clostridium tetani*

Fig. 2: C. *tetani:* Rnf-Open Reading Frame.

Genome sequence of *C. tetani* published by Brüggemann et al. [9] showed the abundance of FeS clusters within the proteins encoded by a putative operon of six genes, homologues to the Rnf complex of *R. capsulatus* and four genes *rnf*C, *rnf*D, *rnf*G

and *rnf*A shows homology to the membrane-bound NQR (NADH:ubiquinone oxidoreductase) found in many aerobic pathogens such as *Vibrio cholerae*, *Salmonella typhimurium*, *Yersenia pestis* and *Haemophilus influenzae* [20]. NQR apparently functions as a Na^+ -translocating NADH:ubiquinone oxidoreductase, but quinones are not reported to be present in *C. tetani.*

Table 1: Characteristics of the Rnf/Nqr subunits of *C. tetani:*

ORF name	CTC1019	CTC1020	CTC1021	CTC1022	CTC1023	CTC1024
Homologues in Rnf/nqr systems	RnfC/NqrF	RnfD/NqrB	RnfG/NqrC	RnfE/NqrD	RnfA/NqrE	RnfB
Hydrophobicity/ putative location	Cytosolic enzyme	16 TM	2 TM	10 TM	12 TM	2 TM
Redox domains	NAD/ FMN binding sites; 2[4Fe-4S]	FMN binding site	FMN binding site		-	4[4Fe-4S] polyferredoxin

It is hypothesised that the Rnf related NADH: ferredoxin oxidoreductase is the missing system for an understanding of electron flow from reduced ferredoxin, generated in the pyruvate:ferredoxin oxidoreductase reaction, via NADH to the NADH-consuming dehydrogenase of the butyrate pathway, which catalyses the reduction of crotonyl-CoA. The electron flow could be coupled with Na^+ translocation by membrane bound NADH: ferredoxin oxidoreductase to conserve energy.
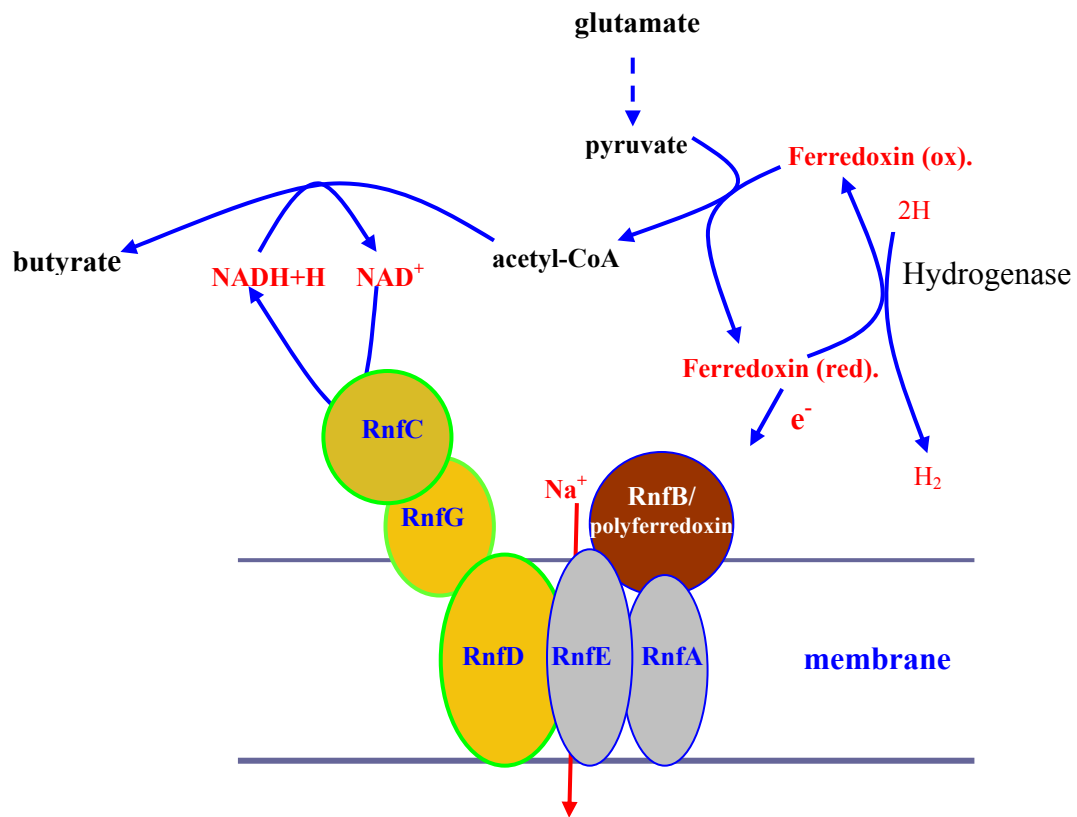
Fig. 3: Role of Rnf complex in *C.tetani* (Brüggemann et al)

1.2.4 The hydroxyglutarate pathway

The pathway has been found in *A. fermentans*, *Clostridium sporosphaeroides*, *C. symbiosum*, *Fusobacterium nucleatum* and *Peptostreptococcus assaccharolyticus.* All these bacteria live in anoxic niches within humans and animals. The hydroxyglutarate pathway is enrouted via (*R*)-2-hydroxyglutaryl-CoA, glutaconyl-CoA and crotonyl-CoA. The latter disproportionates to acetate, butyrate and H_2, the same products as those formed by *C. tetanomorphum* via 3-methylaspartate. Surprisingly, coenzyme B_{12} is absent in the hydroxyglutarate pathway, unlike the methylaspartate pathway where this cofactor plays an important role in the first step.

The first step of the hydroxyglutarate pathway is the oxidative NAD^+-dependent deamination of glutamate to 2-oxoglutarate, which is carried out by glutamate dehydrogenase and followed by hydroxyglutarate dehydragenase and glutaconate-CoA

transferase. The indepth analysis of this pathway revealed the unique reaction that differed from conventional biochemical transformations, the dehydration of (*R*)-2-hydroxyglutaryl-CoA to (*E*)-glutaconyl-CoA. This reversible *syn*-elimination of water is matter of interst in enzyme mechanism. In this reaction 3-*Si* proton has to be removed from the non-activated β position, whereas a hydroxyl anion is expelled from the α-position adjacent to the electron-withdrawing CoA-ester. The dehydratase which carries out this special reaction has been purified from *A. fermentans* and *C. symbiosum*. This enzyme consists of two protein components, A and D. The extremely oxygen sensitive homodimeric component A (hgdC, 2x27 kDa) contains one $[4Fe-4S]^{2+}$ cluster between the two subunits and acts as an activator of the dehydration. Dehydratase activity requires both components A and D, $MgCl_2$, catalytic amounts of ATP and a reducing agent. *In vivo* reduced ferredoxin or flavodoxin and *invitro* Ti(III)citrate or dithionite serve as reducing agents [14,21].

Glutaconyl-CoA decarboxylase found in this pathway is a bioenergetically exciting enzyme, which catalyses the decarboxylation of glutaconyl-CoA to crotonyl-CoA. The salient feature this enzyme is its integration into the membrane, its biotin content and Na^+-dependency of the enzymatic reaction. Similar properties were reported from oxaloacetate decarboxylase from Gammaproteobacteria [Dimroth, 1980 #115]. Glutaconyl-CoA decarboxylases are complexes of four functional domains or subunits,
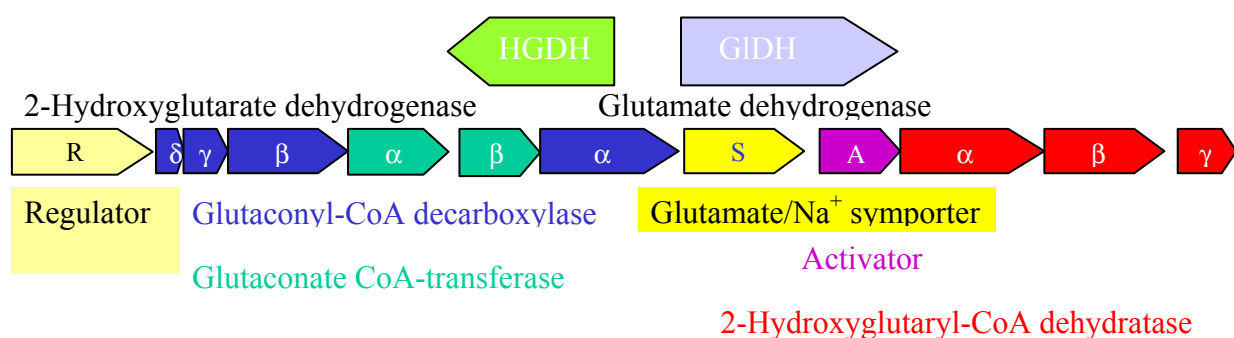
Fig. 4: Genes encoding the specific part of the hydroxyglutarate pathway in *F. nucleatum*.

a carboxytransferase (α), a biotin carrier (γ), a 9-11 membrane-spanning helices-containing Na^+-dependent carboxybiotin decarboxylase (β) and membrane anchor (δ) [22,23].

After decarboxylation of glutaconyl-CoA to crotoconyl-CoA, the 2-hydroxyglutaryl pathway forks into oxidative and a reductive branch. The NAD^+-dependent oxidation of crotonyl-CoA proceeds after normal hydration to (*S*)-3-hydroxylbutyryl-CoA. In the reductive branch, crotonyl-CoA is reduced to butyryl-CoA where NAD is regenerated. The CoA transfer to acetate leads into butyrate production and more acetyl-CoA.

1.3 4-Hydroxybutyryl-CoA pathway

4-Aminobutyrate, which is formed from glutamate by decarboxylation in many organisms, serves as initial substrate for this pathway. It is further converted into 4-hydroxybutyrate by aminotransfer to 2-oxoglutarate, followed by a NADH-dependent reduction of the succinic semialdehyde. A CoA-transferase catalyzes the formation of 4-hydroxybutyryl-CoA with acetyl-CoA or butyryl-CoA as donor. The unusual reaction in this pathway is the reversible dehydration of 2 × 4-hydroxybutyryl-CoA to crotonyl-CoA, which dispropionates to 2 acetyl-CoA and butyryl-CoA to from one ATP. It represents the key step in the fermentation of 4-aminobutyrate to ammonia, acetate and butyrate [14].

1.4. Bacteria

Clostridia belong to the order Clostridiales among the Firmicutes, they are divided into XIX clusters [24]. Only members of cluster I will retain the genus name Clostridium, family Clostridiaceae.

1.4.1. *Clostridium tetanomorphum*: Cluster I

In the 1950's, a histidine fermenting bacterium was isolated at the laboratory of Prof H. A. Barker. This bacterium later turned out to be also a glutamate fementer and identified as *C. tetanomorphum*. It is a spore forming anaerobic bacillus found in soil, human and animal intestinal tract. It is non-pathogenic. Its optimum growth temperature is 37°C. *C. tetanomorphum* shares metabolic feature with *C. tetani* which is a pathogenic bacterium. It produces a neurotoxin which leads to tetanus disease in human.

1.4.2 *Clostridium pascui*: **Cluster I**

C. pascui was first isolated from donkey pasture from Pakistan. It is rod shape, occurs singly or in pairs, and is motile. It forms subterminal elliptical shaped spores. It grows optimally at 37°C.

The phylogenetic tree based on 16S rRNA showed that *C. pascui* could be classified in cluster I of the clostridia where *C. tetanomorphum*, *C. tetani* and *Clostridium malenominatum* are placed (Fig. 5). It has been reported that *C. pascui* can ferment glutamate and histidine but not carbohydrates. The intermediates of glutamate fermentation pathway are not established so far.

1.4.3 *Clostridium pasteurianum*: **Cluster I**

C. pasterianum is a nitrogen fixing bacterium which readily grows on glucose as carbon source. It produces molecular hydrogen from ferredoxin catalyzed by hydrogenase and this system is well characterised. It is anaerobic Gram-positive bacillus, which forms spores.

Glucose + 0.6 H_2O → 2 CO_2 + 0.6 acetate$^-$ + 0.7 butyrate$^-$ + 1.3 H^+ + 2.6 H
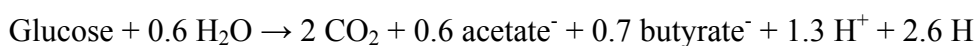
$\Delta G°' = -251$ kJ/mol

1.4.4 *Clostridium aminobutyricum*: **Cluster X**

C. aminobutyricum is a strictly anaerobic, spore forming, rod shaped and Gram-positive bacterium, which has been isolated from North Carolina swamp mud [25,26] and classified in cluster X of the clostridia [24]. It has been listed as *Clostridium* sp. by DSMZ. It grows on the medium containing 4-aminobutyrate as the major nutritional source.

1.4.5 *Clostridium symbiosum*: **Cluster XIVa**

C. symbiosum is a strict anaerobe. Cigar or lemon shaped organism, 2 – 5 of which form chains or pairs. The flagella arranged at the poles. It forms not heat resistant spores and

its GC content is about 48%. It stains Gram-negative despite absence of an outer membrane. Besides fermenting sugars and citrate it can ferment glutamate as main energy source.

1.4.6 *Clostridium propionicum*: Cluster XIVb

C. propionicum is a Gram-positive bacterium, obligate anaerobe; several 3-4 carbon compounds support growth, including acrylate and lactate. The mol% G + C of DNA isolated was 36-37. It degrades alanine and serine to carbon dioxide, ammonia, acetate and propionate, theronine is converted to butyrate.

3 Alanine + 2 $H_2O \rightarrow$ 3 NH_4^+ + CO_2 + acetate$^-$ + 2 propionate$^-$
$\Delta G^{\circ\prime}$ = -138 kJ/mol acetate.
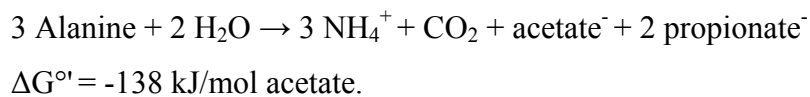
1.4.7 *Eubacterium* (*Clostridium*) *barkeri*: Cluster XV

E. barkeri was isolated from Potomac River (Washington, USA). It is a Gram-positive, rod shaped, strict anaerobe and not pathogenic bacterium with GC content of 55 to 58%. It was reclassified as *Eubacterium*. It ferments nicotinate into pyruvate and propionate.
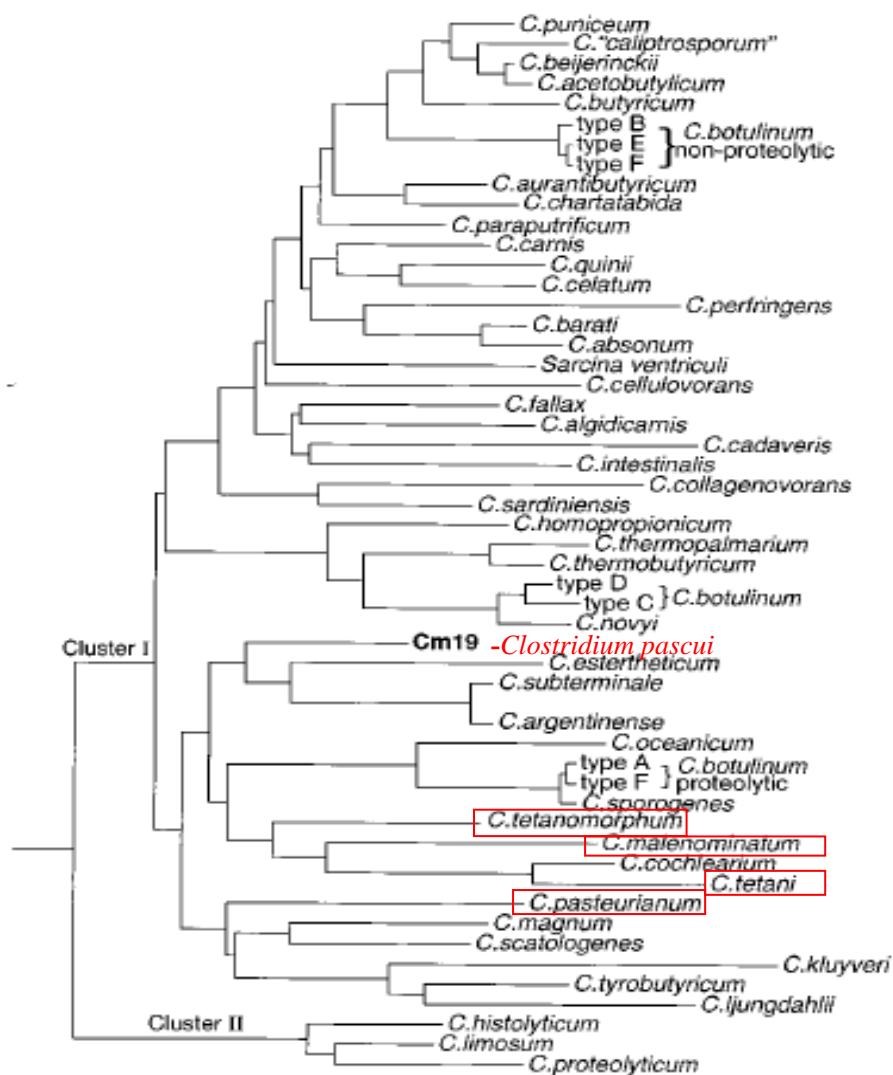
Fig. 5: The phylogenetic of Clostridiaceae, Cluster I and II tree based on 16S rRNA

1.5. Goals of my work

It has been proposed in *C. tetani* that the Rnf complex catalyses the reduction of NAD^+ by reduced ferredoxin generated by pyruvate oxidation, in order to obtain NADH necessary for butyrate synthesis [9]. Therefore, one of the goals of this thesis is to verify this proposal by purification of the Rnf complex and its role in energy conservation in *C. tetanomorphum.*

It has been proposed [27] and confirmed [15] that Bcd/Etf from *C. kluyveri* couples the endergonic reduction of ferredoxin with NADH to the exergonic reduction of crotonyl-CoA to butyryl-CoA. It has not been reported so far that the Bcd/Etf complex from *C. tetanomorphum* can conserve additional energy along with Rnf complex. This thesis focuses on the Bcd/Etf complex purification and confimation of this energy conserving coupling reaction.

Although it has been reported that *C. pascui* ferments glutamate [28], the metabolic pathway has not been established so far. Therefore, this thesis focuses on elucidation of the metabolic pathway in glutamate fermentation.

2. Materials and Methods

All the chemical compounds and reagents were purchased, unless or otherwise mentioned, from the companies Sigma (Steinheim), Merck (Darmstadt), Roth (Karlsruhe), Fluka (Neu-Ulm), Bio-Rad-Laborories (München), Serva (Heidelberg) and Amersham Biosciences (Freiburg). The primers were synthesized by MWG (Ebersberg).

2.1. Instruments

Beckman Ultracentrifuge (München), Sorvall cooling centrifuges (München). Anaerobic glove box was supplied by Coy Laboratories, Ann Arbor, MI (USA). The FPLC, UV-Vis Photometer and Ultrospec 400 which had been installed inside the glove box, were supplied by Amersham Biosciences (Freiburg). The UV visible spectrum was obtained with a HP 8453 UV- Visible diode array spectrophotometer (USA).

2.2. Columns

The columns DEAE sepahrose HR 26/10, Phenyl Sepharose FF HR 26/10, Superdex 200 HR 26/10, Q-Sepharose High performance HiloadTM 26/10, Superdex-G25 (5ml), Hydroxyapatite and Source 15 PHE column were obtained from Amersham Biosciences (Freiburg). HPLC columns were from Merck (Darmsatdt).

2.3. Radioisotopes

^{22}NaCl (1.05 GBq/ mmol) was obtained from Perkin-Elmer (Rodgau, Germany).

2.4. Anaerobic setup

Anaerobic purification was performed under exclusion of air in an anaerobic chamber (Coy Laboratory Products) with a 95% N_2 and 5% H_2 atmosphere. Buffers for enzyme purification were prepared by boiling and cooling under vacuum. Then the buffers were flushed with nitrogen gas to fill the head space of the bottle completely before transferring to the anaerobic chamber where buffers were stirred overnight. An Ultrospec 4000 spectrophotometer placed inside the chamber was used to measure enzyme activity.

2.5. *Clostridium tetanomorphum*

C. tetanomorphum (DSM 576) was cultivated under anaerobic conditions in 100 ml serum bottles. For the 100 L fermentation of culture, 10 L overnight pre-culture was used.

Medium composition:

	Per liter
Sodium glutamate	18 g
Yeast Extract	5 g
Sodium thioglycolate	1 g
Phosphate buffer 1M pH 7.4	20 ml
Trace element (SL10)	10 ml
Resazurin	4 mg

Trace element Composition (SL10):

	Per liter
Hydrochloric Acid (25%; 7.7M)	10 ml
$FeCl_2.4H_2O$	1.5 g
$ZnCl_2$	70 mg
$MnCl_2\ 4H_2O$	100 mg
H_3BO_3	6 mg
$CoCl_2\ 6H_2O$	190 mg
$CuCl_2\ 2H_2O$	2 mg
$NiCl_2\ 6H_2O$	24 mg
$Na_2MoO_4\ 2H_2O$	36 mg

The media (70ml) were prepared in 100 ml serum bottles, they were tightly closed with rubber stoppers and hypodermic needles were introduced for the pressure to be released. The medium was boiled, vacuumed and the air was replaced with nitrogen gas. The reddish blue colour (resazurin) of the anaerobised medium indicated the absence of oxygen. The media were autoclaved and stored at room temperature in a dark place.

2.6. *Clostridium pascui*

C. pascui Cm (DSM 10365) were from DSMZ. The growth conditions were similar to those of *C. tetanomorphum*.

Medium composition for *C. pascui*

	Per liter
Sodium glutamate	18 g
Yeast Extract	5 g
K_2HPO_4	300 mg
$MgSO_4 7H_2O$	100 mg
L-Cysteine hydrochloride	500 mg

pH to 6.5.

2.7. *Clostridium aminobutyricum*

Medium Composition:

	Per liter
KH_2PO_4	1.3 g
K_2HPO_4	7.1 g
$NaHCO_3$	2.0 g
Yeast extract	3.0 g
γ-Aminobutyric acid	10.0 g
$MgCl_2$ x 6 H_2O	0.2 g
$FeCl_3$ x 6 H_2O	0.01 g
$CaCl_2$ x 2 H_2O	0.01 g
$MnSO_4$ x H_2O	1.0 mg
Na_2MoO_4 x 2 H_2O	1.0 mg
Cysteine-Chloride	0.5 g
$Na_2S_2O_4$	0.35 g

Initially the medium was boiled and degassed by connecting it to a vacuum pump. After filling 50 ml medium in 120 ml anoxic serum bottles inside the anaerobic tent, these bottles where closed with rubber stopper and sealed with an aluminum cap. Before sterilizing the medium in the autoclave, the gas phase was changed to N_2 with a pressure of about 30 kPa. The media was inoculated with 10% preculture and incubated for 12 hours at 37° C. The grown cultures were kept at 4° C for storage and passed every four weeks.

2.8. *Clostridium symbiosum*

Medium composition:

	Per liter
Sodium glutamate	18 g
Yeast Extract	5 g
Sodium thioglycolate	1 g
Phosphate buffer 1M pH 7.4	10 ml
Trace element (SL10)	10 ml
D-Biotin (2mg/ml)	50 μl

The cultures were incubated in 50 ml medium in 120 ml serum bottles. The procedure to obtain anaerobic conditions was same as *Clostridium aminobutyricum.* After inoculating the sterilized medium with 1 % pre culture it was incubated at 37° C over night. The grown culture was stored at 4° C.

2.9. Preparation of membranes extracts

The 20 g wet packed cells were suspended in 50 mM Kpp buffer pH 7.4 and the cells were broken by three passages through French press cell at 110 MPa. All the procedures were performed in an anaerobic chamber (Coy, Ann Arbor, Michigan, USA) under a gas phase of 95% N_2 and 5% H_2. Cell debris was removed by centrifugation at 10, 000 × *g* for 20 min at 4°C. Then the crude extract was centrifuged at 120,000 × *g* for 1 h. The membrane extract were collected and washed twice with 50 mM Kpp (pH 7.4) by centrifuging at 120,000 × *g* for 30 minutes. The washed membrane extract were solubilised with 40 mM doecyl maltoside (DM) and homogenized well to solubilise it further. Then solubilised membrane was centrifuged at 120,000 × *g* for 30 minutes. The solubilised membrane extract in the supernatant was collected.

2.10. Purification of Rnf complex from *C. tetanomorphum*

All purification procedure was carried out under strict anaerobic condition inside a glove box under a gas phase of 95% N_2 and 5% H_2. The membrane extracts were prepared as mentioned earlier. The solubilised membrane was loaded onto Q-Sepharose fast-flow column (3 × 10 cm) equilibrated with buffer A (50 mM potassium phosphate

buffer pH 7.4). The column was washed with 70 mL buffer A and the proteins were eluted at a rate of 3 ml per min with a linear gradient of 0 – 2.0 M NaCl in buffer A. The fractions showing Rnf activity were concentrated on an Amicon PM 30 cell and desalted against buffer A and loaded on a DEAE-Sepharose column (3 × 10 cm) equilibrated with buffer A (50 mM Kpp pH 7.0, 2.0 M NaCl). After washing the column with 70 mL buffer A, the active Rnf complex was eluted around 0.55 M NaCl with linear gradient of 0 – 2.0 M NaCl in buffer B at a rate of 3 ml min^{-1}. Active fractions were concentrated loaded on a Red Reactive column (30 ml bed volume) equilibrated with buffer A. After a washing step with 30 ml buffer A, the Rnf complex was eluted with a linear gradient of 0 – 2.0 M NaCl in buffer A at a rate of 0.5 ml min^{-1}. The concentrated sample was loaded onto Superdex 200 (size exclusion column). Purified Rnf complex was finally concentrated with an Amicon Ultra-4 PLTK Ultracel-Pl (30 kDa cut-off).

Columns	Buffers
DEAE-Sepharose (XK 26/120) from Amersham Pharmacia	A: 50 mM Kpp, pH 7.5 B: 50 mM Kpp with 1 M NaCl, pH 7.5
Q-Sepharose from Amersham Pharmacia	A: 50 mM Kpp, pH 7.5 B: 50 mM Kpp with 1 M NaCl , pH 7.5
Red reactive from Sigma	A: 50 mM Kpp, pH 7.5 B: 50 mM Kpp with 1 M NaCl, pH 7.5
Superdex 200	A: 50 mM Kpp, pH 7.5 B: 50 mM Kpp with 150 mM NaCl, pH 7.5

2.11. Ferredoxin purification from *C. tetanomorphum*

Wet packed cells (25 g) were suspended in 50 ml of 50 mM Kpp pH 7.4 (buffer A). Cells were disrupted by sonication at 4°C in intervals of 3 × 5 min using an energy output of 200 W under gas phase (5% H_2/95% N_2). The lysed cells were centrifuged at 100,000 × g and 4°C for 1 h. The supernatant containing ferredoxin was collected and was applied on to DEAE-Sepharose column (XK26/50, 100 ml, Pharmacia) pre-equilibrated with 50 mM Kpp pH 7.4. Ferredoxin was eluted with a linear gradient from 0 to 2 M NaCl in 50 mM Kpp pH 7.4 at NaCl concentration approximately 0.52 to 0.62

M. Fractions containing ferredoxin were pooled and concentrated on 5000 Da Millipore Membrane. The concentrated fractions were applied on a gelfilteration column Superdex-75 (HiLoad 16/60 Superdex). The ferredoxin was eluted with 50 mM Kpp pH 7.4 and 150 mM NaCl. The isolated ferredoxin showed absorption maxima at 280 and 390 nm and the ratio of A_{390}/A_{280} ranged from 0.8 to 0.85, which is typical of a pure ferredoxin and further supports the purity of the preparation [29]. A ε_{390} value of 12.8 $mM^{-1}cm^{-1}$ was used for the determination of ferredoxin concentration.

2.12. Partial purification of hydrogenase from *Clostridium pasteurianum*

Wet packed cells (10 g) were dissolved in 30 ml 50 mM Kpp pH 7.4. Cells were lysed by French press 110 MPa for 3 times. Lysed cells were centrifuged at $10,000 \times g$ for 20 minutes. The collected supernatant (crude extract) was boiled at 55 to 60°C for 10 min under H_2 atmosphere. The boiled sample was kept on ice for 10 min. Then the sample was centrifuged for $20,000 \times g$ for 20 minutes to remove precipitated protein which forms as pellet. The supernatant containing hydrogenase was used for further experiments.

2.13. Purification Bcd-Etf complex from *C. pascui*

Wet packed cells (20 g) of *C. pascui* were suspended in mM Kpp pH 7.4 and lysed by three passages through French press cell at 110 Mpa. The cell free extract was prepared after centrifugation of the lysed cells for 1 hour at $100,000 \times g$. The supernatant was applied on DEAE-Sepharose column (3 x 10 cm) equilibrated with buffer A (50 mM Kpp pH 7.0, 2.0 M NaCl). After washing the column with 70 ml buffer A, the active Bcd/Etf was eluted around 0.4 M NaCl with a linear gradient of 0-2.0 M NaCl in buffer B at a rate of 3 mL min^{-1}, fractions showed good activity with ferrecenium assay were pooled and concentrated with an Amicon Ultra-4 PLTK Ultracel-Pl (30 kDa cut-off). An equal volume of 2.0 M $(NH_4)_2SO_4$ in buffer A was added to the pooled fractions from the first column, which were then loaded on a Source 15 PHE column (3 x 10 cm) equilibrated with buffer B (50 mM Kpp pH 7.0, 1.0 M $(NH_4)_2SO_4$). After washing the column with 70 mL buffer B, the active yellow dehydrogenase eluted with a linear gradient of 1.0 - 0 M $(NH_4)_2SO_4$ in buffer B at a rate of 3 ml min^{-1}. The Bcd-Etf

complex containing fractions were concentrated and loaded on Superdex 200 and purified. Approximately 0.8 mg of pure enzyme was obtained from 20 g cells.

2.14. Purification of BCD-Etf complex from *C. tetanomorphum*

The cells were opened by sonication. The cell free extract was prepared after centrifugation for 1 hour at 100,000 × *g*. The supernatant containing crude extract was subjected to ammonium sulphate precipitation (33% saturation). The precipitated Bcd-Etf complex was applied on DEAE-Sepharose column (3 x 10 cm) equilibrated with buffer A (50 mM Kpp pH 7.0, 2.0 M NaCl). After washing the column with 70 ml buffer A, the active Bcd/Etf was eluted around 0.4 M NaCl with a linear gradient of 0 – 2.0 M NaCl in buffer B at a rate of 3 ml/min. Fractions showing good activity with ferrecenium assay were pooled and concentrated with an Amicon Ultra-4 PLTK Ultracel-Pl (30 kDa cut off) and loaded on a hydroxyapatite column (3 × 10 cm) which was equilibrated with 5 mM Kpp buffer (pH 7.4) and Bcd-Etf complex was eluted with a linear gradient of 5 to 500 mM Kpp buffer pH 7.4. The Bcd-Etf complex containing fractions were loaded on a Superdex 200 column and purified. Approximately 1.9 mg of pure enzyme was obtained from 30 g cells.

2.15. Assays

2.15.1. Rnf with Ferricyanide

NADH dehydrogenase activity was measured anaerobically in 50 mM Kpp pH 7.4, 0.2 mM NADH and 0.1 mM ferricyanide in total volume of 1.0 mL at room temperature. After addition of enzyme, the decrease of ferricyanide (ε_{420} = 1.02 mM^{-1} cm^{-1}) absorbance was followed at 420 nm [30,31].

$$\text{NADH} + 2\,[\text{Fe(CN)}_6]^{\,3-} \xrightarrow[\text{420 nm}]{\text{Rnf}} \text{NAD}^+ + 2\,[\text{Fe(CN)}_6]^{\,4-} + \text{H}^+$$

ferricyanide   ferrocyanide
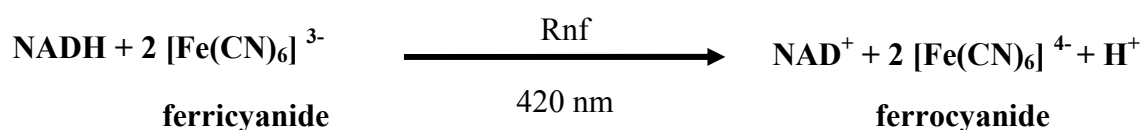
2.15.2. Rnf with ferredoxin and Ti(III)Citrate

The reaction mixtures contained 1mM Ti(III)citrate, 1mM NAD, 1.6 nM Ferredoxin, 100 mM potassium phosphate, pH 7.0. Water was added to make up the final volume 1ml. Then the reaction was started with addition of enzyme NADH-ferredoxin-oxidoreductase (Rnf). The reaction was followed at 340 nm by observing NADH (ε_{340} = 6.3 mM^{-1}cm^{-1}) formation. Ferredoxin was from *C. tetanomorphum*. Control experiments were carried out to make sure that Ti(III)citrate was unable to reduce NAD at pH < 7.4 in the absence of Rnf complex, ferredoxin. The assay, run at pH 7.0, was dependent on ferredoxin and Rnf complex.

$$\text{Ferredoxin} + 2\text{Ti(III)cit} + \text{NAD}^+ + 2\,\text{H}_2\text{O} \xrightarrow[\text{340 nm}]{\text{Rnf}} \text{NADH} + 3\text{H}^+ + \text{Fd}^{2-} + 2\text{TiO}^{2+} + 2\text{citrate}^{3-}$$
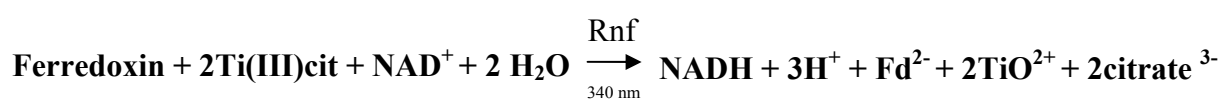
2.15.3. Hydrogenase to generate reduced ferredoxin

The assay (total volume 1 ml) contained 1 mM NAD$^+$, 30 µl hydrogenase- partially purified (82.3 mg/ ml), 3.2 µM Ferredoxin, 30 µl Rnf complex- membrane extract (30 mg/ ml), 100 mM Kpp buffer pH 7.4. The assay was carried out under H$_2$ atmosphere. The reaction was followed at 340 nm by observing NADH (ε_{340} = 6.3 mM^{-1} cm^{-1}) formation [30].

$$\text{H}_2 + \text{NAD}^+ \xrightarrow[\substack{\text{Rnf} \\ \text{340 nm}}]{\substack{\text{Ferredoxin} \\ \text{Hydrogenase}}} \text{NADH} + \text{H}^+$$
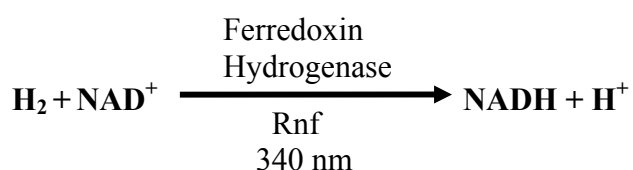
2.15.4. Butyryl-CoA dehydrogenase with ferricenium hexafluorophosphate (FcPF6)

Butyryl-CoA dehydrogenase activity was measured with ferricenium hexafluorophosphate (FcPF$_6$) as artificial electron acceptor. The reaction mixture

contained 100 mM potassium phosphate buffer pH 7.4, 0.2 mM $FcPF_6$ and 0.1 mM butyryl-CoA. The ferricenium hexafluorphosphate was previously prepared in a 10 mM HCl solution to a final concentration of 2 mM set at 617 nm (ε_{617} =0.41 $mM^{-1}cm^{-1}$) [32]. During the catalysis by butyryl- CoA dehydrogenase, ferricenium ions get reduced to ferrocene with a decrease in the absorbance at 300 nm [32](ε_{300} = 4.3mM $^{-1}$cm $^{-1}$).

2.15.5. Bcd/Etf with NADH and crotonyl-CoA

NADH catalyzed by butyryl-CoA dehydrogenase was carried out by observing NADH spectrophotometrically at 340 nm (ε_{340} = 6.3 mM^{-1} cm^{-1}). 1 ml assay mixture contained 50 mM Kpp buffer, 0.1 mM NADH, 0.1 mM crotonyl-CoA, 10 uM ferredoxin, 0.4 U hydrogenase from *C. pasteurianum*. The reaction was started with crotonyl-CoA. The control assays were carried out in the absence of ferredoxin and hydrogenase to confirm the coupled reduction of ferredoxin by BCD-ETF complex

2.15.6. Citramalate lyase

The assay was carried out under aerobic conditions. Lyase was coupled with reduction of pyruvate catalysed by lactate dehydrogenase.

Citramalate $\longrightarrow$ pyruvate + acetate

Pyruvate + NADH + H$^+$ $\longrightarrow$ lactate + NAD$^+$
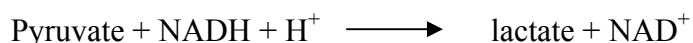
1 ml assay mixture contained Tris/HCl buffer pH 7.4, 50 mM, 50 mM DTT, 1 mM $MgCl_2$, 20 mM (*R,S*)-citramalate, 0.2 mM NADH and 10 µl of lactate dehydrogenase.

1. 100 mM Tris/HCl (pH 7.4)
2. 1 mM DTT
3. 1 mM $MgCl_2$
4. crude extract from *C. tetanomorphum*
5. Mixed and incubated for 30min at room temperature. It was followed by the addition of 800 µl water.

6. 0.01ml of acetic anhydride (a 1:100 solution prepared freshly with ice cold water or dioxane and kept it on ice while in use) mixed and kept for 1-5 min at room temperature.

7. 10 μl of lactate dehydrogenase

8. 0.2 mM NADH

Reaction was started by the addition of 0.01 ml of citramalate at 340 nm. The reaction was observed by monitoring NADH spectrophotometrically at 340 nm (ε_{340} = 6.3 mM^{-1} cm^{-1}).

2.15.7.   2-hydroxyglutarate   dehydrogenase   and   Glutamate dehydrogenase

The assay (total volume 1ml) mixture contained 100 mM Kpp buffer (pH 7.4), 0.2 mM NADH, 1mM α-ketoglutarate, 20 μl crude extract. The reaction was monitored by change in absorbance at 340 nm (ε_{340} = 6.3 mM^{-1} cm^{-1}). 1 mM NH$_4$Cl was added for the glutamate formation.

2.15.8. NADH oxidation assay

The assay (total volume 1ml) contained 100 mM Kpp, 1 mM MgCl$_2$, 1 mM DTT and crude extract. The assay mixture was incubated for 30 minutes at room temperature. The reaction was started with addition of NADH. The NADH oxidation was followed at 340 nm.

2.16. Preparation of inverted vesicles

All preparation steps were carried out under anaerobic conditions. The buffers used were vacuum degassed and anaerobised under gas phase of 95%N$_2$ and 5% H$_2$. About 8 g cells were suspended in 50 mM Kpp buffer (pH 7.4). Lysozyme (68 mg) was added to the suspension and incubated for 1 hr at 37°C. Protoplast was formed and checked by microscopic observation. The protoplasts were passed through a French press cell at 65 MPa, resulting in a vesicle preparation. The vesicles could have 90% inside-out orientation. To remove unbroken protoplasts and cell debris, the crude vesicle

preparation was centrifuged at 6000 × g for 20 min. The membranes were isolated by ultracentrifugation at 120,000 × g for 1 h, suspended in Kpp buffer. The suspension was washed twice with the same buffer by dissolving and centrifuging at 120,000 × g for 1 h at each time. The final preparation of inverted membrane vesicles was resuspended in Kpp buffer to a protein concentration of 1 – 5 mg/ ml.

2.17. Reconstitution Methods

The buffers were vacuumed degassed and anaerobised under N_2 gas. Entire reconstitution procedure and subsequent steps were carried out in an anaerobic chamber (with 95 % N_2 and 5% H_2 gas phase). Wet packed 20 g cells were suspended in 20 ml 50 mM potassium phosphate buffer, pH 7.4 (potassium phosphates used in all steps of reconstitution experiments were purchased from Fluka – 60220 and 60347 – which has only trace amount of Na^+ ions). Cells were broken by three passages through French press cell at 110 MPa. Unbroken cells and debris were removed by centrifugation at 10,000 × g for 10 min. Then the membrane extracts were prepared by centrifugation at 120,000 × g for 60 min and then washed twice with 50 mM Kpp buffer (pH 7.4) and centrifuged. The membrane extract was solubilised with 40 mM dodecylmaltoside (DM) by using the same buffer for 30 min at room temperature. Membrane extract was centrifuged at 120,000 × g for 30 min. The supernatant containing soluble membrane extract were applied over Q-Sepharose HiLoad 26/10 column which is pre-equilibrated and washed with the 50 mM Kpp buffer (pH 7.4) containing DM. The Rnf complex was eluted with an NaCl gradient, linearly increasing from 0 to 2 M NaCl in 50 mM Kpp buffer (pH 7.4). The Rnf complex was concentrated further by Amicon ultra filteration using 30 kDa cut-off membranes. This one column purified Rnf complex was used for reconstitution studies.

2.18. Preparation of liposomes

L-α-phosphatidylcholin (Sigma- P5638) was dissolved in 1 ml of 2:1 (v/v) chloroform/methanol. The solvent was evaporated by roto-evaporation and dried further under vacuum. The Rnf complex (one column purified) was added onto the dried lipids drop wise and further diluted (30 drops min^{-1}) to 5-15 ml of 50 mM Kpp, pH 7.4. The drop wise dilution was carried out until the concentration of dodecylmaltoside was lower than critical miscellar concentration (CMC) of 0.01%. The ratio of protein (Rnf):

lipid was 1:4. The liposomes were sedimented by overnight ultracentrifugation at 120,000 × g. The pellet was resuspended in 2 ml of 50 mM Kpp, pH 7.4. The residual Na^+ concentration of the proteoliposomes was 3 mM when it was measured by atomic absorption spectroscopy.

2.19. Na^+ translocation assay

The Na^+ translocation studies were carried out by using the reconstituted proteoliposomes. The protein concentration obtained of reconstituted proteoliposomes varied from 2 to 3 mg/ml at different preparations. The assay mixture contained 1 mM NAD^+, 5 mM NaCl, 8 μM ferredoxin, hydrogenase (0.04 mg/ml), 0.24 – 0.6 mg lipids (proteoliposomes) and final volume of the assay was made up to 300 μl by addition of 50 mM Kpp, pH 7.4. The reaction was started by addition of 1 mM NAD^+. At different time intervals, 70 μl reaction mixture were applied to a 1 ml plastic syringe containing 0.6 ml Dowex 50 (K^+), pre-equilibrated with 50 mM Kpp buffer, pH 7.4 and the outlet of the syringe was sealed with a HDPE membrane (high-pressure polyethylene, 0.35 μm pore diameter, Reichelt Chemietechnik, Heidelberg). The proteoliposomes were immediately eluted with 0.8 ml deionized water that was quickly pressed through the Dowex material using the piston of the syringe (total handling time < 10 s). Eluted proteoliposomes containing Na^+ were collected and analyzed by atomic absorption spectroscopy with a Shimadzu AA-646 spectrometer. 1 U corresponds to 1 μmol Na^+ transported per minute.

2.20. Determination of protein concentration

Protein concentrations were determined with the Bio-Rad Protein Micro assay (Bio-Rad Laboratories, München, Germany), a dye-binding assay based on the differential colour change of a dye in response to various concentrations of protein [33]. The principle of this method is based on the observation that the absorbance maximum for an acidic solution of Coomassie Brillant Blue G-250 shifts from 465 nm to 595 nm when binding to protein occurs.

Each time the assay was performed, a standard curve was prepared using bovine serum albumin as protein standard (0-10 mg/ ml). The absorbance at 595 nm was corrected for the blank. 0.8 ml of appropriately diluted samples or bovine serum albumin were mixed

with 0.2 ml dye protein reagent and the absorbance of the solution at 595 nm was measured at room temperature with a spectrophotometer (Ultrospec 1100 *pro*, Amersham Biosciences, Freiburg, Germany) after 30 minutes.

2.21. SDS-PAGE

The purity of the enzyme preparations was checked by polyacrylamide gel electrophoresis under denaturing conditions. For the preparation of two 14 × 16 mm gels with 15 % polymerisation grade, the running gel was cast followed by stacking gel. Before electrophoresis the protein samples were diluted 1:2 with protein loading buffer (63 mM Tris/HCl pH 6.8, 10% (w/v) SDS, 10% (w/v) glycerine, 16 mM DTT, 0.01% (w/v) bromophenol blue) and denatured at 95°C for 5 min. Subsequently, 3-20 μl (5-15 μg protein) of the samples were loaded to the gel. The electrophoresis was started at 70 V until the bromophenol blue marker reached the top of the separating gel then performed at 150 V until the tracking dye reached the bottom of the separating gel, Protein was stained with Coomassie Brillant Blue R-250 (Serva, Heidelberg, Germany) and destained with a mixture of 30 % Methanol/ 10 % acetic acid.

	Separating gel	Stacking Gel
Buffer A [(1)]	2.5 ml	-
Buffer B [(2)]	-	2.5 ml
Acrylamide 30 % [(3)]	5.0 ml	1.1 ml
Water	2.5 ml	6.5 ml
TEMED	42 μl	20 μl
APS [(4)]	60 μl	50 μl

[(1)] Buffer A   1.5 M Tris-HCL (pH 8.8) / 0.4 % SDS
[(2)] Buffer B   0.5 M Tris-HCl (pH 6.8) / 0.4 % SDS
[(3)] Acrylamide 30 %   (37.5:1) Acrylamide : bisacrylamide, Rotiphorese Gel 30
[(4)] APS   10 % (w/v) Ammonium persulfate (fresh)

2.22. Amino acid sequence analysis

The subunits of the Rnf complex were seperated by SDS-PAGE. The protein samples were transferred from an unstained SDS-PAGE gel to methanol-soaked polyvinylidene fluoride membrane (PVDF Westran S^{TM}-Membrane, Schleicher & Schuell GmbH Dassel, Germany). The system was stacked with six layers of gel blotting filter paper which was previously equilibrated with transfer buffer. By using Bio-Rad transfer-blot cell (16 x 20) cm, filled with transfer buffer (25 mM Tris-glycine, 20 % methanol). The electro transfer was performed applying a constant current of 300 mA for 1 h at 4°C. The gel was shortly stained with Coomassie blue R-250 stain and immediately destained in 80% methanol/ 10 % acetic acid, six bands corresponding to the size of RnfC, D, G, A, E and B were excised from the membrane for N-terminal sequence by Edman degradation which was done by Dr. Linder at the Biochemisches Institut des Fachbereichs Humanmedizin, Justus-Liebig-Universität in Gießen, Germany .

2.23. Spectral analysis

The UV-Visible absorption spectra of Rnf complex, ferredoxin were recorded by using diode array spectrophotometer HP 8453 UV-Visible diode array spectrophotometer (USA). Fluorescence spectrum of covalently bound flavins was measured on a Cary Eclipse fluorescence photometer.

Covalently bound flavin analysis

2. 24. Method 1

The Rnf complex was diluted 1:2 with loading buffer containing DTT and denatured by boiling at 95°C for 5 min. Subsequently samples were loaded on a SDS-PAGE gel and separated. The unstained SDS-PAGE gel was subjected to UV illumination to find out the bands which had covalently bound flavin which could be illuminated under UV light.

2.25. Method 2

The Rnf complex was treated with 10 % TCA to precipitate the covalently bound flavins. The nature of the covalently bound flavins were achieved by treating the enzyme with 0.5 % SDS and incubated with phospohodiesterase I from *Crotalus atrox* (0.2 mg/ ml, pH 7.4) at 37°C for 3 h. The change in fluorescence intensity was monitored with a Cary Eclipse fluorescence photometer. The fluorescence was measured at excitation maximum at 350 and 445 nm and the emission maximum at 525 nm.

2.26. Flavin quantification by HPLC

The flavin content of Rnf complex was characterized with HPLC. The enzyme solution was denatured with 3 % TCA and centrifuged to remove the denatured protein. The yellow supernatant was analysed using a hydrophobic reverse phase column, RP-18 column (5 μm). The sample was eluted with 25 % methanol in 50 mM ammonium formate. Riboflavin, FMN and FAD (10 μM) were used as standards, which were treated in the same way as the enzyme solution. A flow rate of 1 ml/min was used and the absorbance at 266 nm was used for detection of flavin.

2.27. Non-heme iron determination

The iron complex in the protein was liberated by treatment with hydrochloric acid. Excess acid was neutralized with ammonium acetate; Fe^{3+} is converted to Fe^{2+} by reduction with ascorbic acid. Precipitated protein formed complex with sodium dodecylsulfate. Finally the iron chelator was added to form a blue Fe^{2+}- chelator complex (35).

Reagents:

1 % (m/v) HCl

7.5 % (m/v) Ammoniumacetate

2.5 % (m/v) Sodium dodecylsulfate (SDS)

4 % (m/v) Ascorbic acid, (freshly prepared)

1.5 % (m/v) Iron chelator, (3-(2-pyridyl)-5, 6-bis (5-sulfo-2-furyl)-1, 2, 4-triazine, disodium salt

0.2 mM $(NH_4)_2Fe(SO_4)_2 \times 6H_2O$ (freshly prepared)

Three samples of the Rnf complex and ferredoxin, two blanks and six samples of iron standard (2, 4, 8, 12, 16 and 20 μM final concentrations) were diluted to 100 μl with water in Eppendorf tubes, subsequently, 100 μl 1 % HCl was added. The samples were mixed by gentle shaking, incubated at 80 °C for 10 minutes and cooled down to room temperature. 500 μl ammonium acetate, 100 μl 4 % ascorbic acid, 100 μl sodium dodecylsulfate and 100 μl iron chelator were added sequentially with vortex and short centrifugation. The reaction mixtures were centrifuged at 9000 × g for 10 minutes and the absorbance at 593 nm was measured against water. A standard curve was plotted using iron standards and iron content of the Rnf complex and ferredoxin was determined.

2.28. CoA thioester synthesis

Acetyl-CoA, Butyryl-CoA and Crotonyl-CoA thioesters were synthesized from their corresponding anhydrides [34]. A 1.2-fold excess of anhydride over CoASH was applied. The anhydride was dissolved in 1 ml acetonitrile and dissolved into a solution of 80 mg coenzyme A tri-lithium salt (ICN Biochemicals, Eschwege Germany) in 10 ml of a 100 mM $KHCO_3$ solution. The mixture was incubated for 15 minutes at room temperature and then acidified to pH 2.0 with 1 M HCl. Freshly synthesized acyl-CoA esters, as well as all the enzymatic reaction mixtures involving CoA derivates as a substrate, were purified by reversed phase method using solid phase extraction C18 Sep-Pak cartridges (Waters, Massachusetts USA). The columns (20 ml/2g material) were equilibrated with methanol prior use. The columns used for the isolation of 100 μmol synthesized CoA ester were washed with 10 ml TFA 0.1 % (v/v) before and after probe loading. As final step 5 ml 50 % (v/v) acetonitrile in TFA 0.1 % (v/v) was added for CoA-esters elution. Solvent free probes were obtained after evaporation. The CoA esters were dissolved in water (pH 3.0) and stored at –20°C. The probes analysed by MALDI-TOF were dropped directly on a gold grid platform and mixed 1:1 with the matrix alpha-Cyano-4-hydroxycinnamic acid at final volume of 1 μl.

Molecular Biological methods

2.29. Genomic DNA isolation

Wet packed cells (50 mg) of *C. tetanomorphum* were suspended in 567 µl Tris EDTA buffer (10 mM Tris/ HCl, pH 7.5, 1 mM EDTA, pH 8.0). Then, 30 µl of proteinase K (20 mg/ml) was added to give a final concentration of 100 µg of proteinase K in 0.5 % SDS and incubated for 1 h at 37°C. 100 µl NaCl (5M) was added and mixed thoroughly which was by followed with addition of 80 µl of CTAB/Nacl solution [10% CTAB (hexadecyltrimethyl ammonium bromide) in 0.7 M NaCl] and mixed thoroughly and incubated for 10 minutes at 65°C. Then the solution was treated with 700 µl chloroform/isoamyl alcohol and after centrifugation equal volume of phenol/chloroform/isoamyl alcohol was added and centrifuged again. The nucleic acids were precipitated by 0.6 volume of isoproponal to get stingy white DNA precipitate. The precipitated DNA was washed with ethanol and dried. The DNA was re-dissolved with TE buffer and stored at -20°C. The protocol was adapted from Current protocols in Molecular Biology [35].

2.30. Determination of DNA concentration

The DNA concentration and purity were determined by measuring the absorption at 260 nm and then at 280 nm. $OD_{260} = 1$ corresponds to 50 µg/ml of dsDNA. The ratio of A260/280 is an indication of nucleic acid purity. A value more than 1.8 shows > 90% nucleic acid.

2.31. DNA Agarose Gel Electrophoresis preparation

The appropriate amount of agarose, depending on the percentage of the gel, was dissolved in 1 × TAE buffer. After boiling in microwave for few minutes, the melted agarose was cast on a tray with sample comb placed inside. Then the gel was placed in the electrophoresis chamber. DNA was mixed with loading buffer (0.21% Bromophenol Blue, 0.21% Xylene Canol FF, 0.2 M EDTA, pH 8.0, and 50% glycerol) were then loaded into the gel wells, and electrophoresis was started at 80-120 V. Bromophenol blue and xylene cyanol dyes migrate through agarose gels along with double stranded DNA fragments of 300 and 4000 bp. After completion of electrophoresis, the gel stained with ethidium bromide and examined on UV transillumnator and documented.

2.32. DNA Extraction from Gel

DNA bands were examined on UV-illuminator by using short wavelength for a short time and excised from the agarose gel. Extraction was done by following the manual provided with kit (from Omni Life Sciences, Germany).

2.33. Restriction and Ligation

Restriction reactions were usually performed following the manual provided with enzyme by suppliers. DNA ligations were done by using T4-DNA ligase (Amersham Biosciences) and ligation reaction was carried as per the manual.

2.34. Preparation of competent *E. coli* cells for electrotransformation

For the preparation of electro competent cells, a flask containing 500 ml LB medium was inoculated at an OD_{578} of 0.1 with an overnight *E. coli* DH5α culture and incubated at 37°C with agitation. The cells were harvested by a pre-cooled (4 °C) high-speed centrifuge at $6000 \times g$ for 20 minutes. The harvested cells were washed twice with 500 ml ice-cold sterile H_2O and one time with 20 ml 10 % glycerol. The washed cells were resuspended with 1 ml 10 % glycerol and 40 μl aliquots in a small 500 μl Eppendorf tubes were stored at −80°C.

2.35. Electrotransformation

The dialysed ligation mixture was added to 40 μl competent cells and transferred to an Electroporation Cuvette (Molecular BioProducts, cat#5510). A pulse was given to the cuvette using the following settings: 25 μF, 1.8 kV and 200 Ohm. The cuvette was washed with 500 μl Standard I medium and transferred to a sterile 1.5 ml Eppendorf tube. The transformation mixture was incubated for 1 h at 37°C before plating on a LB agar plate containing antibiotic(s). The agar plate was incubated overnight at 37°C to screen the positive clone.

2.36. PCR reactions

PCR reactions were performed using a *Taq* polymerase (Fermentas), Phusion polymerase (Finzymes) and FideliTaq polymersase (USB). The PCR reaction mixtures were made with following concentration of the ingredients.

2.37. Concentration of ingredients: Final concentration

dNTP 200 μM

Forward primer 500 nM

Reverse primer 500 nM

Template DNA 2 to 50 ng/ μl

Polymerase 1 U

2.38. Cycle Conditions

2.38.1. For Taq polymerase

Cycling program

1. 95 °C 3 min

2. 95 °C 90 sec

3. 55 °C 90 sec (gradient with 10 different temperatures)

4. 72 °C 3 min (depending on the length of target gene expected)

5. 72°C 8 min

29 × cycles - step 2 to 4.

2.38.2. For Phusion polymerase

Cycling program

1. 98 °C 30 sec

2. 98 °C 10 sec

3. 55 °C 90 sec (gradient with 10 different temperatures)

4. 72 °C 15 sec (depending on the length of target gene expected)

5. 72 °C 5 min

29 × cycles - step 2 to 4.

2.38.3. For FideliTaq polymersase

Cycling program

1. 94 °C 90 sec

2. 94 °C 30 sec

3. 55 °C 30 sec (gradient with 10 different temperatures)

4. 68 °C 1 min 30 sec (depending on the length of target gene)

5. 68 °C 5 min

29 × cycles – step 2 to 4.

2.39. List of primers

EJ01_for `TTYAARAAYGGWGTWCAYCCWCCWCAYGG` (degenerate)

EJ03_rev `TCYTTDATDATWCCRTTRTAWARTCTTTC` (degenerate)

rnfG_iPCR_as1 `GCAGCTATTAACAGTAGAACCATTCC`

rnfG_iPCR_s1 `AGCAGCATCAGGAGAAGATG`

ela E3: `GTGTAGGAGCATCCTTCTTTGACG`

Ela_RnfB2: `ACADSTWCCWARWCCYAWACATCC`

Internal primer for sequencing:

For: `TGAAATATATTATGCAGTTGTAAATGGTA`

Rev: `TAAAATACCGATGACTAATACGATGTAGT`

2.40. Sequencing of Rnf ORF from *C. tetanomorphum*

The first fragment of the *Rnf* operon was PCR amplified from the chromosomal DNA of the *C. tetanomorphum* using degenrated primers forward-EJ01_for and reverse EJ03_rev based on sequence homology between conserved regions, located in the N-terminal sequence of different *Rnf* operons of *C. tetani*. Amplification products with the expected size of about 2800 bp were ligated into TOPO TA cloning (Invitrogen) and transformed to *E. coli* TOP 10. From ten random clones, plasmid DNA was isolated and analyzed by restriction using *Eco*RI. Subsequently five of the ten clones were sequenced (MWG, Germany), revealing identical nucleotide sequences and confirming *Rnf* gene identity.

Fig. 6: Rnf- Open Reading Frame from *C. tetanomorphum*

Fig. 7: First step- by using degenerated primer

The 2800 bp amplified fragment was used to design the primers rnfG_iPCR_as1 and rnfG_iPCR_s1. Chromosomal DNA from *C. tetanomorphum* was digested with EcoRI and EcoRI1355) and ligated, yielding circular DNA molecules. PCR with diverging primers rnfG_iPCR_as1 and rnfG_iPCR_s1 with the circular ligation products as template yielded amplicons of 891bp (upstream-sequence) and 882 bp (downstream-sequence), respectively. After cloning of both fragments into TOPO- TA (Invitrogen) their nucleotide sequences were determined (MWG, Germany).
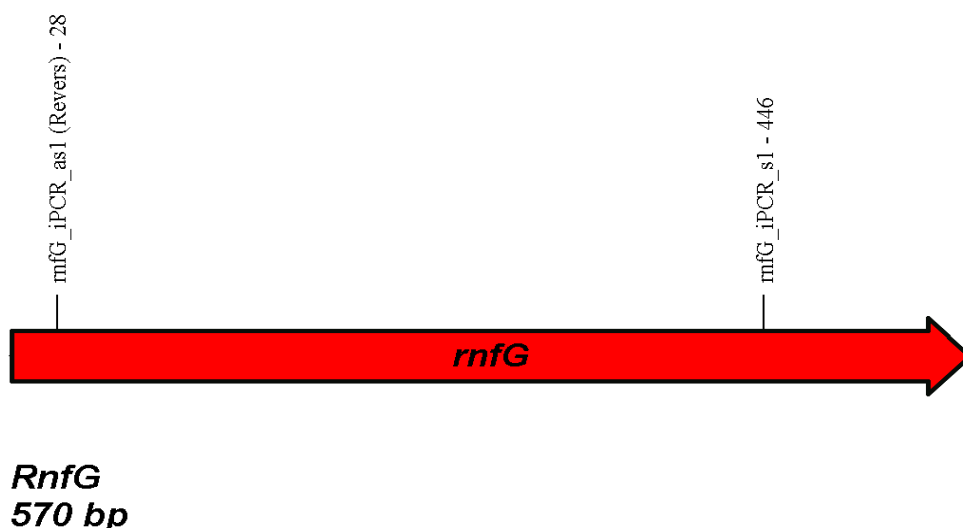
Fig. 8: Second step- inversed PCR

By using the known sequence of 891 bp obtained from forward primer- ela E3 was synthesised and degenerate primers were designed for reverse primer Ela_RnfB2 based on sequence homology between conserved regions located in RnfB which was assumed

as last subunit in the Rnf operon. Amplification product size of 2000 bp was ligated into TOPO TA cloning and followed by sequencing. (MWG, Germany)
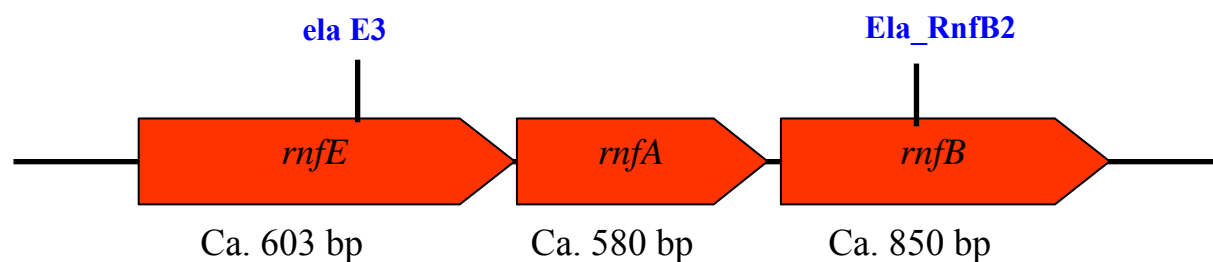
Fig. 9: Third step- by using known sequence and degenerated primer from conserved region.

Methods for deuterium incorporation and NMR studies

2.41. Preparation of labeled glutamate

Sodium metal (1.15g) was dissolved into 10 ml D_2O solution containing 0.9 g of glutamate. The solution was heated at $120^\circ C$ for 5 days. Sample was drawn time to time and analyses under NMR to check incorporation of deuterium in glutamate.

(*S*)-[2-$^2H_1$,4-$^2H_2$]Glutamate:
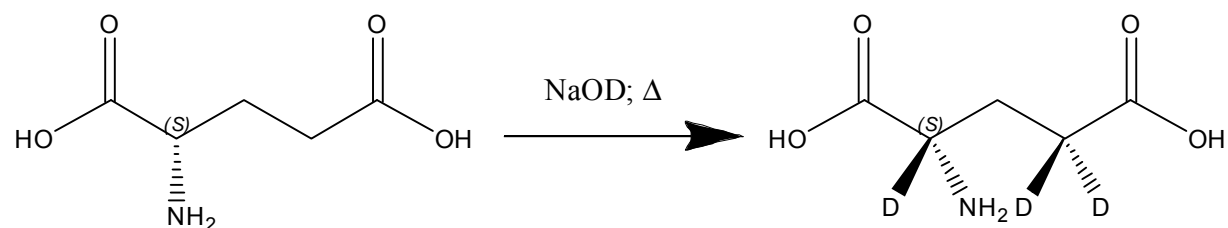
^1H NMR (H_2O) δ 2.58 (0.03H, m, CD(*H*)NH$_2$) δ 1.52 (0.07H, m, CD(*H*)$_2$COO) δ 1.13 (2H, dd, $J_1 = 36.5$, $J_2 = 13.4$, C*H*$_2$)
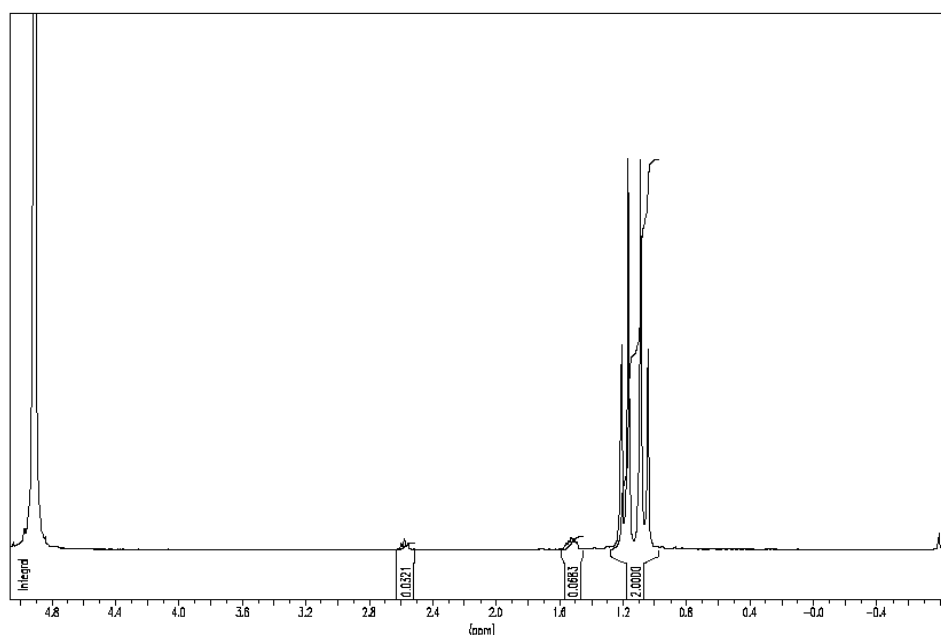
Fig. 10: D-Incorporation levels at C2 (98.5 %) and C4 (96.5 %)

^{13}C NMR (CDCl$_3$) δ 176.66 (*C*OO) δ 67.16 (t, *J* = 23.12, *C*DHO) δ 26.77 (*C*H$_2$COO) δ 21.05 (*C*H$_2$)

2.42. Preparation of medium (with labeled glutamate) and bacterial growth

The solution containing labeled glutamate was neutralised with 1M HCl solution. To avoid high salt concentration in the growth medium the neutralized solution was diluted by water to a ratio of 1:1. The 20 ml solution was added into growth medium of *C. pascui*, *C. tetanomorphum, F. nucleatum* and *C. symbiosum* which can metabolise the glutamate with final concentration of 50 mM. The medium was inoculated with bacteria and incubated for 2 to 4 days as the growth rate was slower due deuterium incorporated glutamate.

2.43. Separation of products from the medium

The bacterial culture was centrifuged at 10,000 × *g* 20 min to get the cell free supernatant. The supernatant containing fermented products were acidified to pH 1.0 (below the pKa of butyric acid) and further steam distilled. The distillate was collected and made into alkaline (pH 9.0 and above) and dried.

2.44. Preparation of NMR samples

For Deuterium only NMR

Dried powder containing metabolic product was collected. 0.8 ml was transferred to the NMR tube for D-NMR.

For H-NMR

Water in the sample was dried by applying vacuum. Deuterated water was added and evaporated to remove the remains of water. This step was repeated to make sure the absence of water. Thereafter, 0.8ml of deuterium oxide was added to dissolve the butyrate. This was transferred to NMR tube for H-NMR.

3. Results

It was suggested that in *A. fermentans,* the reverse electron transport from NADH to hydrogen was carried out by a membrane-bound NADH dehydrogenase [7]. The NADH dehydrogenase activity was measured photometrically by following the reductio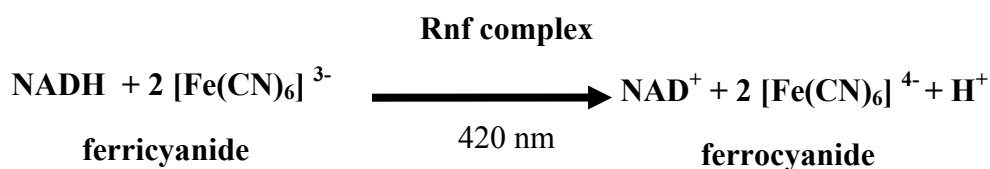n of iodonitrosotetrazolium (INT) at 492 nm (ε_{492} = 19.6 mM^{-1}cm^{-}1) [36]. From the genome of *C. tetani*, Brüggemann et al. suggested that the Rnf complex could be involved in electron transfer from ferredoxin to butyrate synthesis of *C. tetani.* This conclusion was based on a finding of highly active NADH dehydrogenase activity in washed membranes of the closely related *C. tetanomorphum* reported by W. buckel [9]. The NADH dehydrogenase activity was measured by following the reduction of artificial electron acceptor hexacyanoferrate(III) (ferricyanide). In our lab this assay was carried out with membrane extracts of *A. fermentans*, *C. tetanomorphum*, *C. symbiosum* and *F. nucleatum*. Here I describe the ferricyanide assay, and the development of two ferredoxin dependent assays. Reduced ferredoxin was either generated non-enzymatically by Ti(III)citrate or by hydrogen catalysed by hydrogenase from *C. pasterianum.*

3.1. Ferricyanide assay

The ferricyanide assay was generally used during purification of NADH dehydrogenase. The activity was measured anaerobically in 50 mM Kpp pH 7.4, 0.2 mM NADH and 0.1 mM ferricyanide in total volume of 1.0 ml at room temperature. After addition of enzyme, the decrease of ferricyanide absorbance (ε = 1.02 mM^{-1} cm^{-1}) was followed at 420 nm.

$$\text{NADH} + 2\,[\text{Fe(CN)}_6]^{\,3-} \xrightarrow[\text{420 nm}]{\text{Rnf complex}} \text{NAD}^+ + 2\,[\text{Fe(CN)}_6]^{\,4-} + \text{H}^+$$

$$\text{ferricyanide} \qquad\qquad\qquad\qquad \text{ferrocyanide}$$

3.2. Assay with Ti(III)citrate and NAD$^+$

In order to keep ferredoxin in the reduced state, Ti(III)citrate was added to the reaction mixture. Before that, it was imperative to check NAD+ reduction by Ti(III)citrate in the

absence of the Rnf complex and ferredoxin. The assay (total volume 1ml) contained 100 mM Kpp, 1 mM Ti(III)citrate and 1 mM NAD$^+$. The NAD$^+$ reduction was followed at 340 nm. The pH of the assay was varied from pH 5.8 to pH 8.8. NAD$^+$ was reduced by Ti(III)citrate when assayed at pH 7.2 and above. The possible reaction that leads to NAD$^+$ reduction by Ti(III)citrate at the pH 7.2 and above is shown (equation 2).

$$2\ Ti3+ \ + \ 2\ H2O \ + \ NAD+ \ \longrightarrow \ 2\ TiO2+ \ + \ NADH \ + \ 3\ H+$$
$$(equation\ 2)$$
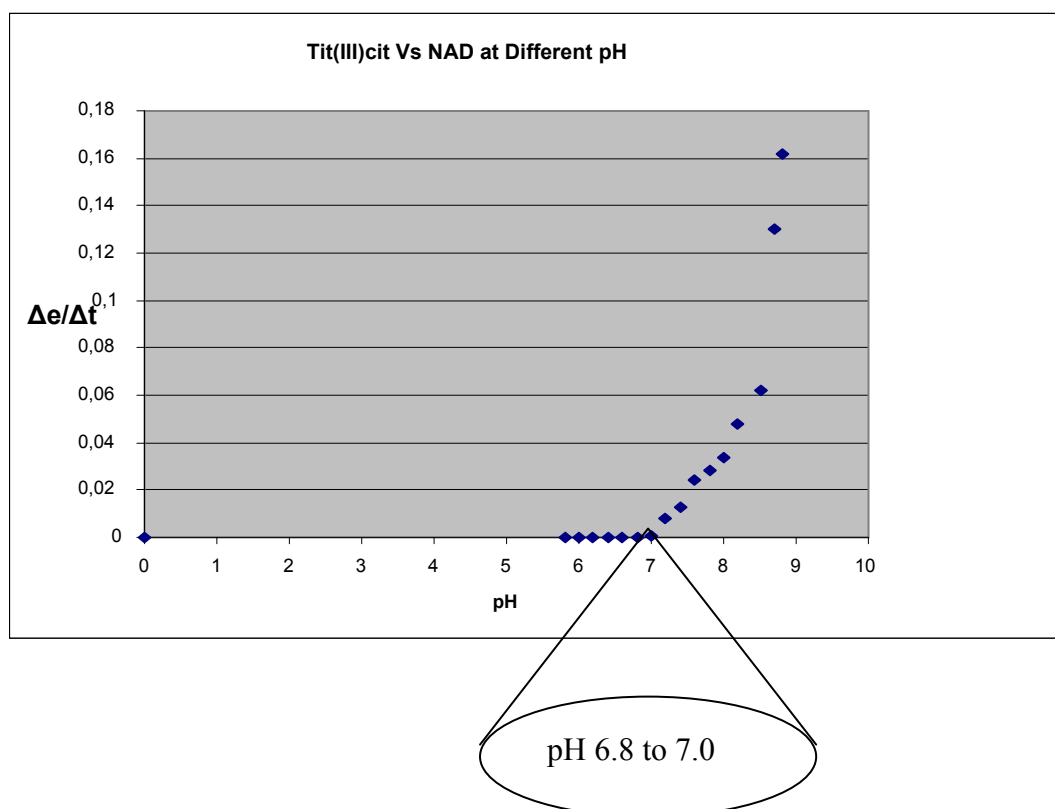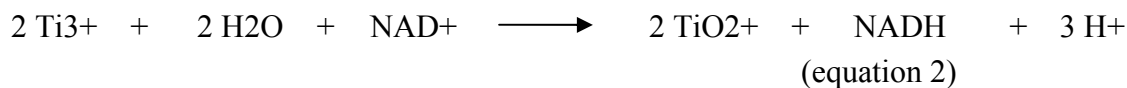
Fig. 11: Reduction of NAD$^+$ by Ti(III)citrate at different pH, control assay - NAD$^+$ reduction by Ti(III)citrate at the pH 7.2 and above. NAD$^+$ was not reduced by Ti(III)citrate at pH 7.0 and below.

3.3. Rnf activity - ferredoxin dependent assay

The activity of Rnf has been measured by the ferredoxin dependent assay, where the increase in absorbance of NADH was observed at 340 nm (ε = 6.3 mM^{-1}cm^{-1}). The

reaction was started by adding the enzyme. Ti(III)citrate was used to generate reduced ferredoxin. The assay was carried at pH of 7.0.

$$2H_2O + 2Ti^{3+} + Fd \quad \rightarrow \quad 2TiO^{2+} + Fd^{2-} + 4H^+ \quad - \quad \text{spontaneous reaction}$$

$$NAD^+ + Fd^{2-} + H^+ \rightarrow NADH + Fd \qquad - \quad \text{Rnf mediated reaction}$$
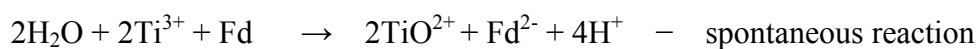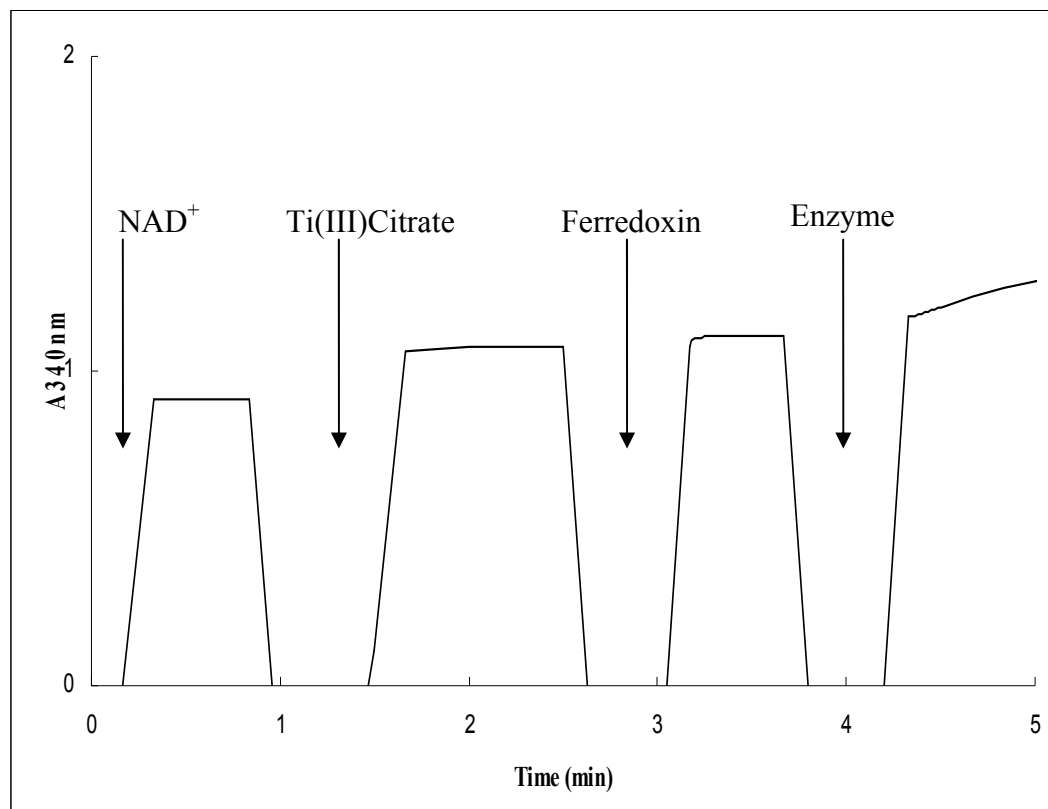
Fig. 12: Rnf Activity - The assay was started by adding the enzyme. The increase in absorbance due to Rnf was observed at 340 nm.

3.4. Rnf assay with ferredoxin and hydrogenase

The activity of Rnf in crude membranes has been measured by ferredoxin dependent assay where the increase in absorbance of NADH was observed at 340 nm. The reaction was started by adding the enzyme. Hydrogenase was used to generate reduced ferredoxin under H_2 atomosphere.
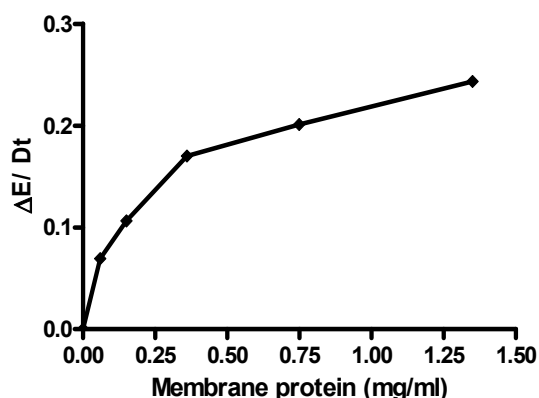
Fig. 13: Rnf activity with reduced ferredoxin generated by hydrogenase. The reaction is formation of NADH from NAD$^+$ by the Rnf system.

3.5. Rnf activity

Table 2: Specific activities of the Rnf complex with different assay systems.

Ferricyanide	Ferredoxin/Ti(III)citrate	Ferredoxin/Hydrogenase
26 (U/mg)	1.5 (U/mg)	0.18 (U/mg)

All assays were carried out with membrane extracts. The ferricyanide assay showed highest activity as 26 U/ mg, followed by ferredoxin assay which showed 1.5 U/ mg and hydrogenase activity showed 0.18 U/ mg. The hydrogenase assay showed very less activity, the probable reason could be the depleting hydrogen atmosphere in the cuvette and rate limiting hydrogenase.

2.5. Rnf activity of different organisms

The Rnf complex, which plays a major role in methylaspartate as well as hydroxyglutarate pathways in many Clostridiaceae, was checked by using the ferricyanide assay. The membrane extracts were prepared and tested for the Rnf acitivity at anaerobic conditions.

Table 3: Rnf activity from membrane extracts of different bacteria. The activity was based on ferricyanide assay.

Name of the bacteria	Specific Activity (U/mg)
C. tetanomorphum	26
C. pascui	20
C. propionicum	3.2
C. aminobutyricum	12
E. barkeri	0.01

3.7. Rnf purification
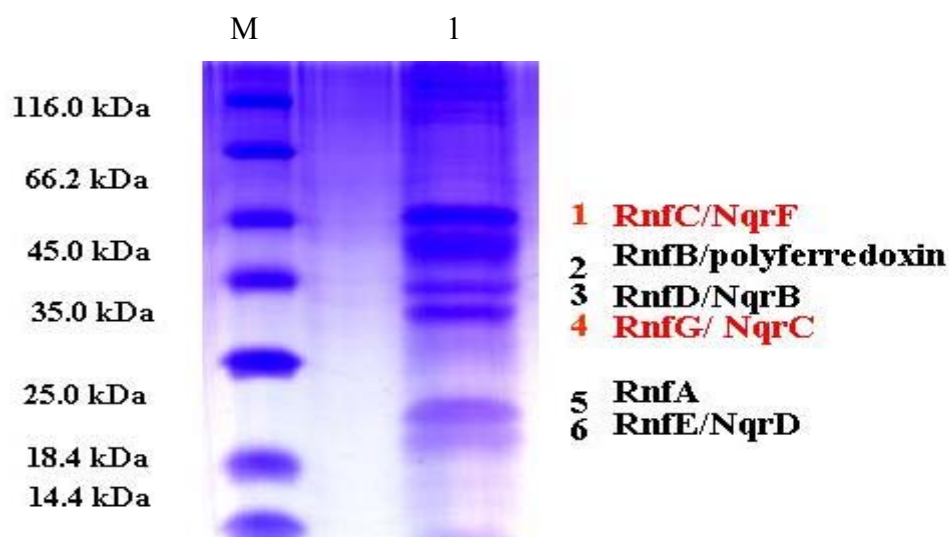
Fig. 14: SDS-PAGE: Analysis of purified Rnf complex from *C. tetanomorphum*. M – Marker and Lane 1- Rnf/Nqr subunits. Proteins were denatured by incubation in Laemmli-buffer containing 10 mM DTT and 2% SDS for 5 min at 95°C and were subsequently separated on a 15% slab gel (8 to 7 cm). Gels were stained with Coomassie Brilliant Blue R250.

The Rnf complex was purified from 30 g wet cells of *C. tetanomorphum*. The cells were opened by French press. The membrane extract was prepared by ultra centrifugation.

After protein solubilisation, purification of Rnf was carried out by chromatography on DEAE Sepharose, Q Sepharose, Red Reactive and Superdex 200. Approximately 0.9 mg protein was obtained. SDS-PAGE revealed protein bands with apparent molecular masses of 49 kDa, 33 kDa, 30 kDa, 25 kDa, 23 kDa and 22 kDa. Rnf activity of the purified enzyme was determined by using NADH and the artifical electron acceptor ferricyanide at 420 nm.

Table 4: Purification of Rnf complex from *C. tetanomorphum*

Sample/ method	Total protein mg	Total activity (U)	Specific acvity (U/mg)	Yield	Purification factor
Crude extract	65	2275	35	100	1
Q Sepharose	16	1760	110	77	3
DEAE Sepharose	5.7	1128	198	50	6
Red Reactive	1.1	957	870	42	25
Superdex 200	0.9	837	930	36	27

The specific activity shown here was from the best preparation; the usually obtained specific activity was 400 U/ mg.

3.8. N Terminal Sequence

The Rnf complex was separated by SDS-PAGE and transferred on a PVDF membrane. The subunits were excised and N-terminal sequenced by Edman degradation. The N-terminal sequences were compared with those are from Rnf complex of *C. tetani* which showed sequence identities of about 60% to 80%.

1 MELLTFKNGVHPPHGKIYTE 20 *C. tetanomorphum*
15 MEILTFKNGVHPPHGKHYSE 34 **85%** identity with **RnfC/Nqr**F *C. tetani* [E88]

```
1   MKKVSSFKLGMVLLLIAAV  19  C. tetanomorphum
1   MKKNGILKLG I VLLI IAGV  19  63% identity with RnfG/NqrC C. tetani [E88]


1   MSETTMYTVSSSGCT      15  C. tetanomorphum
1   MSETTMYTVSSSPH I     15  80% identity with RnfD/NqrB C. tetani [E88]


1   MVVSERLYNGIIKEN      15  C. tetanomorphum
1   MSMGDRLYNGIIREN      15  65% identity with RnfE/NqrD C. tetani [E88]
```

RnfA and RnfB subunits could not be sequenced.

3.9. Na$^+$ translocation experiment

Sodium ion translocation of inverted membrane vesicles from *C. tetanomorphum* measured by observing the change of intravesicular Na$^+$ concentration using ^{22}Na$^+$, where ferredoxin was reduced and NADH is generated by Rnf complex. The assay contained NAD$^+$, ferredoxin and Ti(III)citrate, in order to reduce the ferredoxin. V-type ATPase, which couples hydrolysis of ATP with Na$^+$ translocation in *C. tetani*, was chosen as positive control. In these experiments it was shown that ATP hydrolysis coupled with Na$^+$ translocation in *C. tetanomorphum*. The assay contained 100 mM Kpp buffer (pH 7.4), Mg^{2+} and inverted membrane vesicles.
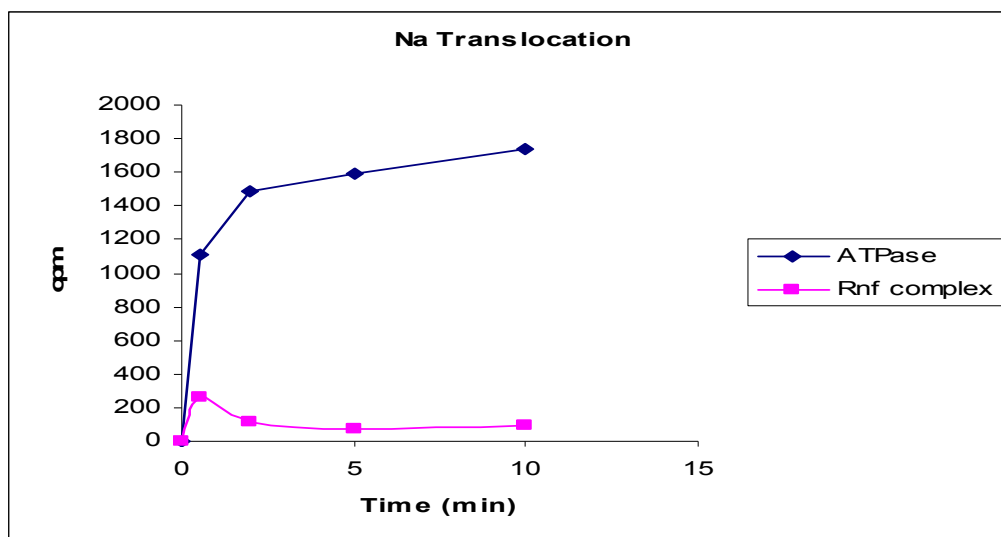
Fig. 15: ^{22}Na$^+$ translocation in inverted vesicles driven by Ti(III)citrate, ferredoxin, NAD$^+$ and Rnf (pink line) or ATP (blue line). The assays were performed at 37°C. 1 ml

assay mixture contained 100 mM Kpp buffer pH 7.4, 1 mM NAD$^+$, 0.37 MBq ^{22}Na$^+$, 20 mM KCl, 1.6 µM ferredoxin, 1 mM Ti(III)citrate, 2 mM DTT, and inverted vesicles (0.8 mg protein). The assay mixture was incubated at 37°C at different time points in the range of 1 min to 30 min. Each 5 minutes samples were analysed for ^{22}Na$^+$ entrapped in vesicles (see Materials and Methods).

3.10. Kinetics of Na$^+$ uptake into proteoliposomes by Rnf complex

The solubilised Rnf complex was reconstituted with L-α-phosphatidylcholin with several steps, which were explained in materials and methods section. Na$^+$ was accumulated within the proteoliposomes when the reaction was started with addition of substrate NAD$^+$. A four fold increase of internal Na$^+$ content of the proteoliposomes as compared with control experiment and sudden decrease of Na$^+$ concentration along with time was observed. The decrease in the Na$^+$ concentration of the proteoliposomes after 60 seconds can be attributed either to leakage of the proteoliposomes or due to the hydrogenase used in this reaction. The hydrogenase was purified from *Methanosarcina barkeri* containing dodecyl maltoside as detergent might have destroyed the reconstituted proteoliposomes. (Hydrogenase from *Methanosarcina barkeri* was a gifted by PD. Dr. Hedderich).
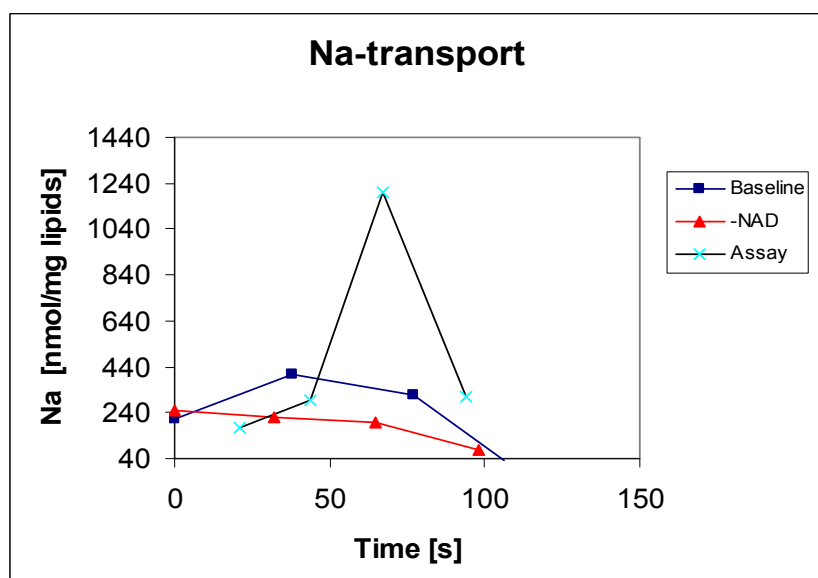
Fig. 16: Na$^+$ transport by proteoliposomes containing one column purified Rnf complex from C. tetanomorphum. The reaction mixture contained 0.1 mg reconstituted protein,

5M NaCl, 8 µM ferredoxin and hydrogenase (0.04 mg/ml). The reaction was started by addition of NAD^+ at the time point of zero seconds. At each time interval 70 µl assay mixture were passed over Dowex columns to remove the external Na^+ and the Na^+ content trapped inside the proteoliposomes was determined by atomic absorption spectroscopy. (■) Base line- control with 0.1 mg protein (NAD^+, ferredoxin and hydrogenase were absent); (▲) control in the absence of NAD^+ (×) reaction with 0.1 mg protein.

3.11.1. Flavins in Rnf complex

The Rnf complex from *C. tetanomorphum* was treated with trichloroacetic acid. The UV- Vis spectra from the supernatant showed the peaks at 360nm and 450 nm characteristic of oxidised flavins. But the shape of the spectrum was quite different from that of the standards (FMN or riboflavin).

A. Standard   B. Rnf complex (from the supernatant)
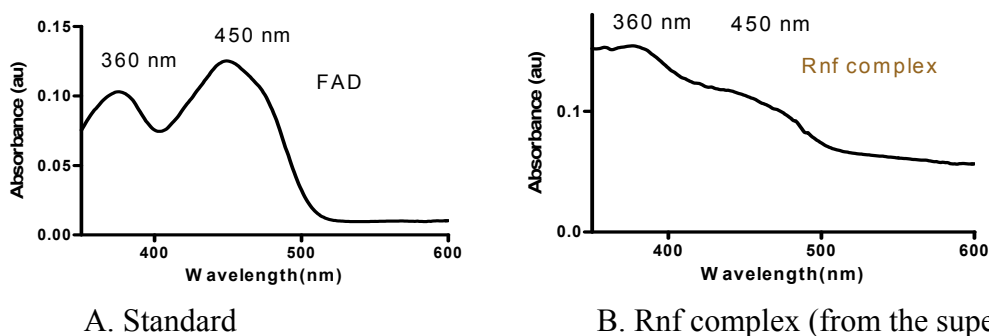
Fig. 17: UV-vis spectrum: Absorption spectra of denatured Rnf complex from C. tetanomorphum. The flavins were analysed by HPLC.

3.11.2. Flavin analysis

Rnf complex contains noncovalently bound flavins. The flavin analysis of Rnf complex by HPLC showed that the Rnf complex contained 0.6 mol FMN+riboflavin per 180 kDa protein. FMN and riboflavin found in a 1:1 stoichiometric ratio within the protein.
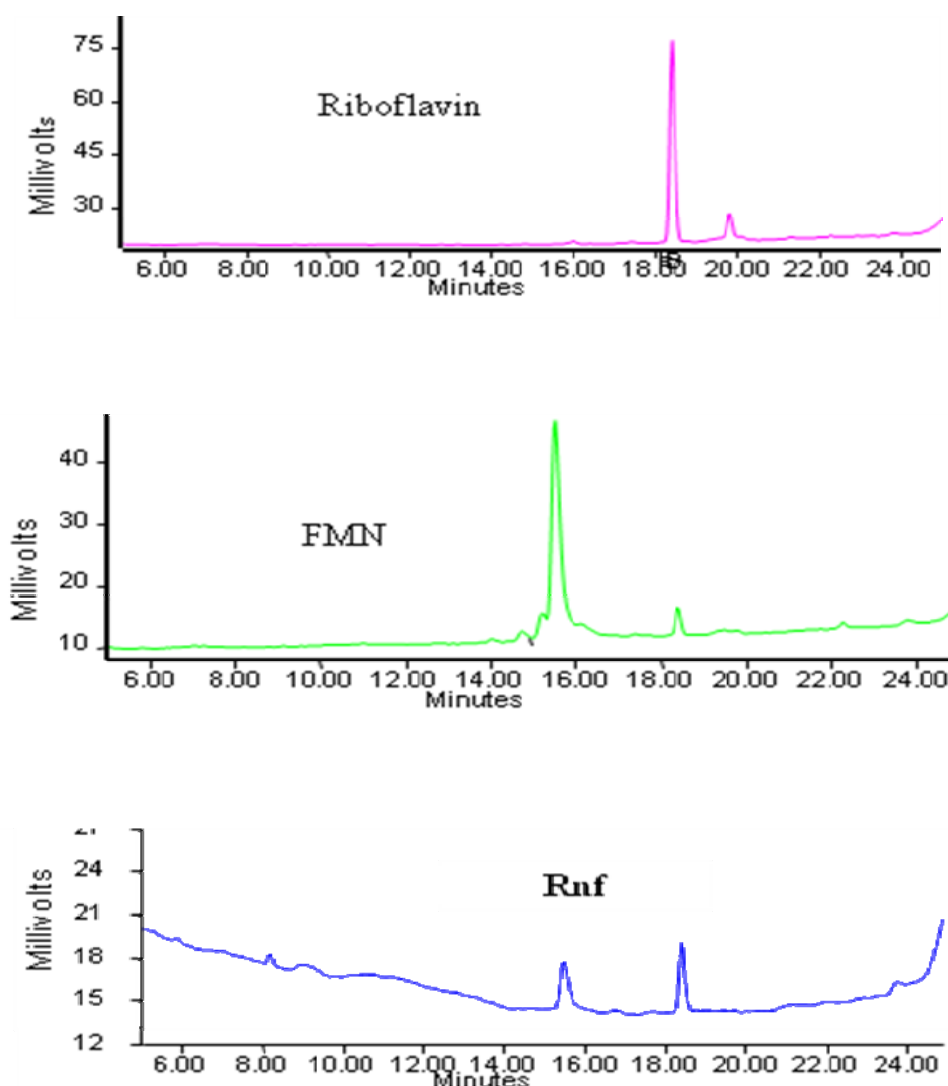
Fig. 18: Flavin identification by HPLC. The pink elution profile shows riboflavin as standard, the green elution profile shows FMN as standard and blue elution profile corresponds to the Rnf complex from *C. tetanomorphum,* which indicates the presence of FMN and riboflavin in the complex (1:1).

3.11.3. Distribution of covalently bound Flavins in Rnf complex

The covalently bound flavin was revealed by separating the Rnf complex at 15 % polyacrylamide gel. It should be noted that the sample loaded on the SDS PAGE was subjected to heat treatment (5 min at 95°C) and SDS (0.1%). The separated gel was subjected to UV illumination which shows two fluorescent bands corresponding in molecular mass to RnfD and RnfG subunits of the Rnf complex from *C.*

tetanomorphum. RnfG exhibited a much stronger fluorescent intensity as compared to RnfD.
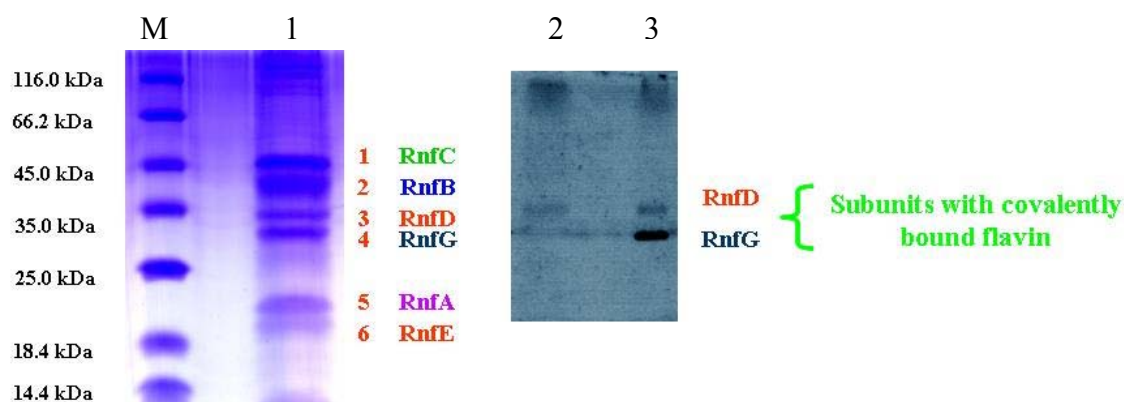
Fig. 19: Existance of covalently bound fluorescent compound in the RnfD and RnfG subunits of the Rnf complex from *C. tetanomorphum.* Purified Rnf complex was separated by SDS PAGE at 15% polyacrylamide. M - Marker. Lane 1 is Coomassie-stained Rnf complex, and the lanes 2 and 3 are a fluorescent photograph. Lane 2 - RnfG that disappeared after treatment with phosphodiestarase. Lane 3- fluorescent bands of RnfG and RnfD.

3.11.4. Covalently bound FAD or FMN?

In order to check the nature of covalently bound flavin, the Rnf complex was treated with TCA to precipitate covalently bound flavin. The precipitates were treated with SDS and phosphodiesterase which can cleave phosphodiester bonds. Fluorescence was measured on a Cary Eclipse fluorescence photometer using an excitation wavelength of 445 nm and an emission wavelength of 520 nm. Four fold increases in the fluorescence intensity of the flavins was observed when it was treated with phosphodiesterase compared with precipitated protein. The result indicated that covalently bound flavin is either FMN which was released with phosphodiesterase treatment or FAD from which the quenching adenosine moiety was removed.
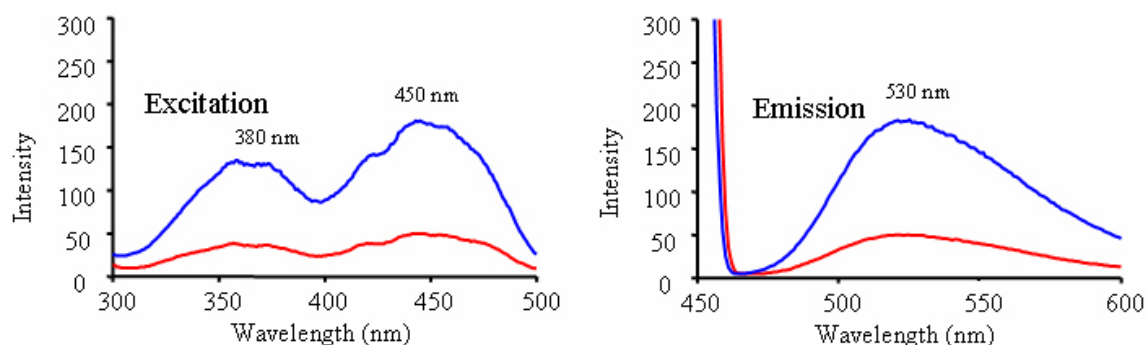
Fig. 20: Fluorescence spectra of covalently bound flavins from the Rnf complex: pellet containing flavin (red colour line), covalently bound flavin (blue colour line). The sample was diluted with 50 mM Kpp (pH 7.7) to record fluorescence spectra. The excitation spectrum was measured with the emission at 525 nm, and the emission spectrum was measured with excitation at 445 nm.

3.14. The putative flavin binding site of RnfG and RnfD

Rnf subunits D and G are homologous to subunits B and C of Na$^+$-Nqr, respectively. The covalently bound flavins of Na$^+$-Nqr was reported and characterized by Nakayama, Y., et al.,[37]. The binding site of flavin was estimated to be a threonine residue in both the NqrB and NqrC; the sequence around the threonine residue was compared and shown below in the sequence alignment. The similar case was reported for Rnf subunits D and G in *V. cholerae*, [38] and it was reported that flavins are linked at the position of RnfG-T175 (SGAT) and RnfD-T187 (TMAT). It is observed that, in the case of RnfD, the flavin was bound, not to the SGAT sequence but to the final threonine residue of the sequence, TMAT.
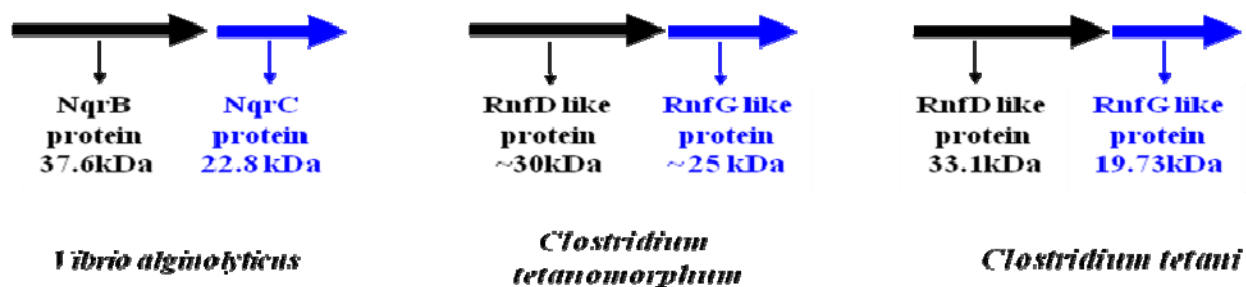
RnfG

NqrC- *Vibrio alginolyticus*	DGLSGA**T**LTSNGVQHTF
RnfG/NqrC- *C. tetanomorphum*	VAITGA**T**ITSKAVTLGV
RnfG/NqrC- *C. tetani*	VAITGA**T**ITSKAVTLGV
RnfG/NqrC- *Vibrio cholerae*	DQFTGA**T**ITSKAVTLGV

Alignment of the amino acid sequence around the flavin-linked threonine of the NqrC of *V.alginolyticus* and the conserved sequence of RnfG of *C. tetani, C. tetanomorphum* and *V. cholerae*. Flavin-linked threonine is shown marked with blue colour.

RnfD

Flavin conserved region 1

RnfD/NqrB- *C. tetanomorphum*	DGVTTATPLAI
RnfD/NqrB- *C. tetani*	DGATTATPLAI
RnfD/NqrB- *V. cholerae*	DGITMATPLDA

Flavin conserved region 2

NqrB- *Vibrio alginolyticus*	TAADGFSGA**T**ALSQWAQGGN
RnfD/NqrB- *C. tetanomorphum*	LKGNEATGAAAPDLMSVFIG
RnfD/NqrB- *C. tetani*	LKGAEATGA**T**LPGVMDAFIG
RnfD/NqrB- *Vibrio cholerae*	PMIHLLSGA**T**MLGAFFIATD

Alignment between RnfDs from different sources showing that possible flavin binding sequence. A Flavin binding motif conserved in *Vibrio alginolyticus, C. tetani, and C. tetanomorphum* and *Vibrio cholerae*. RnfD includes two partially conserved flavin binding motifs of NqrB. Flavin-linked threonine is shown marked with blue colour. Flavin binding motif SGAT is not conserved in RnfD from *C. tetanomorphum*.

3.15. Iron determination

By chemical analysis, non-heme iron was determined as 25±1 mol per Rnf complex (180 kDa). The purified ferredoxin was estimated to contain 8±1 mol per one ferredoxin (6 kDa). It suggested the presence of up to 6[4Fe-4S] clusters in Rnf complex and 2[4Fe-4S] clusters in ferredoxin.

3.16. Sequence analysis

The sequences were obtained by different strategies. The N-terminal sequences were used to design degenerated primers. The first fragment of the Rnf operon was amplified by PCR. By using the known fragment, inverse PCR technique was applied to obtain flanking regions. Full experiment details were described in the material and methods section. The sequence from *C. tetanomorphum* showed high identities with C. tetani when it was compared by sequence alignment by ClustalW2 programme from EMBL. The obtained nucleotide sequence was translated into amino acid sequence. The translated amino acids were analysed under Motif scan to check the flavin binding site and iron-sulphur binding region signature and transmembrane helices were checked.

Rnf C

Translated amino acid sequence of RnfC from *C. tetanomorphum*

```
MELLTFKNGVHPPHGKIYTEENKPIEGYLPKGDIVIPMSQHIGAPAEPIVKKGDRVLVG
QKIGEAKGFVSANIHASVSGTVKNVAPVTLFNGVKSTAVIIENDGQYEEIETEKRDYTK
LSNEEIINIIKEAGIVGMGGATFPTHVKLAPPLDKNIDSIVVNAAECEPYLTCDHRMML
EKTNEIVEGLKIVLKLFPKATGYIGIEDNKMNAIKAMQEAVKNIANIEVKAVKTKYPQG
AEKQLIYAITKREVPSGGLPADAGCIVQNVDTIYEIYNAVVNGKPLTSRVVTVTGDAIK
EPKNLRFKIGTSVRELVEAATSGVLCLTKKVAEIEEESNCINCGKCVQVCPMNLMPTKL
ATASAVSNLDMFNEFSGRDCIECGCCSFVCPARRHLLQRIRSG
```

Respiratory-chain NADH dehydrogenase 51 kDa subunit

Na$^+$-translocating NADH-quinone reductase subunit A (NqrA)

[4Fe-4S] ferredoxins, iron-sulfur binding region signature- CINCGKCVQVCP and

DCIECGCCSFVCP

Sequence alignment - Rnf C from *C. tetanomorphum* and *C. tetani*

```
RnfC-C.tetanomorphum    --------------MELLTFKNGVHPPHGKIYTEENKPIEGYLPKGDIVIPMSQHIGAPA
RnfG-C.tetani           MQLIKCKLRDRRVFMEILTFKNGVHPPHGKHYSE-NKAIEEYLPEGDIVIPMSQHIGAPA
                                      **:************ *:* **.** ***:**************

RnfC-C.tetanomorphum    EPIVKKGDRVLVGQKIGEAKGFVSANIHASVSGTVKNVAPVTLFNGVKSTAVIIENDGQY
RnfG-C.tetani           EPIVKKGDRVLVGQKIGEAKGFISANVHASVSGTVKNVSEITQFNGAKCKAVIIENDGQY
                        *********************:***:************: :* ***.*.:*********

RnfC-C.tetanomorphum    EEIETEKRDYTKLSNEEIINIIKEAGIVGMGGATFPTHVKLAPPLDKNIDSIVVNAAECE
RnfG-C.tetani           EEVETQKRDYTKLSNEEIINIVKEAGIVGMGGATFPTNVKLTPPPDKKIEYIVVNAAECE
                        **:**:*************** :***********:**.****:** **.*: *********

RnfC-C.tetanomorphum    PYLTCDHRMMLEKTNEIVEGLKIVLKLFPKATGYIGIEDNKMNAIKAMQEAVKNIANIEV
RnfG-C.tetani           PYLTCDHRMMLEHSKEIIKGLKVILKLFPNAKGLIGIEDNKPNAIKAMKEAASGEERIEV
                        ************:::**::***::*****:*.* ******* ******:**..  .***

RnfC-C.tetanomorphum    KAVKTKYPQGAEKQLIYAITKREVPSGGLPADAGCIVQNVDTIYEIYNAVVNGKPLTSRV
RnfG-C.tetani           KSVKTKYPQGAEKQLIYALIGKEVPSGGLPADAGCIVQNVDTVYEIYNAVVNGKALVSRV
```

```
                        *.***************:   :*******************:*********** .* ***
RnfC-C.tetanomorphum    VTVTGDAIKEPKNLRFKIGTSVRELVEAA-------FKSYISGPMMGMAMYSLDVPSTKE
RnfG-C.tetani           VTVTGDAIKEPKNIRFRIGTSVKELVEAAGGFLEEPYKVISGGPMMGIAMYSLDVPAAKG
                        *************:**:*****:******      :*   .*****:*********::*

RnfC-C.tetanomorphum    TSGVLCLTKKVAEIEEESNCINCGKCVQVCPMNLMPTKLATASAVSNLDMFNEFSGRDCI
RnfG-C.tetani           TSGILCLTKKVAEIEDESNCINCGKCVQVCPMNLIPTKLAVASSIRNYDMFNEFNGRDCI
                        ***:*********:****************:*****.**:: * ******.*****

RnfC-C.tetanomorphum    ECGCCSFVCPARRHLLQRIRSG--------
RnfG-C.tetani           ECGCCSFICPARRHLLQRIRSGKKAASRKK
                        *******:**************
```

The underlined (MELLTFKNGVHPPHGKIYTE) was obtained from N-terminal by Edman degradation.

Rnf G

Translated amino acid sequence of RnfG from *C. tetanomorphum*

MKKVSSFKLGMVLLLIAAVCGLILGGVNQVTAEPIAIQNKKTLDEANKAILPEASEFAE
KTDIKGEGIVLGVTEGKSGSDLKGYTIKVAPK**GYAGAIEMMVGVSTEGKVTGIKILNHA
ETPGLGANATDPKFSGQYANKPAKELKVVKGAASGEDEIVAITGATITSKAVTLGVNEA
IKFY**DTKLKGG

FMN-binding domain

TMhelix - 2

Sequence alignment - Rnf G from *C. tetanomorphum* and *C. tetani*

```
RnfG-C.tetanomorphum    MKKVSSFKLGMVLLLIAAVCGLILGGVNQVTAEPIAIQNKKTLDEANKAILPEASEFAEK
RnfG-C.tetani           MKKNGILKLGIVLLIIAGVCGLILGGINQVTAEPIAIQAKKTIDEANKEILPVASTFEEK
                        ***:***:**.********:********** ***:***** *** ** * **

RnfG-C.tetanomorphum    TDIKGEGIVLGVTEGKSGSDLKGYTIKVAPKGYAGAIEMMVGVSTEGKVTGIKILNHAET
RnfG-C.tetani           KDVELDEGILSLSEGKEGSEVKGYTIKVAPKGYGGAIEMMVGISTEGKITGIKVLNHSET
                        .*:: :  :*.::***.**::*************.********:*****:****:***:**

RnfG-C.tetanomorphum    PGLGANATDPKFSGQYANKPAKELKVVKGAASGEDEIVAITGATITSKAVTLGVNEAIKF
RnfG-C.tetani           PGLGAHADSPDFSDQYKDKPTEKLSVVKGTASKDTEIAAITGATITSNAVTDGVNKAIEF
                        *****:* .*.**.** :**:::*.****:** : **.*********:*** ***:**:*

RnfG-C.tetanomorphum    YDTKLKGG-
RnfG-C.tetani           YNSKLKGGN
                        *:::*****
```

The underlined (MKKVSSFKLGMVLLLIAAV) was obtained from N-terminal by Edman degradation.

RnfD

MSETTMYTVSSSGCTRAKDTTQSIMRDVVIALLPATIAGVYFFKLQGLLVILASVLSCV
VAEYIWQKASKKKVTVGDYSAVVTGLLLAFNVPASIPLWIPVVGGFFAIIVVKQFFGGL
GQNIVNPALAARAFLLASWPVQMTSWTLDGVTTATPLAILKGNEATGAAAPDLMSVFIG

```
HVGGCIGETSALALLIGGAYLFYKLIGGAYLFYKHIIDWRIPVSFIGTTFIFTAIAGRG
SSPVYELFAGGLMLGAIFMATDYATSPITPLGRIIFGVGCGVITSLIRIFGGYPEGVSY
SILVMNLFVPLIERWTAPKIFGKV
```

NQR2, RnfD family
TMhelix - 17

```
RnfD-C.tetanomorphum    MSETTMYTVSSSGCTRAKDTTQSIMRDVVIALLPATIAGVYFFKLQGLLVILASVLSCVV
RnfD-C.tetani           MSETTMYTVSSSPHIREKDTTQSIMRDVIIALLPATVAGVYFFKMEALLVILASVISCVL
                        ********** ***********:*******.*******::.********:***:

RnfD-C.tetanomorphum    AEYIWQKASKKKVTVGDYSAVVTGLLLAFNVPASIPLWIPVVGGFFAIIVVKQFFGGLGQ
RnfD-C.tetani           AEYIWQKATKQKVTISDLSAVVTGLLLAFNLPASVPLWLPVIGGFFSIIIVKQFFGGLGQ
                        ********:*:***.* *************:***.***:**:****:**:**********

RnfD-C.tetanomorphum    NIVNPALAARAFLLASWPVQMTSWTLDGVTTATPLAILKGNEATGAAAPDLMSVFIGHVG
RnfD-C.tetani           NVVNPALAGRAMLLASWPVQMTTWTLDGATTATPLAILKGAEATGATLPGVMDAFIGHVG
                        *:******.**:**********:*****.*********** *****: *.:*..******

RnfD-C.tetanomorphum    GCIGETSALALLIGGAYLFYKLIGGAYLFYKHIIDWRIPVSFIGTTFIFTAIAGRGSSPV
RnfD-C.tetani           GCIGETSALALLLG----------GAYLLYKRVIDWKIPVTFIGTTLIITAIAGRSGNVI
                        *************.*          ****:**::***:***:*****:*:******... :

RnfD-C.tetanomorphum    YELFAGGLMLGAIFMATDYATSPITPLGRIIFGVGCGVITSLIRIFGGYPEGVSYSILVM
RnfD-C.tetani           YELFVGGLMIGAIFMATDYATCPITPKGRIIFGIGCGIITSLIRIFGGYPEGVSYSILIM
                        ****.****:*********** .**** ******:***:*************** *****:*

RnfD-C.tetanomorphum    NLFVPLIERWTAPKIFGKV-
RnfD-C.tetani           NLFVPLIERWTTPRTFGKVK
                        ***********:*: ****
```

The underlined (MSETTMYTVSSSGCT) was obtained from N-terminal by Edman degradation.

Rnf A

Translated amino acid sequence of RnfA from *C. tetanomorphum*

```
MSIFTIFISALLVNNFVLSRFLGICPFLGVSKKVETATGMGAAVTFVMALAAIMTFLVE
RFILIPLNIQYLSTLAFILVIASLVQFVEMVIKKVSPDLYKALGIYLPLITTNCAVLGM
AVINSNEKYNLIQSIINSVGAALGFTLALVLLAGIREKMETNEYIPEALKGLPITLVTA
GLMAIAFLGFQGLI
```

Rnf-Nqr subunit, membrane protein

TMhelix - 12

Sequence alignment - Rnf A from *C. tetanomorphum* and *C. tetani*

```
RnfA-C.tetanomorphum    MSIFTIFISALLVNNFVLSRFLGICPFLGVSKKVETATGMGAAVTFVMALAAIMTFLVER
RnfA-C.tetani           MKIFTIFLSALLVNNFVLSRFLGICPFLGVSKKVETATGMGAAVTFVMALASIMTYLVEK
                        *.*****:****************************************** **:***:***:

RnfA-C.tetanomorphum    FILIPLNIQYLSTLAFILVIASLVQFVEMVIKKVSPDLYKALGIYLPLITTNCAVLGMAV
RnfA-C.tetani           FILVKFEITYLSTLAFILVIASLVQFVEMVIKKVSPDLYKALGIFLPLITTNCAVLGVAV
                        ***: ::* ************************************:************:**

RnfA-C.tetanomorphum    INSNEKYNLIQSIINSVGAALGFTLALVLLAGIREKMETNEYIPEALKGLPITLVTAGLM
RnfA-C.tetani           INSDEGYTLIESLVNSVGAALGFTLALVLLAGIREKLDTNEYIPEALKGLPITLVTAGLM
```

```
                                 ***:*  *.**:*::*********************::********************
RnfA-C.tetanomorphum             AIAFLGFQGLI
RnfA-C.tetani                    AIAFLGFQGLI
                                 ***********
```

N-terminal sequence could not be sequenced.

RnfE

MVVSERLYNGIVKENATFVQVLGMCPTLAVTTSAINGIGMGLSATVVLIGSNVVISLLK
KVIPDEIRIPAYITVIATLVTVLQFLLQAYLPDLNKSLGIFIPLIVVNCIILGRAEAYA
NKNSVGASFFDGLGMGLGFTVSLAALGIIREFLGTGKVFGAQITPDAFQPALIMILAPG
GFFTLGILMAILNQRKLKKAK

Rnf-Nqr subunit, membrane protein
11 Tm – Helix

```
RnfE-C.tetanomorphum     MVVSERLYNGIVKENATFVQVLGMCPTLAVTTSAINGIGMGLSATVVLIGSNVVISLLKK
RnfE-C.tetani            MSMGDRLYNGIIRENPTFVQVLGMCPTLAVTSSAMNGAGMGLSTTVVLIGSNVAISLLRK
                         :.:******::**.*****************:**.** *****:*********.****.*

RnfE-C.tetanomorphum     VIPDEIRIPAYITVIATLVTVLQFLLQAYLPDLNKSLGIFIPLIVVNCIILGRAEAYANK
RnfE-C.tetani            VIPDEIRIPAYITIIATFVTVLQFLLKAYLPDLNKSLGIFIPLIVVNCIILGRAEAYASK
                         *************:***:********:*********************************.*

RnfE-C.tetanomorphum     NSVGASFFDGLGMGLGFTVSLAALGIIREFLGTGKVFGAQITPDAFQPALIMILAPGGFF
RnfE-C.tetani            NGIVSSLFDGLGMGLGFTLSLTVLGIIRELLGNGTVFGWRLMPQAYNPALIMILAPGAFF
                         *.: :*:************:**:.******:**.*.*** :: *:*:::**********.**

RnfE-C.tetanomorphum     TLGILMAILNQRKLKKAK--
RnfE-C.tetani            TLGILLAILNARKLKKAKNN
                         *****:**** *******
```

The underlined (MVVSERLYNGIVKEN) was obtained from N-terminal by Edman degradation.

RnfB

GYASKKFAVEVDERVPMVRAALPGANCGGCGFAGCDAYADAVVNAGAKPNGCPVGGAAC
AAKIAEIMGVVVDSSEPKKAYVKCQGTCDKAKEKYEYYGAMTCVDDAANIAGSKTCGFG
CLGLGSCVQVCAFDAIHVENGIAVVDEEACTGCGACVSICPKSVIELTPMSKKVRISCN
SHDKGIEVKNACSVGCLSCGLCVRNCPSEAITMVNNLPVIDYDKCTQCGVCVGKCPTKA
IVNL

[4Fe-4S] ferredoxins, iron-sulfur binding region signature

Putative Fe-S cluster- **CtGCGaCVsICP, ClSCGlCVrNCP and CtQCGvCVgKCP**

2 TM – Helix

```
RnfB-C.tetanomorphum     ----------------------GYASKKFAVEVDERVPMVRAALPGANCGGCGFAGCD
RnfB-C.tetani            MDLNNLIAPVLSLGGLGIIFGALLGYASKKFAVEVDPRVPQVRDALPGANCGGCGFAGCD
```

```
                               *********** *** ** ***************
RnfB-C.tetanomorphum  AYADAVVNAGAKPNGCPVGGAACAAKIAEIMGVVVDSSEPKKAYVKCQGTCDKAKEKYEY
RnfB-C.tetani         AYADAVVNAGASPSGCPVGGAACASKIAEIMGVTVDTSEPKKAYVKCQGTCNNAKEKYEY
                      ***********.*.***********:********.**:***************::*******

RnfB-C.tetanomorphum  YGAMTCVDAANI--AGSKTCGFGCLGLGSCVQVCAFDAIHVENGIAVVDEEACTGCGACV
RnfB-C.tetani         YGAMTCVDAANIPGAGSKQCSYGCMGLGSCTQVCLFDAITIEDGIAVIDEEKCTGCGACV
                      ************   **** *.:**:*****.*** **** :*:****:*** ********

RnfB-C.tetanomorphum  SICPKSVIELTPMSKKVRISCNSHDKGIEVKNACSVGCLSCGLCVRNCPSEAITMVNNLP
RnfB-C.tetani         DICPKAVIELTPMSKKVRIACNSHDKGISVKNSCAVGCISCGLCARNCPVEAIEMVDNLP
                      .****:*************:********.***:*:***:*****.**** *** **:***

RnfB-C.tetanomorphum  VIDYDKCTQCGVCVGKCPTKAIVNL------------------------
RnfB-C.tetani         VINYDKCVQCGICVKKCPTKAIANLKKDQKVAPKAKPATEVKEAKKTEDK
                      **:****.***:** *******.**
```

Here, the sequence alignment was done with the known fragment of RnfB. With the known sequence the polyferredoxin signature was observed that is consistent with RnfB of C. tetani. N-terminal sequence could not be sequenced.

3.17. Ferredoxin purification from *C. tetanomorphum*

In order to carry out the ferredoxin dependent assay of the Rnf complex, ferredoxin was purified from *C. tetanomorphum*. The ferredoxin was recognized by its dark brown colour after subjecting cell free extracts to DEAE Sepharose column chromatography. The purification was done anaerobically in two steps column DEAE Sepharose and Superdex 200. Figure shows the ferredoxin fraction from size exclusion column chromatography, Sephadox 200 column. The yield of ferredoxin from 20 g wet packed cells was 0.7 mg.
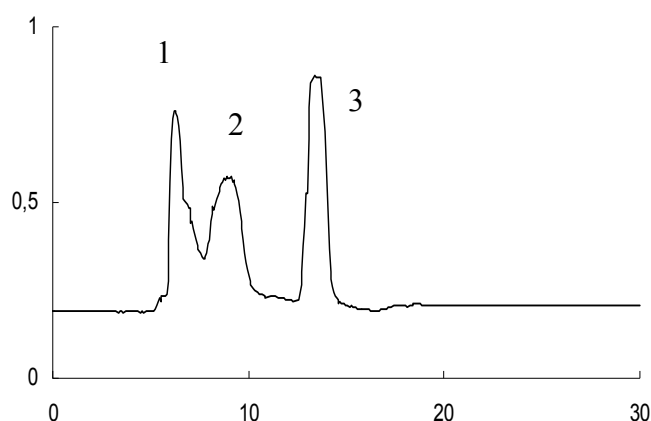

Fig. 21: Elution pattern of from size exclusion column (Superdex 75, GE Health Care). 3rd peak corresponds to ferredoxin fractions

3.18. Amino acid sequence of ferredoxin

The amino acid sequence by the Edman degradation method yielded up to 56 cycles which completed the whole ferredoxin. It showed upto 80 to 95 % sequence identity with ferredoxins from *C. pasteurianum, Clostridium perfringens* and *C. tetani*. The amino acid sequence showed the cysteine motifs typical for two ferredoxin-like Fe-S-clusters. It contains two C-X_2-C-X_2-C-X_3-C-P motifs.

Clostridium tetanomorphum	MAYKILDT**C**IS**C**GA**C**ASE**CP**VNAISQGDTQFVIDEAA**C**ID**C**GN**C**ANV**CP**VGSPVQE
Clostridium tetani	MAYVINDT**C**IS**C**GA**C**ASE**CP**VNAISQGDGLFVVDADT**C**ID**C**GN**C**ANV**CP**VGAAVAE
Clostridium perfringens	MAYKILDT**C**VS**C**GA**C**AAE**CP**VDAISQGDTQFVIDADT**C**ID**C**GN**C**ANV**CP**VGAPVQE
Clostridium pasteurianum	MAYKIADS**C**VS**C**GA**C**ASE**CP**VNAISQGDSIFVIDADT**C**ID**C**GN**C**ANV**CP**VGAPVQE

Complete amino acid sequence of ferredoxin

Iron-sulphur motif: CXXCXXCXXXCP

3.19. UV- Visible spectrum

The oxidised and reduced forms of purified ferredoxin exhibited UV-visible absorption spectra of typical of [4Fe-4S] type ferredoxin. The spectrum of the oxidised form revealed absorption peaks at 340 nm and 420 nm which are characteristic of iron-sulphur chromophores. The ferredoxin, which was reduced by Ti(III)citrate, showed decrease in absorbance centred around 400 nm.
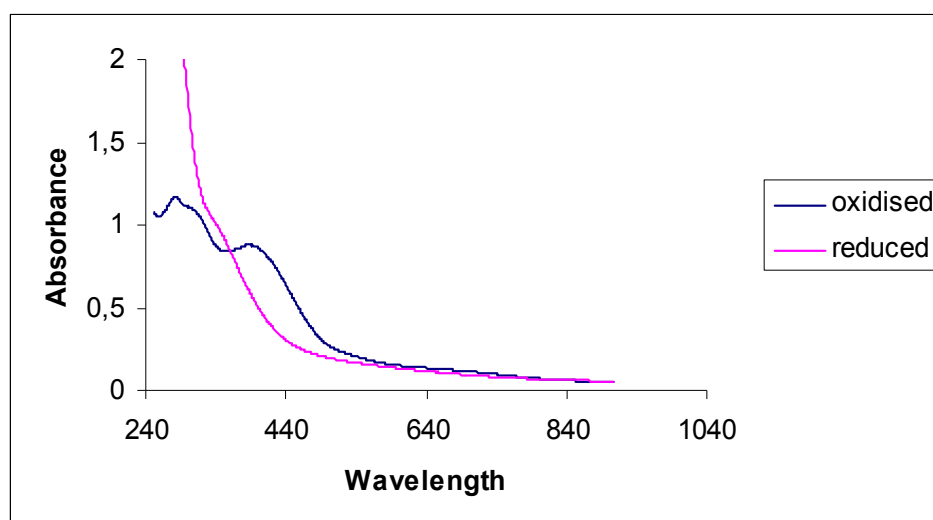
Fig. 22. UV-visible spectra of ferredoxin. Blue line, oxidised ferredoxin (0.9 mg/ml); pink line, reduced ferredoxin.

3.20. K_m determination

The K_m value of ferredoxin for Rnf complex was determined. Two K_m were observed with values of 9 nM and 2 nM. It could be that ferredoxin has two different binding sites. Possibly, Rnf is a homodimer of heterohexamer, in which the first binding of ferredoxin reduces the affinity for the second binding site resulting, in two different apparent K_m.
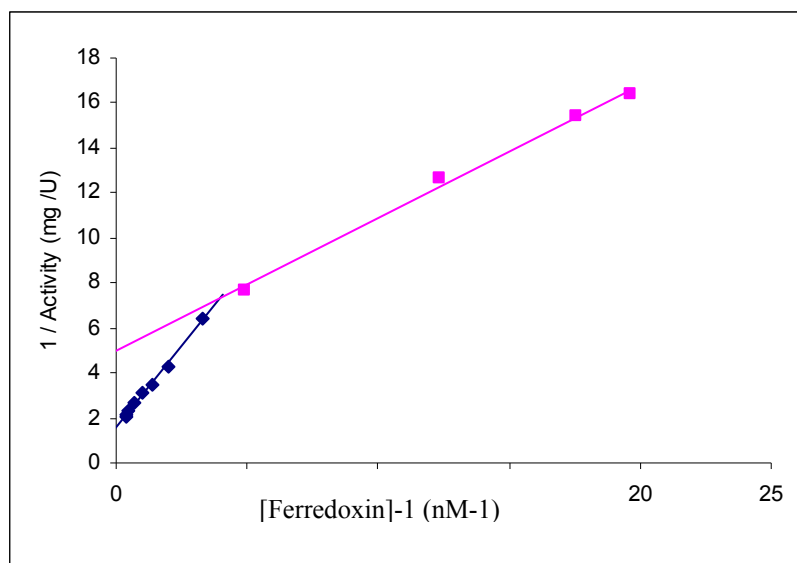

Fig. 23: Lineweaver-Burk plot of the ferredoxin-dependence. Reaction mixture contained were incubated in 50 mM Kpp (pH 7.4), 1 mM NAD$^+$, 1 mM Ti(III)citrate, 30 µl Rnf complex (1 mg/ml) and different concentration of ferredoxin. The measurement of Rnf activity was started by adding NAD$^+$ and monitored the formation of NADH.

3.21. Purification of butyryl-CoA dehydrogenase-Etf complex from *C. pascui*

In order to elucidate the metabolic pathway of *C. pascui,* the enzyme activites were measured. The crude extracts showed high NADH oxidase acitivty in the presence of DTT. This lead to purify the enzyme which showed NADH oxidase and turned out to be Bcd/Etf complex. For the purification of butyryl-CoA dehydrogenase and Etf complex (Bcd-Etf complex) from *C. pascui,* the cells (15 g) were opened by French press after passing three times at 110 MPa. The crude extract was purified over three column

chromatography like DEAE Sepharose, Source 15 PHE and Superdex 200. The SDS-PAGE revealed protein bands with apparent molecular masses of 40 kDa, 36 kDa and 28 kDa. Bcd-Etf complex activity of the purified enzyme was determined by using ferrocenium reduction at 300 nm. The putative physiological reaction, the reduction of crotonyl-CoA by NADH could not be measured, probably because the enzyme was almost inactive.

Table 5: Purification of Bcd-Etf complex from *C. pascui*

Sample/ method	Total protein mg	Total activity (U)	Specific acvity (U/mg)	Yield	Purification factor
Crude extract	22	5.6	0.25	100	1
DEAE Sepharose	32	5.9	0.18	105	0.7
Source 15 PHE	4	1.4	0.35	25	1.4
Superdex 200	0.8	0.5	0.30	9.0	1.2

3.22. N Terminal Sequence of Bcd-Etf complex from *C. pascui*

The Bcd/Etf complex subunits were transferred on PVDF membrane and excised. N-terminal were sequenced by Edman degradation. The N- terminal sequences showed sequence identity of about 85% to 100% compared with Bcd/Etf complex of *C. tetani* and *C. tetanomorphum.*

α - Subunit:

C. pascui	**MNFSLTREQEFVRQMVREFA**
C. tetani	**MNFALTREQEFVRQMVREFA** – 95**%** identity
C. tetanomorphum	**MNFALTREQEFVKQMVREFA** – 90% identity

β - Subunit:

C. pascui	**MNIADYKGVWVFAEQRDGEL**
C. tetani	**MNIADYKGVWVFAEQRDGEL** – 100**%** identity
C. tetanomorphum	**MQPADYKGVWVFAEQRDGQL** – 85% identity

γ - Subunit:

C. pascui	**MNIIVCLKQVPDTNEVKIDP**
C. tetani	**MNIVVCVKQVPDTTEVKIDP** – 85**%** identity
C. tetanomorphum	**MNIVVCLRQVPDTNEVKIDP** – 90% identity

3.23. Purification of Butyryl-CoA dehydrogenase-Etf complex from *C. tetanomorphum*

Purified Bcd/Etf complex from *C. pascui* was almost inactive. Eventually, the reduction of crotonyl-CoA by NADH could not be measured. So we tried to purify butyryl-CoA dehydrogenase and Etf complex (Bcd-Etf complex) from *C. tetanomorphum*. The cells were opened by sonication. The cell free extract were prepared after centrifugation the opened cells for 1 h at 100,000 × *g*. The supernatant containing crude extract was subjected to ammonium sulphate precipitation (33% saturation). Then the precipitated Bcd-Etf complex was applied on DEAE Sepharose, Hydroxyapatite and Superdex 200. Approximately 1.9 mg of pure enzyme was obtained from 30 g cells. The preparations thus obtained were analysed by SDS-PAGE, which revealed protein bands with apparent molecular masses of 40 kDa, 36 kDa and 28 kDa.
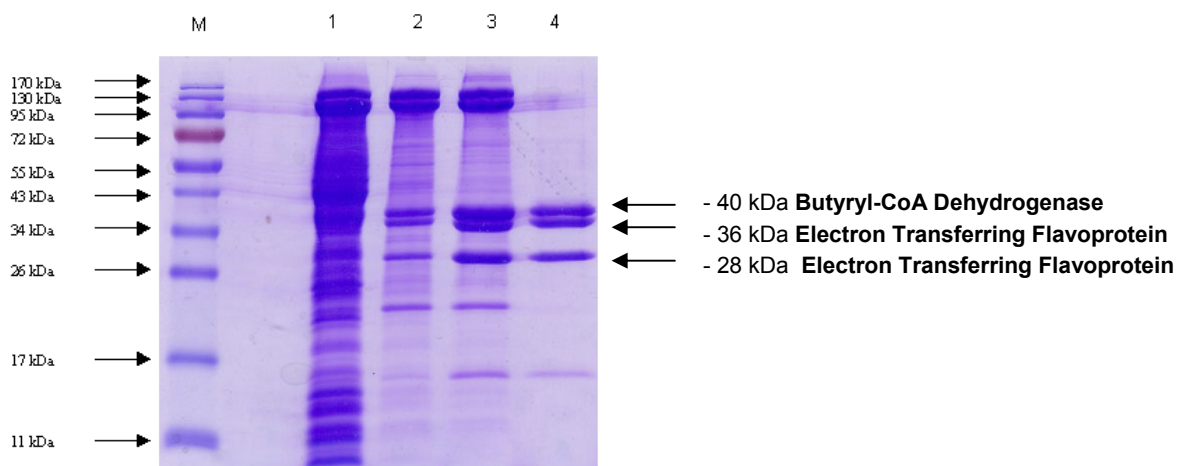

Fig. 24: SDS-PAGE – purification of Bcd/Etf complex from *C. tetanomorphum*. M Marker; 1 cell free extract; 2 (NH$_4$)$_2$SO$_4$ precipitation; 3 DEAE Sepharose; 4. Hydroxyapatite.

3.24. The NADH assay

The NADH oxidation catalysed by the BCD-ETF complex was assayed spectrophotometrically by monitoring NAD^+ formation at 340 nm. The assay mixture (total volume 1 ml) contained 50 mM Kpp pH 7.4, 0.1 mM NADH, 0.1 mM crotonyl-CoA, 10 µM ferredoxin, 0.4 U hydrogenase from *C. pasteurianum*. The reaction was started by crotonyl-CoA addition. The assays were carried out in the absence of ferredoxin and hydrogenase to confirm the coupled reduction of ferredoxin by BCD-ETF complex. The formed H_2 was not quantified.
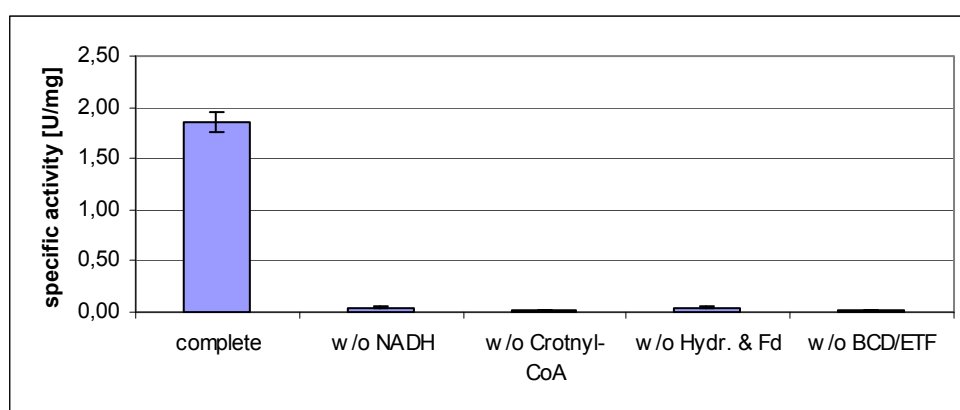

Fig. 25: The NADH assay: complete- the reaction mixture has NADH, crotonyl-CoA, hydrogenase, ferredoxin and BCD-ETF complex. W/o: the respective compound was excluded from the complete reaction mixture.

3.25. Enzyme assays - to find out the intermediates in *C. pascui* metabolic pathway

Based on the presence and absence of enzyme activities, the biochemical pathways for the fermentation of glutamate by *C. pascui* were analysed. Activities of the enzymes citramalate lyase, glutamate dehydrogenase, 2-hydroxyglutarate dehydrogenase and NADH oxidase were measured in crude extracts prepared from C. pascui. Crude extracts from *C. tetanomorphum* and *F. nucleatum* were used to carry out the same enzymatic assays to elucidate and conclude the biochemical pathway of C. pascui.

3.26. Citramalate lyase assay

The assay was carried out under anaerobic conditions. The assay contained 100 mM Tris/HCl pH 7.4, 2mM DTT, 0.1 mM MgCl2, 0.01 ml acetic anhydride, 0.01 ml lactate dehydrogenase, 0.02 mM NADH, crude extract from *C. pascui* and *F.nucleatum*. The reaction mixture was incubated for 30 min at room temperature before the addition of acetic anhydride, lactate dehydrogenase, NADH. (Ref. Table 6). The assay was started with (*R,S*)citramalate.

3.28. NADH Oxidase Assay

The assay (total volume 1ml) contained 100 mM Kpp (pH 7.4), 1 mM $MgCl_2$, 1 mM DTT and crude extract. The mixture was incubated for 30 minutes at room temperature. The reaction was started with addition of NADH. The NADH oxidation was followed at 340 nm. (Ref. Table 6). The assays were measured in the absence of DTT, MgCl2 and crude extracts.

3.29. Glutamate and 2-hydroxyglutarate dehydrogenase assay

The assay contained 0.1 mM NADH, 100 mM Tris/HCl pH 7.4, 0.02 ml crude extract and the reaction was started by the addition of 100 mM α-ketoglutarate. The reaction was monitored by following NADH at 340 nm. Adding NH4Cl to the above reaction mixture increase the rate when the glutamate dehydrogenase was present. (Ref. Table 6).

Table 6: Enyzmes activites in U/ mg.

Name of the bacteria	Citramalate assay (U/mg)	NADH oxidase Assay (U/mg)			GlDh + HGDh* assay (U/mg)	
		A	B	C	-NH4Cl	+NH4Cl
C. pascui	0.9	0.2	0.01	0.01	0.01	0.01
C. tetanomorphum	0.8	0.01	0.01	0.01	0.04	0.1
F. nucleatum	0.001	0.08	0.07	0.1	22	32

* GlDh – Glutamate dehydrogenase; HGDh – 2-hydroxygluterate dehydorgenase

3.30. Elucidation of the metabolic pathway in *C. pascui* by using deuterium labelled glutamate

The scheme below shows two pathways involved in the fermentation of glutamate to ammonia, butyrate, acetate, CO_2 and hydrogen - The methylaspartate pathway and the hydroxyglutarate pathway which are used by *C. tetanomorphum* and *C. symbiosum*, respectively. Though these pathways give rise to same products, they should distinguishable by the different labeling patterns of the butyrate, when deuterium labelled glutamate was used as substrate. *C. pascui* was grown on deuterium labelled glutamate as a substrate to elucidate the fermentation pathway. *C. tetanomorphum* and *C. symbiosum* were used as controls.

In case of *C. tetanomorphum*, which uses the methylaspartate pathway, deuterium at C2 position of glutamate should be conserved in the acetic acid. The label in the C4 position will be relocated by the rearrangement of C3 and C4 of 3-methylaspartate which are later occurs in acetic acid and finally in the butyrate [6].

The condensation reaction of acetyl-CoA by thiolase would lead to a loss of about 20% deuterium label from the methyl group of acetyl-CoA, if one considers the possible intramolecular isotopic effect of about $K_{D/H} = 4$. Therefore butyrate formed from *C.*

tetanomorphum will have 1, 0, 0.4 deuterium at positions C4, C3 and C2 respectively. And also acetic acid will contain 1 deuterium.

The butyrate formed from *C. symbiosum* through the hydroxyglutarate pathway, on the other hand, will have 2, 0, 0.5 deuterium at positions C4, C3 and C2 respectively. The deuterium stems from the C2 position of glutamate is lost by deamination and oxidation to oxoglutarate. This deuterium is transferred to NADD and might be partially reintroduced at C2 in the reduction to 2 hydroxyglutarate or to C3 of butyrate (Buckel, 1980). Conversion to 2 hydroxyglutaryl-CoA, dehydration to glutaconyl-CoA and decarboxylation to crotonyl-CoA should retain the deuterium at C2 and C4 positions. crotonyl-CoA is reduced to butyryl-CoA and butyrate is released. By comparing the deuterium incorporation with bacteria of which biochemical pathways are known, the *C. pascui* metabolic pathway could be assigned.

Scheme: Glutamate fermentation pathway

Incorporation of Deuterium in Glutamate by heating in NaOD/D$_2$O

Table 7: Percentage of deuterium incorporation in glutamate.

Labelled Glutamate	
% incorporation of deuterium	
At C-2	At C-4
97 (one deuterium)	2 × 97 (two deuterium)

3.31. Labelled butyrate produced during glutamate fermentation

The products butyric acid and acetic acid of glutamate fermentation were isolated together by steam distillation. Thus labeled butyrate could be analyzed by NMR spectrum.

3.32. Deuterium labelled butyrate from *C. pascui*

^{1}H-NMR (H$_2$O) δ 2.05 (2.07H, t, *J* = 7.46, CD(H)$_2$COO) δ 1.81 (7.56H, s, COOCH(D)$_3$) δ 1.45 (2H, m, C*H*$_2$) δ 0.78 (2.73H, t, *J* = 7.37, CH(D)$_3$). ^{2}H NMR δ 2.12 (0.13D, s, CD(H)$_2$COO) δ 1.89 (0.43D, s, COOCH(D)$_3$) δ 1.53 (0.03D, s, CH(D)$_2$) δ 0.86 (0.26D, s, CH(D)$_3$)

The figure 26 shows the aligned ^{2}H NMR and ^{1}H-NMR spectra. Acetic acid at δ 1.81 which is coextracted with the used method, in a molar ratio to butyric acid of 1 to 2.53, under the assumption that C2 contains no deuterium incorporation. If the signal at C2 is scaled to the natural abundance of deuterium the attributed signals at a shift of δ 2.12 and 0.86 show the deuterium incorporation at C2 and C4 respectively. The ratio of deuterium content at C4 is 9% and at C2 is 6%. The deuterium content of acetic acid is 6%.
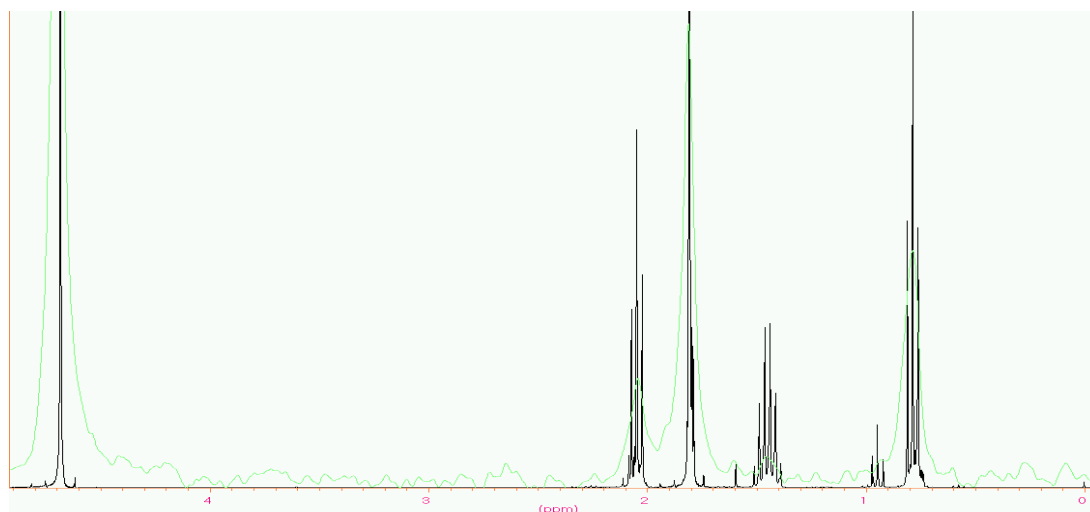
Fig. 26: NMR spectrum of butyrate + acetate produced by *C. pascui.*

3.33. Deuterium incorporated into butyrate from *C. tetanomorphum*

^{1}H NMR (H$_2$O) δ 2.18 (1.97H, t, *J* = 7.27, CD(H)$_2$COO) δ 1.77 (5.69H, s, COOCH(D)$_3$) δ 1.43 (2H, m, C*H*$_2$) δ 0.75 (2.59H, t, *J* = 7.37, CH(D)$_3$). ^{2}H NMR δ 2.12 (0.19D, s, CD(H)$_2$COO) δ 1.89 (0.19D, s, COOCH(D)$_3$) δ 1.51 (0.03D, s, CH(D)$_2$) δ 0.86 (0.43D, s, CH(D)$_3$). Aligned ^{2}H NMR and ^{1}H-NMR spectra data are presented in the table 8.
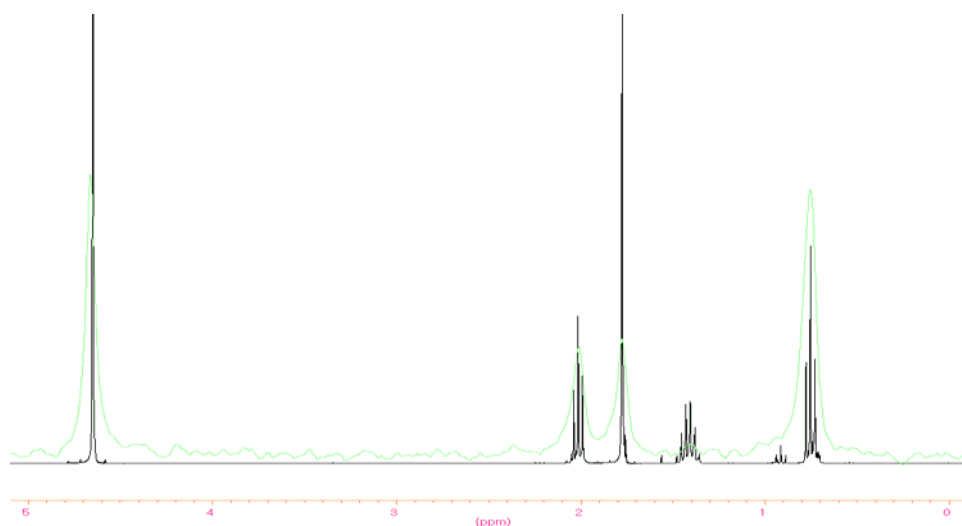

Fig. 27: NMR spectrum of butyrate + acetate produced by C. *tetanomorphum*

3.34. Deuterium incorporated into butyrate from *C. symbiosum*

^{1}H NMR (H$_2$O) δ 2.00 (1.89H, t, *J* = 7.27, CD(H)$_2$COO) δ 1.76 (5.26H, s, COOCH(D)$_3$) δ 1.39 (2H, m, C*H*$_2$) δ 0.71 (1.60H, m, , CH(D)$_3$). ^{2}H NMR δ 2.12 (0.08D, s, CD(H)$_2$COO) δ 1.88 (0.75D, s, COOCH(D)$_3$) δ 1.50 (0.03D, s, CH(D)$_2$) δ 0.85 (0.61D, s, CH(D)$_3$). Aligned ^{2}H NMR and ^{1}H-NMR spectra data are presented in the table 8.
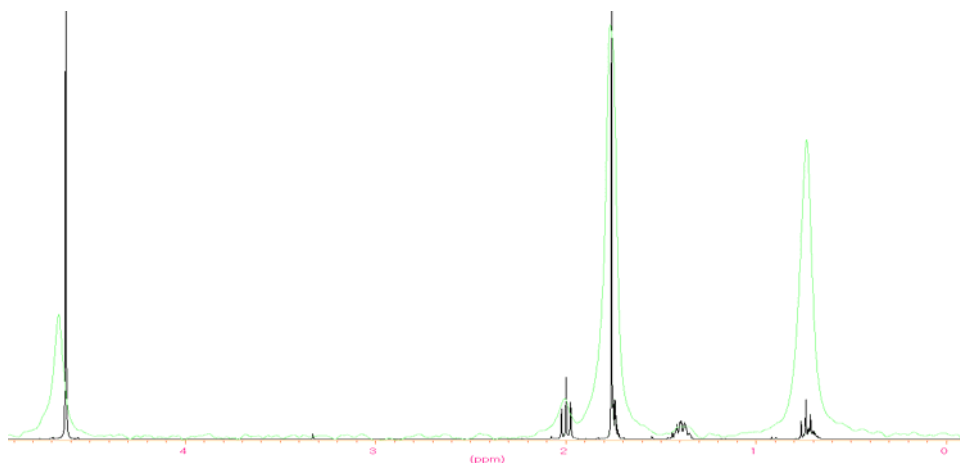
Fig. 28: NMR spectrum of butyrate + acetate produced by *C. symbiosum*.

3.35. Deuterium incorporated into butyrate from *F. nucleatum*

^{2}H-NMR δ 1.8789 (1 D, s, COOCD(H)$_2$) 0.8483 (1,26 D, s, CD(H)$_3$).^{1}H-NMR δ 1.9251 (2.0H, t = 7.27, COOCH$_2$) 1,6910 (5.76, s, CH$_3$) 1.3827 (2.0H, m, CH$_2$) 0.8206 (0.35, t = 7.65, CH$_3$) 0.6616 (2.3H, t = 7.37, CH$_3$)
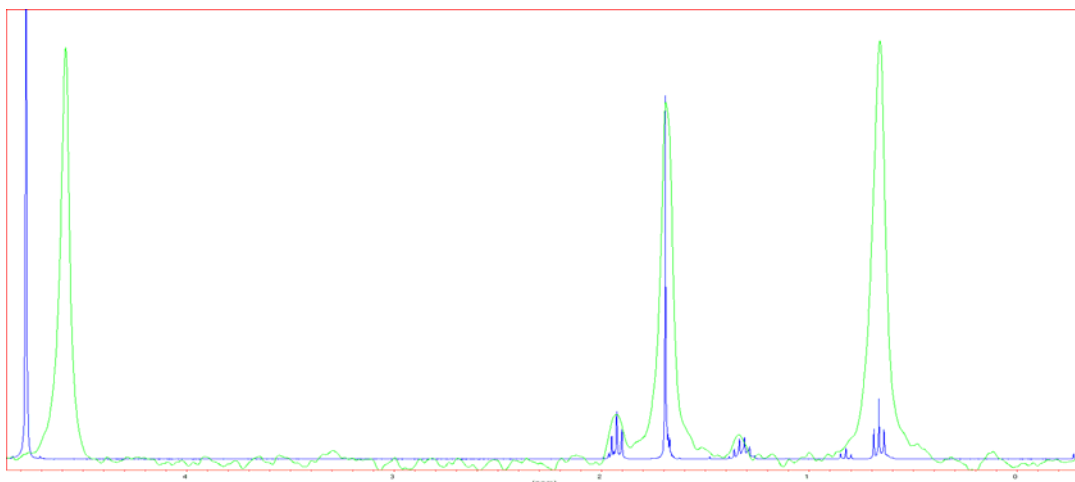

Fig. 29: NMR spectrum of butyrate + acetate produced by *F. nucleatum*.

Table 8: ^{2}H NMR and ^{1}H-NMR - Deuterium contents and chemical shifts shown for functional groups of fermentation products.

	C. pascui			*C. tetanomorphum*			*C. symbiosum*			*F. nucleatum*		
	Acetic acid	Butyric acid		Acetic acid	Butyric acid		Acetic acid	Butyric acid		Acetic acid	Butyric acid	
δ(ppm)	1.81	2.05	0.78	1.77	2.18	0.75	1.76	2	0.71	1.69	1.93	0.66
Group	C2	C2	C4	C2	C2	C4	C2	C2	C4	C2	C2	C4
% D	6	9	6	6	6	9	3	4	28	9	31	37

3.36. Summary-Deuterium incorporation studies

As it is presented in the Table 8, *C. pascui,* assumed to have the methylaspartate pathway based on enzymatic assays, showed 9% deuterium at C2 position and 6 % deuterium at C4 position. Whereas *C. tetanomorphum* which ferments glutamate by methylaspartate pathway, showed 6% and 9 % deuterium retention at C2 and C4 position, respectively. *C. symbiosum* showed 28% deuterium incorporation at C4 position and *F. nucleatum* showed 31% at C2 and 34% at C4 position. This is consistent with its fermentation of glutamate by the hydroxyglutarate pathway. Over all, the deuterium incorporation in butyrate was found to be lower than expected for both pathways. In the methylaspartate pathway, during group translocation reactions which lead to distribution of the label between C2 and C4 might lead to an exchange with the solvent. Whereas, in the hydroxyglutarate pathway, the reinsertion of the dehydrated deuterium at C2 in 2 hydroxyglutarate is dependent on the ratio of deuterated NADD and NADH.

Table 9: Butyrate (Deuterium incorporated) produced- by *C. pascui, C. tetanomorphum, F. nucleatum* and *C. symbiosum.*

	% of expected deuterium		% of observed deuterium	
	C2	C4	C2	C4
C. pascui	≤ 50	≤ 50	9	6
C. tetanomorphum	≤ 50	≤ 50	6	9
C. symbiosum	≤ 50	≤ 100	4	28
F. nucleatum	≤ 50	≤ 100	31	37

4. Discussion

4.1. Elucidation of the glutamate fermentation in *Clostridium pascui* by deuterium lebelling and enzymatic assays

C. pascui phenotypically resembles the classic glutamate-fermenting clostridia, such as *Clostridium cochlearium, C. tetanomorphum, C. tetani,* and especially *C. malenominatum* [28]. All these bacteria ferment glutamate by the methylaspartate pathway, but differ in their sugar utilization, cellular fatty acid composition, and cellular protein pattern and by 16S rRNA sequence divergence of approximately 4 to 8%. It is reported that *C. pascui* ferments glutamate to yield acetate, butyrate, hydrogen and CO_2 [28]. The end products of glutamate fermentation by *C. pascui* clearly indicates the involvement of either methylaspartate or hydroxyglutarate pathway. In this work, we analysed the butyrates obtained by fermentation of [2,4,4-^{2}H]glutamate and measured enzymatic activities in *C. pascui* with positive controls for the methylaspartate pathway in *C. tetanomorphum* and the hydroxyglutarate pathway in *F. nucleatum.*

C. pascui and *C. tetanomorphum* contain high levels of citramalate lyase whereas in *F. nucleatum* this activity was absent. Citramalate lyase mediates one of the unique reactions of the methylaspartate pathway which is leading to the formation of pyruvate from glutamate. The carbon skeleton rearrangement of glutamate to 3-methylasparate is mediated by glutamate mutase. The conversion of glutamate to 3-methylaspartate is followed by two important reactions, the facile elimination of ammonia from the α,β-aminoacid methylaspartate to mesaconate catalyzed by methylaspartate ammonia lyase [39] and subsequent hydration to (*S*)-citramalate [40,41]. Citramalyl-ACP is formed while acetate is released. Citramalyl-ACP is then cleaved to pyruvate, whereby acetyl-ACP is regenerated and pyruvate is formed [13]. Thus, the presence of citramalate lyase activity in crude extracts of *C. pascui* along with that known from *C. tetanomorphum* clearly indicates the glutamate fermentation by methylaspartate pathway. The presence of 2-hydroxyglutarate dehydrogenase and glutamate dehydrogenase in the crude extract of *F. nucleatum* [6] and absence of *C. pascui* respectively, is an excellent indication that the hydroxyglutarate pathway is absent in *C. pascui*. Since (*R*)-2-hydroxyglutarate is not a very common substrate, it is regarded as the first specific intermediate of the hydroxyglutarate pathway [6].

Although glutamate fermentation by the methylaspartate pathway and the hydroxyglutarate pathway yield the same end products, the intermediates formed in the pathway are distinctly different from each other [6]. In this work, it is described that [2,4,4-^{2}H$_3$]glutamate yields butyrate with different labelling patterns [42]. The butyrates obtained with *C. pascui* and *C. tetanomorphum* showed huge loss of deuterium at C2 position as well as C4 position. Significant deuterium labelling is observed at C2 and C4 positions of hydroxyglutarate pathway in *F. nucleatum*. The deuterium label at C4 position from *C. symbiosum* is also significant though loss at C2 poisition is observed. In the methylaspartate pathway, 50% loss at C4 position could be contributed by the rearrangement step and the subsequent elimination of ammonia.

4.2. Functions of Rnf Complex

The Rnf complex catalyzes the reduction of NAD$^+$ by using reduced ferredoxin as an electron donor. The reaction proceeds in the physiological direction with its most probable natural substrate. Thus, clostridial Rnf acts as ferredoxin-NAD$^+$ reductase, which is certainly involved in the reoxidation of reduced ferredoxin (Fd^{2-}) generated by the oxidative decarboxylation of pyruvate catalyzed by pyruvate-ferredoxin oxidoreductase (PFOR). The resulting NADH is required for butyrate synthesis. Thus, Rnf is the missing link between pyruvate oxidation and butyrate systhesis.

4.2.1. Na$^+$ translocation studies

In *C. tetani*, it is proposed that part of the ATP synthesized in the course of the fermentative metabolism is hydrolyzed by a V-type ATPase to generate a Na$^+$-motive force at the membrane. The same could be attributed to the amino acid fermentation in *C. tetanomorphum*. The Na$^+$ translocation experiment with inverted vesicles shows that ATP hydrolysis drives sodium translocation, whereas NAD$^+$ oxidation mediated by Rnf complex with ferredoxin and Ti(III)citrate shows no translocation. The reason for this could be that the Ti(III)citrate used to reduce the ferredoxin destroys the inverted vesicles or influences the reaction. An alternative system to generate reduced ferredoxin in translocation studies can solve this problem. Controls with Ti(III)citrate and ferredoxin in the ATP hydrolysis experiments are required to check whether their the influence could give more information about Na$^+$ translocation.

The established reconstitution protocol to investigate Na^+ translocation for Nqr [43,44] applied to the Rnf complex shows Na^+ translocation with a sudden decrease after a few minutes. The membrane bound hydrogenase used in this assay was purified from *Methanosarcina barkeri* and solubilized with the detergent DM (dodecyl maltoside) which could destroy the reconstitution experiment. The other reason could be either low partial hydrogen pressure in the assay system or a rate limiting hydrogenase. The spontaneous insertion of hydrogenase into the proteoliposomes can influence the H^+ or Na^+ pump [45-47].

4.2.2. Sequence analysis

The N- terminal sequences of RnfC, D, E and G from *C. tetanomorphum* showed the high sequence identities with deduced Rnf proteins from *C. tetani* [9]. This paved the way to synthesize degenerated primers from the conserved regions and sequence the ORF with 2 more steps. The sequences encoding the Rnf complex showed identities of about 65% to 85% with the deduced sequences from *C. tetani*. Analysis of the translated polypeptide sequences indicated that the presence of redox domains, conserved Nqr homologues and transmembrane helices (TM) was identical to the sequence analysis of *C. tetani* (Table 1) [9].

Table 10: Rnf subunits of *C. tetanomorphum*- TM and redox domains predictions.

C. tetanomorphum	RnfC/NqrF	RnfD/NqrB	RnfG/NqrC	RnfE/NqrD	RnfA/NqrE	RnfB
Hydrophobicity/ putative location	Cytosolic enzyme	17 TM	2 TM	11 TM	12 TM	2 TM
Redox domains	NAD/FMN binding sites; 2[4Fe-4S]	FMN binding site	FMN Binding site		-	3[4Fe-4S] polyferredoxin

4.2.3. Flavin analysis

The yellowish brown Rnf complex contains covalently and non-covalently bound flavins. The HPLC analysis of non-covalently bound flavin shows FMN and riboflavin in a 1:1 stoichiometric ratio. Usually, riboflavin has been viewed only as a precursor for the synthesis of FMN and FAD cofactors. However, Blanca Barquera et al,[48]

reported that riboflavin is a component of the Na^+ - pumping NADH-quinone oxidoreductase from *V. cholerae*. It has been suggested that phosphate and adenylate groups of FMN and FAD could be responsible for the interaction between the protein and cofactors [48]. Riboflavin may be functionally important in long range electron transfer or the sodium translocation mechanism [49][12]. It has been proposed that riboflavin is buried within the membrane domain of the enzyme since it lacks the hydrophilic groups unlike FAD and FMN [50]. Nevertheless riboflavin was also found in 2-hydroxyacyl-CoA dehydratases from *A. fermentans*, *F. nucleatum* and *C. propionicum* [51-54]. This enzyme has been found in clostridia and fusobacteria, which ferment α-amino acids via (*R*)-2-hydroxyacyl-CoA that is dehydrated to enoyl-CoA by radical mediated syn-elimination mechanism. The 2-hydroxyacyl-CoA dehydratases are two-component systems composed of an extremely oxygen-sensitive component A, an activator, and component D, the actual dehydratase [55].

The covalently bound flavin has been visualized on an unstained SDS-PAGE gel as fluorescent bands under UV illumination, corresponding to the RnfG/NqrC and RnfD/NqrB subunits [56]. It had been confirmed by the same method that NqrB and NqrC from *V. alginolyticus* also have covalently bound flavins [57]. In order to determine the linkage of covalently bound flavin, the Rnf complex was denatured and treated with phosphodiesterase whereby the flavins were released. The Rnf G complexes of *V. cholerae* and NqrC of *V. alginolyticus* have been shown to contain the same linkage. In *V. cholerae*, RnfG binds FMN through a phosphodiester bond between the phosphate group of FMN and threonine-175, which is the final threonine of the conserved flavin binding motif S(T)GA**T** [38]. The sequence analysis of RnfG from *C. tetanomorphum* shows a conserved TGA**T** sequence that coincides with the FMN binding motif of NqrC and RnfG of *V. cholerae*. The Rnf D subunit of *V. cholerae* includes two partially conserved sequences similar to the SGAT flavin binding motif of NqrB. One of the flavin binding motifs TMA**T** (183 – 187), represents a new version of the S(T)GAT flavin binding motif. The mutated proteins, in which the threonine of NqrB was replaced by serine, appear to have the same properties as the wild type enzyme, confirming the viability of serine as an alternative to threonine [38]. It has been reported that flavin is linked to threonine-187 in *V. cholerae*, although it has two partially conserved flavin binding motifs. In comparision, analysis of the amino acids encoding RnfD in *C. tetanomorphum* showed the first of the two flavin binding motifs
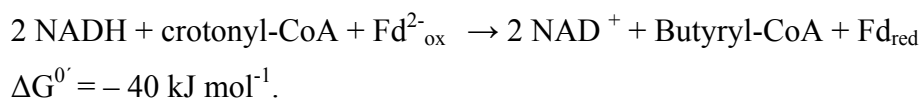
is TTAT, the final threonine should be covalently linked with flavin. The second flavin binding motif site SGAT is not conserved in *C. tetanomorphum,* whereas it is conserved in all *Vibrio* sp. and *C. tetani*.

The high activity of the Rnf complex in the presence of ferricyanide could be explained by the presence of FMN/riboflavin, the [4Fe-4S] cluster, and the NADH binding motif in RnfC. It is probable that its FMN-[4Fe-4S] group is the initial electron acceptor from NADH and donates directly to ferricyanide, thereby excluding the role of other subunits of the complex in this reaction. The Rnf activity in the presence of ferredoxin and Ti(III)citrate is moderately low when compared with the ferricyanide assay. The results are consistent with the model proposed by Brüggemann et al., in which RnfB with its three [4Fe-4S] clusters accepts the electrons from ferredoxin and transfers them further to the membrane-bound subunits RnfADE. The electrons are further transferred to RnfG and finally to the largest subunit RnfC, where NAD^+ is reduced.

Although the mode of electron transfer is probably the same in the ferredoxin-Ti(III)citrate and hydrogenase assays, even lower Rnf activity is observed in the latter. This can be explained by significant loss of the H_2 in the quvette during substrate addition or by the low and rate limiting hydrogenase activity.

4.2.4. Bcd/Etf complex

Electron transfer flavoprotein is present in a wide range of organisms from mammals to anaerobic bacteria. The mammalian Etf transfers electrons to the mitochondrial membrane enzyme Etf-quinone oxidoreductase and subsequently to ubiquinone in the respiratory chain [27]. In the anaerobic bacterium *C. propionicum,* Etf was isolated as a complex with propionyl-CoA dehydrogenase [18]. Etf is found in *C. tetanomorphum* as a tight complex with butyryl-CoA dehydrogenase [17]. Herrmann et al. [27] proposed that the Bcd/Etf complex mediates the exergonic reduction of crotonyl-CoA to butyryl-CoA ($E^{\circ\prime}$ = -10 mV) by NADH ($E^{\circ\prime}$ = -320 mV) that is coupled with the endergonic reduction of ferredoxin ($E^{\circ\prime} \leq$ -420 mV) with NADH.

$$2 \text{ NADH} + \text{crotonyl-CoA} + Fd^{2-}_{ox} \rightarrow 2 \text{ NAD}^+ + \text{Butyryl-CoA} + Fd_{red}$$
$$\Delta G^{0\prime} = -40 \text{ kJ mol}^{-1}.$$

This hypothesis was proven by Li et al. who showed that in *C. klyuveri*, Bcd/Etf complex generates reduced ferredoxin, which forms hydrogen and reduces NAD^+ mediated by the presumably ion pumping Rnf complex. The Bcd-Etf complex from *C. kluyveri* has been purified and determined to contain three subunits having apparent molecular masses of 41, 36, and 28 kDa. This finding along with Herrmann's et al. hypotheis paved the way to solve the 40 years enigma in energy conservation in *C. klyuveri* [15,58].

In our work, the purified Bcd/Etf complex from *C. tetanomorphum* shows the ferredoxin-dependent NADH oxidation with crotonyl-CoA. It has been reported that additional FAD is required to measure a crotonyl-CoA dependent NADH oxidation [17], probably FAD acted as a substitute for ferredoxin. In our study, butyryl-CoA dehydrogenase-ETF complex catalyzed the oxidation of NADH with crotonyl-CoA at a specific activity of 0.1 U/mg, when ferredoxin and hydrogenase were absent in the reaction mixture. But in their presence the activity increased about 20 fold, i.e., to 1.8 U/mg. The above experiment showed that ferredoxin was required as an electron acceptor for efficient enzyme activity. In the fully coupled reaction system, the reduction of 1 mol crotonyl-CoA required 1.8 mol NADH. The concomitantly formed amount of H_2 has not been determined yet.

Here, the Bcd-Etf complex bifurcates the two electrons from NADH via FAD, one to the more negative ferredoxin or flavodoxin and the other to the more positive crotonyl-CoA. Thus the exergonic reduction of crotonyl-CoA drives the endergonic reduction of ferredoxin [15]. The reduction of ferredoxin with NADH catalyzed by Bcd/Etf complex resembles the coenzyme Q cycle. The electrons from QH_2 are energetically bifurcated upto cytochrome b and down to via the Rieske [2Fe-2S] cluster to cytochrome c_1. Interstingly, a similar kind of reaction where the reduction of crotonyl-CoA is coupled to a high demanding energy process without an investment of ATP was reported in *Rhodobacter sphaeroides* [59]. In this organism the enzyme crotonyl-CoA carboxylase/reductase catalyzes the reductive carboxylation of crotonyl-CoA to ethylmalonyl-CoA. Even though the mechanism of coupling is different from Bcd/Etf, it can be seen as another example where free energy change associated with the reduction of crotonyl-CoA with NAD(P)H can be used to drive an endergonic reaction [15].

4.3. Energy conservation in *C. tetanomorphum* during glutamate fermentation by the Rnf and Bcd/Etf complexes
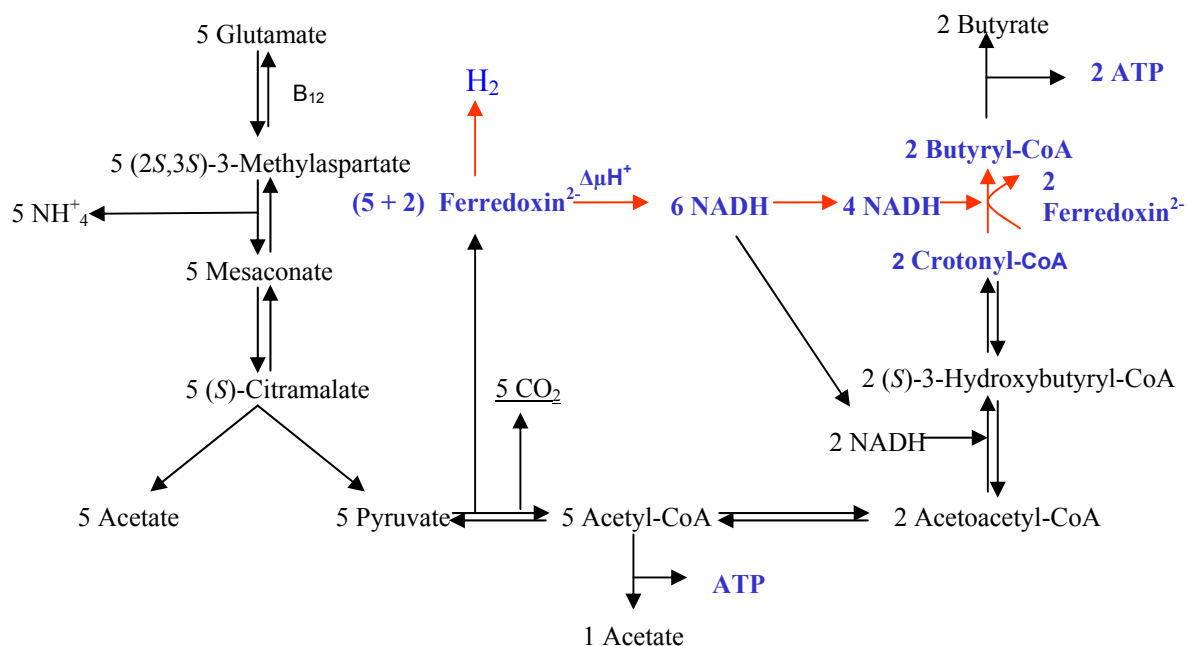

Fig. 30: Methylaspartate pathway- Glutamate fermentation by *C. tetanomorphum*.

Glutamate fermentation by *C. tetanomorphum* using the methylaspartate pathway yields 3 ATP per 5 glutamate ($\Delta G^{\circ\prime}$= -63.4 kJ/mol glutamate) via SLP (Substrate level phosphorylation). But the free enthalpy required to synthesize 1 ATP (-317/3 = -106 kJ mol^{-1}) is higher when compared with other systems. Usually -75 $\pm$ 5 kJ mol^{-1} is considered the maximum enthalpy for ATP [60][9, 10]. The oxidation of pyruvate derived from glutamate yields ferredoxin ($E^{\circ\prime} \leq$ -420 mV), whereas NADH ($E^{\circ\prime}$ -320 mV) is the reductant in butyrate synthesis. The difference ($\geq$ 100 mV) could be used for additional energy conservation of approximately 0.25 ATP/ 100 mV via Rnf. In addition to 5 ferredoxin formed from pyruvate decarboxylation, 2 ferredoxins are supplied by the Etf-Bcd complex [27] which will give rise to the formation of 6 NADH via the Rnf complex and one ferredoxin is used in H$_2$ production catalyzed by hydrogenase. Thus six Fd^{2-} would yield additional 1.5 ATP and the required enthalpy to from 1 ATP would decrease to 70 kJ/mol.

4.4. Rnf complex in other systems

C. pascui ferments glutamate by the methylaspartate pathway (shown in the Results section) and conserves the additional energy in a similar manner as *C. tetanomorphum.* This corroborates with the presence of Rnf complex in membrane and Bcd/Etf complex in the soluble fraction.

C. aminobutyricum ferments $2 \times$ 4-aminobutyrate to yield 2 acetate, 2 NH_4, 1 butyrate and 1 hydrogen. [25,26,61,62]. Growth experiments with *C. aminobutyricum* yielded 7.6 mg (dry weight) cells (mmol 4-aminobutyrate)$^{-1}$, which is more than the expected yield of 5 mg mmol^{-1} calculated from a Y_{ATP} of 10 [10 g (dry weight) cells mol ATP^{-1}) (average value based on many fermentations)] [61]. The conservation of more than 1.0 ATP equivalent from the two 4-aminobutyrate thermodynamically attainable, because the -90 kJ mol butyrate^{-1} released in 4-aminobutyrate fermentation is sufficient for about 1.3 ATP. The detection of membrane-bound NADH dehydrogenase activity in this work explains this additional energy conservation. Probably, the Bcd/Etf complex catalyses the reduction of crotonyl-CoA to butyryl-CoA to generate reduced ferredoxin which is reoxidised by NAD$^+$ catalyzed by Rnf complex (note that *C. aminobutyricum* is not producing H_2 as product). Thus cycling of NADH could conserve additionaly 0.25 ATP via $\Delta\mu H^+$ or $\Delta\mu Na^+$.

E. barkeri catabolizes nicotinate to ammonia, acetate, CO_2 and propionate via a unique fermentation [63,64]. Nicotinate is converted into pyruvate via many intermediates, where it generates NADPH and ferredoxin (oxidised) and NADH is consumed. The generated ferredoxin is reduced in the conversion of pyruvate to acetyl-CoA [64]. The membrane extracts show absence of Rnf activity, which is understandable because there is no available ferredoxin to generate NADH and conserve additional energy. It is proposed that NADPH:NAD$^+$ transhydrogenase could supply an additional source of energy via the difference in electrochemical potentials of nicotinate/6-hydroxynicotinate [-380 mV (Holcenberg, 1969 #141)] vs. 2-(hydroxymethyl)-/2-formyl-glutarate couples ca -200 mV [64].

C. propionicum ferments 3 alanine to 3 ammonia, 1 CO_2, 1 acetate, and 2 propionate [8]. SLP gives rise to only 1 ATP via acetyl-CoA, which is derived via pyruvate in the oxidative branch. In the reductive cycle, acryloyl-CoA generated from the dehydration of lactyl-CoA is reduced to propionyl-CoA. Propionyl-CoA dehydrogenase/Etf complex has been purified [18] and shown to catalyze the reduction of acryloyl-CoA by NADH without coupling to reduction of ferredoxin. It could be postulated that the absence of this coupling causes a more efficient reduction of the higly toxic acryloyl-CoA to avoid cell death. The Rnf activity in membrane extracts indicates that reduced ferredoxin from pyruvate ferredoxin oxidoreductase is used to conserve the additional energy up to 0.25 ATP.

The energy conservation in *C. sporophaeroides* is not well established so far. It ferments glutamate via the hydroxyglutarate pathway to yield acetate, butyrate and H_2. It is also able to grow on crotonate, whereas *A. fermentans* and *C. symbiosum* failed to grow. It ferments 3 crotonate to yield 4 acetate, 1 butyrate and 1 H_2 (Härtel et al.). NADH is generated in the oxidation of (*S*)-3-hydroxybutyryl-CoA to acetoacetyl-CoA. The crotonyl-CoA is reduced by NADH to butyryl-CoA catalyzed by Bcd/Etf complex and thereby formed ferredoxin gives rise to hydrogen. It could be the direct evidence of electron bifurcation by Bcd/Etf complex and its role in energy conservation. The high H_2 production and energy conservation by Bcd/Etf complex allows to predict that Rnf complex may be absent in these bacteria.

Frank et al [65], showed that the Rnf complex also plays a role in the energy conservation by caffeate respiration in *Acetobacterium woodii.* The H_2-dependent caffeate reduction causes the ATP synthesis by a chemiosmotic mechanism. NADH serves as the electron donor for cytosolic reduction of caffeate. Recently an Rnf complex has been found in this organism and the enzyme catalysing the reduction of caffeate has been characterized as an NADH-dependent Etf-Bcd related caffeoyl-CoA reductase [66,67]. Hence, energy can be conserved from reduced ferredoxin generated directly from hydrogen and by reduction of caffeoyl-CoA to 3-(3,4-hydroxyphenyl)propionyl-CoA. It can be postulated that energy is conserved by Rnf complex along with Etf complex.

The Rnf complex is widespread in many bacteria and archaea with various functions, ranging from energy conservation to DNA repair mechanisms. Two copies of Rnf genes are found in *Azotobacter vinelandii*. The *rnf1* is regulated by the *nif* genes, whereas *rnf2* is expressed independently of the nitrogen source present in the medium. The deletion of *rnf* clusters in these bacteria leads to slow *nifHDK* gene expression, and subsequent impairment of nitrogenase function [68]. Hence, reduced ferredoxin is involved in nitrogenase maturation but not nitrogen fixation. Probably in this organism the fix gene products provide reduced ferredoxin for nitrogen fixation [27,69-71]. It has been reported that *E. coli* is protected from nitric oxide and superoxide by the *soxRS* regulon. It keeps SoxR in the reduced state mediated by *rsxABCDGE* that is highly homologues to the Rnf genes [72].

Acetate conversion to methane is paramount to the development of process parameters for control and optimization of large scale biomethanation of renewable biomass. Proteome Studies on *Methanosarcina acetivorans* grown on acetate paved the way to identify the essential core enzymes in the acetate pathway. The proteins (MA0659-0664) show amino acid sequence identities to the Rnf complex of *C. tetani* [73]. *Syntrophus acidotrophicus* SB´s genome sequence reveals the presence of Rnf and Bcd/Etf complexes [74]. The role of Rnf can be explained in these bacteria by considering the previous observations made with whole-cell suspensions of *Syntrophomonas wolfei* grown on either butyrate or crotonate [5,75]. They observed that addition of protonophore CCCP completely inhibited the formation H_2 when the cells were grown on buyrate. Hence the oxidation of butyryl-CoA to crotonyl-CoA requires ferredoxin reduced by NADH, which is catalysed by the probably ion pumping Rnf complex. However, upon incubation of butyryl-CoA, ferredoxin, NAD^+ with Bcd/Etf complex did not yield crotonyl-CoA (Work done in our lab which is not mentioned in this thesis).
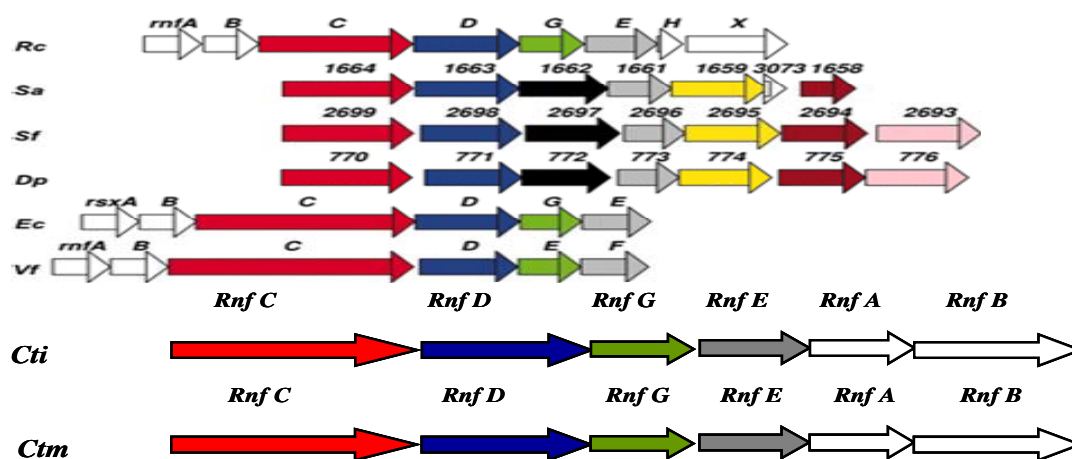
Rnf-type gene cluster: The *rnfABCDGEH* genes of *R. capsulatus* (Rc), the putative *rnf* genes of *S. aciditrophicus* (Sa), *S. fumaroxidans* (Sf), and *D. psychrophila* (Dp) are aligned 5' to 3'. The *rsxABCDEF* genes of *E. coli* (Ec), *rnfABCDEF* genes *Vibrio fisheri* (Vf), *rnfABCDEG* genes *C. tetani* (Cti) and *rnfABCDEG* genes *C. tetanomorphum* (Ctm) are shown below. Identically colored genes are homologous. Modified from McInerney et al., [8].

5. Outlook

The energy conservation in *C. tetanomorphum* by Rnf complex will be confirmed by Na^+/H^+ ion translocation studies. This is an ongoing project in collaboration with Prof. Julia Fritz Steuber, University of Zürich. The genes encoding the Rnf complex will be cloned and expressed to produce recombinant protein. The RnfG and RnfD subunits will be analyzed under HPLC followed by peptide analysis by MALDI-TOF to confirm the amino acids to which the flavins are covalently bound. The EPR spectroscopy of Rnf complex and Bcd/Etf complex will reveal the presence of radicals and insight into the enzyme mechanism. (Collaboration with Antonio Pierik, University of Marburg). RnfB and RnfC subunits can be analyzed for their Fe-S clusters. The metabolic pathway involved in glutamate fermentation in *C. pascui* will be confirmed further by using [^{13}C]glutamates as a substrate. The same experiment may give some more insight in to the metabolic pathway of *Fusobacterium nucleatum.*

References

1. Wächtershäuser G: **Before enzymes and templates: theory of surface metabolism**. *Microbiol Rev* 1988, **52**:452-484.

2. Wächtershäuser G: **Evolution of the first metabolic cycles**. *Proc Natl Acad Sci U S A* 1990, **87**:200-204.

3. Decker K, Jungermann K, Thauer RK: **Energy production in anaerobic organisms**. *Angew Chem Int Ed Engl* 1970, **9**:138-158.

4. Thauer RK, Kaster AK, Seedorf H, Buckel W, Hedderich R: **Methanogenic archaea: ecologically relevant differences in energy conservation**. *Nat Rev Microbiol* 2008, **6**:579-591.

5. Schink B: **Energetics of syntrophic cooperation in methanogenic degradation**. *Microbiol Mol Biol Rev* 1997, **61**:262-280.

6. Buckel W, Barker HA: **Two pathways of glutamate fermentation by anaerobic bacteria**. *J Bacteriol* 1974, **117**:1248-1260.

7. Härtel U, Buckel W: **Sodium ion-dependent hydrogen production in** *Acidaminococcus fermentans*. *Arch. Microbiol.* 1996, **166**:350-356.

8. Barker HA: **Fermentations of nitrogenous organic compounds**. In *The Bacteria*. Edited by Gunsalus IC: Academic Press Inc.; 1961:151-207. vol 2.]

9. Brüggemann H, Baumer S, Fricke WF, Wiezer A, Liesegang H, Decker I, Herzberg C, Martinez-Arias R, Merkl R, Henne A, et al.: **The genome sequence of *Clostridium tetani*, the causative agent of tetanus disease**. *Proc. Natl. Acad. Sci. U S A* 2003, **100**:1316-1321.

10. Reitzer R, Gruber K, Jogl G, Wagner UG, Bothe H, Buckel W, Kratky C: **Glutamate mutase from *Clostridium cochlearium*: the structure of a coenzyme B12-dependent enzyme provides new mechanistic insights**. *Structure* 1999, **7**:891-902.

11. Schneider K, Dimroth P, Bott M: **Identification of triphosphoribosyl-dephospho-CoA as precursor of the citrate lyase prosthetic group**. *FEBS Lett* 2000, **483**:165-168.

12. Schmellenkamp H, Eggerer H: **Mechanism of enzymic acetylation of des-acetyl citrate lyase**. *Proc Natl Acad Sci U S A* 1974, **71**:1987-1991.

13. Buckel W, Bobi A: **The enzyme complex citramalate lyase from *Clostridium tetanomorphum*. *Eur J Biochem* 1976, **64**:255-262.

14. Buckel W: **Unusual enzymes involved in five pathways of glutamate fermentation**. *Appl Microbiol Biotechnol* 2001, **57**:263-273.

15. Li F, Hinderberger J, Seedorf H, Zhang J, Buckel W, Thauer RK: **Coupled ferredoxin and crotonyl coenzyme A (CoA) reduction with NADH catalyzed by the**

butyryl-CoA dehydrogenase/Etf complex from *Clostridium kluyveri*. *J Bacteriol* 2008, **190**:843-850.

16. Boiangiu CD, Jayamani E, Brügel D, Herrmann G, Forzi L, Hedderich R, Vgenopoulou I, Kim J, Pierik AJ, Steuber J, et al.: **Sodium ion pumps and hydrogen production in glutamate fermenting anaerobic bacteria**. *J. Mol. Microbiol. Biotechnol.* 2005, **10**:105-119.

17. Herrmann GE: **Enzymes of two clostridial amino-acid fermentation pathways**. Marburg: Universität Marburg: 2008.

18. Hetzel M, Brock M, Selmer T, Pierik AJ, Golding BT, Buckel W: **Acryloyl-CoA reductase from** *Clostridium propionicum*. **An enzyme complex of propionyl-CoA dehydrogenase and electron-transferring flavoprotein**. *Eur. J. Biochem.* 2003, **270**:902-910.

19. Schmehl M, Jahn A, Meyer zu Vilsendorf A, Hennecke S, Masepohl B, Schuppler M, Marxer M, Oelze J, Klipp W: **Identification of a new class of nitrogen fixation genes in** *Rhodobacter capsulatus*: **a putative membrane complex involved in electron transport to nitrogenase**. *Mol Gen Genet* 1993, **241**:602-615.

20. Hase CC, Fedorova ND, Galperin MY, Dibrov PA: **Sodium ion cycle in bacterial pathogens: evidence from cross-genome comparisons**. *Microbiol Mol Biol Rev* 2001, **65**:353-370, table of contents.

21. Hans M, Bill E, Cirpus I, Pierik AJ, Hetzel M, Alber D, Buckel W: **Adenosine triphosphate-induced electron transfer in 2-hydroxyglutaryl-CoA dehydratase from** *Acidaminococcus fermentans*. *Biochemistry* 2002, **41**:5873-5882.

22. Braune A, Bendrat K, Rospert S, Buckel W: **The sodium ion translocating glutaconyl-CoA decarboxylase from** *Acidaminococcus fermentans:* **cloning and function of the genes forming a second operon**. *Mol Microbiol* 1999, **31**:473-487.

23. Wendt KS, Schall I, Huber R, Buckel W, Jacob U: **Crystal structure of the carboxyltransferase subunit of the bacterial sodium ion pump glutaconyl-coenzyme A decarboxylase**. *EMBO J.* 2003, **22**:3493-3502.

24. Collins MD, Lawson PA, Willems A, Cordoba JJ, Fernandez-Garayzabal J, Garcia P, Cai J, Hippe H, Farrow JA: **The phylogeny of the genus** *Clostridium*: **proposal of five new genera and eleven new species combinations**. *Int. J. Syst. Bacteriol.* 1994, **44**:812-826.

25. Hardman JK, Stadtman TC: **Metabolism of amega-amino acids. III. Mechanism of conversion of gamma-aminobutyrate to gamma-hydroxybutryate by** *Clostridium aminobutyricum*. *J Biol Chem* 1963, **238**:2081-2087.

26. Hardman JK, Stadtman TC: **Metabolism of omega-amino acids. IV. gamma Aminobutyrate fermentation by cell-free extracts of** *Clostridium aminobutyricum*. *J Biol Chem* 1963, **238**:2088-2093.

27. Herrmann G, Jayamani E, Mai G, Buckel W: **Energy conservation via electron transferring flavoprotein (Etf) in anaerobic bacteria**. *J. Bacteriol.* 2008, **190**.

28. Wilde E, Collins MD, Hippe H: *Clostridium pascui* **sp. nov., a new glutamate-fermenting sporeformer from a pasture in Pakistan**. *Int J Syst Bacteriol* 1997, **47**:164-170.

29. Terlesky KC, Ferry JG: **Purification and characterization of a ferredoxin from acetate-grown *Methanosarcina thermophila***. *J Biol Chem* 1988, **263**:4080-4082.

30. Rex M. C. Dawson DCE, William H. Elliott and K. M. Jones: *Data for Biochemical Research*. Edited by Dawson RMC: Oxford University Press

31. Carrillo N, Ceccarelli EA: **Open questions in ferredoxin-NADP+ reductase catalytic mechanism**. *Eur J Biochem* 2003, **270**:1900-1915.

32. Lehman TC, Hale DE, Bhala A, Thorpe C: **An acyl-coenzyme A dehydrogenase assay utilizing the ferricenium ion**. *Anal Biochem* 1990, **186**:280-284.

33. Bradford MM: **A rapid and sensitive method for the quantification of microgram quantitiesof protein utilizing the principle of protein dye binding**. *Anal. Biochem.* 1976, **72**:248-254.

34. Simon EJaS, D: **The preparation of S-succinyl coenzyme A**. *J. Am. Chem. Soc.* 1953, **75**:2520.

35. Wilson K: **Preparation of Genomic DNA from Bacteria**. *Current Protocols in Molecular Biology* 2001.

36. Härtel U, Buckel W: **Fermentation of *trans*-aconitate via citrate, oxaloacetate, and pyruvate by *Acidaminococcus fermentans***. *Arch. Microbiol.* 1996, **166**:342-349.

37. Nakayama Y, Yasui M, Sugahara K, Hayashi M, Unemoto T: **Covalently bound flavin in the NqrB and NqrC subunits of Na$^+$-translocating NADH-quinone reductase from *Vibrio alginolyticus***. *FEBS Lett.* 2000, **474**:165-168.

38. Backiel J, Juarez O, Zagorevski DV, Wang Z, Nilges MJ, Barquera B: **Covalent binding of flavins to RnfG and RnfD in the Rnf complex from *Vibrio cholerae***. *Biochemistry* 2008, **47**:11273-11284.

39. Barker HA, Kahn JM, Hedrick L: **Pathway of lysine degradation in *Fusobacterium nucleatum***. *J. Bacteriol.* 1982, **152**:201-207.

40. Wang CC, Barker HA: **Activation of L-citramalate hydrolyase from *Clostridium tetanomorphum***. *J Biol Chem* 1969, **244**:2527-2538.

41. Wang CC, Barker HA: **Purification and properties of L-citramalate hydrolyase**. *J Biol Chem* 1969, **244**:2516-2526.

42. Hartrampf G, Buckel W: **The stereochemistry of the formation of the methyl group in the glutamate mutase-catalysed reaction in *Clostridium tetanomorphum***. *FEBS Lett* 1984, **171**:73-78.

43. Gemperli AC, Dimroth P, Steuber J: **Sodium ion cycling mediates energy coupling between complex I and ATP synthase**. *Proc Natl Acad Sci U S A* 2003, **100**:839-844.

44. Steuber J, Schmid C, Rufibach M, Dimroth P: **Na+ translocation by complex I (NADH:quinone oxidoreductase) of *Escherichia coli***. *Mol Microbiol* 2000, **35**:428-434.

45. Meuer J, Kuettner HC, Zhang JK, Hedderich R, Metcalf WW: **Genetic analysis of the archaeon *Methanosarcina barkeri* Fusaro reveals a central role for Ech hydrogenase and ferredoxin in methanogenesis and carbon fixation**. *Proc Natl Acad Sci U S A* 2002, **99**:5632-5637.

46. Albracht SP, Hedderich R: **Learning from hydrogenases: location of a proton pump and of a second FMN in bovine NADH--ubiquinone oxidoreductase (Complex I)**. *FEBS Lett* 2000, **485**:1-6.

47. Vgenopoulou I: **On the mechanism of Na+ transport by the respiratory NADH:quinone oxidoreductase (complex I) from *Klebsiella pneumoniae***: ETH, Zürich.

48. Barquera B, Zhou W, Morgan JE, Gennis RB: **Riboflavin is a component of the Na+-pumping NADH-quinone oxidoreductase from *Vibrio cholerae***. *Proc Natl Acad Sci U S A* 2002, **99**:10322-10324.

49. Barquera B, Ramirez-Silva L, Morgan JE, Nilges MJ: **A new flavin radical signal in the Na(+)-pumping NADH:quinone oxidoreductase from *Vibrio cholerae*. An EPR/electron nuclear double resonance investigation of the role of the covalently bound flavins in subunits B and C**. *J Biol Chem* 2006, **281**:36482-36491.

50. Page CC, Moser CC, Chen X, Dutton PL: **Natural engineering principles of electron tunnelling in biological oxidation-reduction**. *Nature* 1999, **402**:47-52.

51. Müller U, Buckel W: **Activation of (R)-2-hydroxyglutaryl-CoA dehydratase from *Acidaminococcus fermentans***. *Eur J Biochem* 1995, **230**:698-704.

52. Klees AG, Linder D, Buckel W: **2-Hydroxyglutaryl-CoA dehydratase from *Fusobacterium nucleatum* (subsp. nucleatum): an iron-sulfur flavoprotein**. *Arch Microbiol* 1992, **158**:294-301.

53. Kuchta RD, Abeles RH: **Lactate reduction in *Clostridium propionicum*. Purification and properties of lactyl-CoA dehydratase**. *J Biol Chem* 1985, **260**:13181-13189.

54. Kim J, Hetzel M, Boiangiu CD, Buckel W: **Dehydration of (R)-2-hydroxyacyl-CoA to enoyl-CoA in the fermentation of alpha-amino acids by anaerobic bacteria**. *FEMS Microbiol Rev* 2004, **28**:455-468.

55. Kim J, Darley DJ, Buckel W, Pierik AJ: **An allylic ketyl radical intermediate in clostridial amino-acid fermentation**. *Nature* 2008, **452**:239-242.

56. Singer TP, McIntire WS: **Covalent attachment of flavin to flavoproteins: occurrence, assay, and synthesis**. *Methods Enzymol* 1984, **106**:369-378.

57. Hayashi M, Nakayama Y, Yasui M, Maeda M, Furuishi K, Unemoto T: **FMN is covalently attached to a threonine residue in the NqrB and NqrC subunits of Na$^+$-translocating NADH-quinone reductase from *Vibrio alginolyticus*.** *FEBS Lett.* 2001, **488**:5-8.

58. Seedorf H, Fricke WF, Veith B, Bruggemann H, Liesegang H, Strittmatter A, Miethke M, Buckel W, Hinderberger J, Li F, et al.: **The genome of *Clostridium kluyveri,* a strict anaerobe with unique metabolic features**. *Proc Natl Acad Sci U S A* 2008, **105**:2128-2133.

59. Erb TJ, Berg IA, Brecht V, Muller M, Fuchs G, Alber BE: **Synthesis of C5-dicarboxylic acids from C2-units involving crotonyl-CoA carboxylase/reductase: the ethylmalonyl-CoA pathway**. *Proc Natl Acad Sci U S A* 2007, **104**:10631-10636.

60. Thauer RK, Jungermann K, Decker K: **Energy conservation in chemotrophic anaerobic bacteria**. *Bacteriol Rev* 1977, **41**:100-180.

61. Stadtman ER, p. In(ed.), *Some considerations of the energy metabolism of anaerobic bacteria*. Edited by Kennedy. New York ,NY: Academic Press; 1966.

62. Hardman JK, Stadtman TC: **Metabolism of Omega-Amino Acids. V. Energetics of the Gamma-Aminobutyrate Fermentation by *Clostridium Aminobutyricum***. *J Bacteriol* 1963, **85**:1326-1333.

63. Stadtman ER, Stadtman TC, Pastan I, Smith LD: ***Clostridium barkeri* sp. n**. *J Bacteriol* 1972, **110**:758-760.

64. Alhapel A, Darley DJ, Wagener N, Eckel E, Elsner N, Pierik AJ: **Molecular and functional analysis of nicotinate catabolism in *Eubacterium barkeri***. *Proc Natl Acad Sci U S A* 2006, **103**:12341-12346.

65. Imkamp F, Biegel E, Jayamani E, Buckel W, Muller V: **Dissection of the caffeate respiratory chain in the acetogen *Acetobacterium woodii*: identification of an Rnf-type NADH dehydrogenase as a potential coupling site**. *J Bacteriol* 2007, **189**:8145-8153.

66. Imkamp F, Muller V: **Chemiosmotic energy conservation with Na(+) as the coupling ion during hydrogen-dependent caffeate reduction by Acetobacterium woodii**. *J Bacteriol* 2002, **184**:1947-1951.

67. Müller V, Imkamp F, Biegel E, Schmidt S, Dilling S: **Discovery of a ferredoxin:NAD+-oxidoreductase (Rnf) in *Acetobacterium woodii*: a novel potential coupling site in acetogens**. *Ann N Y Acad Sci* 2008, **1125**:137-146.

68. Curatti L, Brown CS, Ludden PW, Rubio LM: **Genes required for rapid expression of nitrogenase activity in *Azotobacter vinelandii*. ***Proc Natl Acad Sci U S A* 2005, **102**:6291-6296.

69. Edgren T, Nordlund S: **The fixABCX genes in *Rhodospirillum rubrum* encode a putative membrane complex participating in electron transfer to nitrogenase**. *J Bacteriol* 2004, **186**:2052-2060.

70. Edgren T, Nordlund S: **Electron transport to nitrogenase in *Rhodospirillum rubrum*: identification of a new fdxN gene encoding the primary electron donor to nitrogenase**. *FEMS Microbiol Lett* 2005, **245**:345-351.

71. Edgren T, Nordlund S: **Two pathways of electron transport to nitrogenase in *Rhodospirillum rubrum*: the major pathway is dependent on the fix gene products**. *FEMS Microbiol Lett* 2006, **260**:30-35.

72. Koo MS, Lee JH, Rah SY, Yeo WS, Lee JW, Lee KL, Koh YS, Kang SO, Roe JH: **A reducing system of the superoxide sensor SoxR in *Escherichia coli***. *Embo J* 2003, **22**:2614-2622.

73. Li Q, Li L, Rejtar T, Lessner DJ, Karger BL, Ferry JG: **Electron transport in the pathway of acetate conversion to methane in the marine archaeon *Methanosarcina acetivorans***. *J. Bacteriol.* 2006, **188**:702-710.

74. McInerney MJ, Rohlin L, Mouttaki H, Kim U, Krupp RS, Rios-Hernandez L, Sieber J, Struchtemeyer CG, Bhattacharyya A, Campbell JW, et al.: **The genome of *Syntrophus aciditrophicus*: Life at the thermodynamic limit of microbial growth**. *Proc. Natl. Acad. Sci. USA* 2007, **104**:7600-7605.

75. Schink B, Wallrabenstein C: **Evidence of reversed electron transport in syntrophic butyrate or benzoate oxidation by *Syntrophomonas wolfei* and *Syntrophus buswellii***. *Archives of Microbiology* 1994, **162**:136-142.

Acknowledgements:

I appreciate my Indians friends for their technical discussions and moral support.

I am indebted to my parents and family for their support throughout my studies.

Persönliche Daten

Name, Vorname	Elamparithi, Jayamani
Straße	Neue Kasseler Straße 4
PLZ/Wohnort	35039/Marburg
Geburtsdatum	04.07.1978
Nationalität	Indisch

Schulbildung

1993-1995	High School-KGF First Grade college
1995-1998	Bachelor of Science in Microbiology, Pee Gee College of Arts and Sciences
1999-2001	Master of Science in Applied Microbiology, Vels College of Sciences
2002-2003	Research Scientist- R & D at Poseidon Biotech, Chennai.
2004-	Mitglied des Graduiertenkollegs ''Proteinfunktion auf atomarer Ebene'' und der IMPRS am MPI für terrestrische Mikrobiologie

Erklärung

Ich versichere, dass ich meine Dissertation mit dem Titel

A unique way of energy conservation in glutamate fermenting clostridia

selbständig, ohne unerlaubte Hilfe angefertigt und mich dabei keiner anderen als der von mir ausdrücklich bezeichneten Quellen und Hilfen bedient habe.

Die Dissertation wurde in der jetzigen oder einer ähnlichen Form noch bei keiner anderen Hochschule eingereicht und hat noch keinen sonstigen Prüfungszwecken gedient.

Marburg, 24.11.2008   Elamparithi Jayamani

(Ort, Datum)